2017

MODULATING THE INNATE IMMUNE RESPONSE TO ELECTROSPUN SCAFFOLDS AND POLYMER DEGRADATIVE BYPRODUCTS

Daniel Abebayehu
Virginia Commonwealth University

MODULATING THE INNATE IMMUNE RESPONSE TO ELECTROSPUN SCAFFOLDS AND POLYMER DEGRADATIVE BYPRODUCTS

A dissertation submitted in partial fulfillment of the requirements for the degree of Doctor of Philosophy in Biomedical Engineering at Virginia Commonwealth University.

by

DANIEL ABEBAYEHU
Bachelor of Science, University of Virginia, 2011

Director: JOHN J. RYAN, PH.D.
Professor, Biology

Virginia Commonwealth University
Richmond, Virginia
May 2017

Acknowledgements

I would like to first thank my advisor and mentor, Dr. John J. Ryan. He took on an orphaned graduate student from another discipline and made him one of his own, and that seemingly simple decision has set me on a course that has radically improved my future prospects. While I am incredibly thankful for the endless supply of cokes and pies throughout the years, I am particularly thankful for his guidance and encouragement that has helped me to become a better scientist, teacher, husband, and father. Next, I would like to say thank you to my committee members, Dean Barbara Boyan, Jamie Sturgill, Chris Lemmon, and Rebecca Heise. I appreciate the encouragement and input they have given me over the years to help me navigate through my research. I would also like to thank all of the members of the Bowlin and Ryan lab who have helped me over the years. To Scott Sell who helped me get started on my research and helped me feel at home at VCU. To Gary Bowlin in believing in me and giving me a first lab to call home. To Brian Barnstein for being incredibly patient and showing me how to do nearly everything. A huge thank you to Andrew Spence who was my partner in crime and did a large part of this work alongside of me. Because there have been so many people over the years that have been helpful and supportive, I'll list them here. I'd like to say thank you to Travis Faber, Motunrayo Kolawole, Marcela Taruselli, Amina Abdul-Qayum, Anuya Paranjape, Heather Caslin, Tamara Haque, Jamie McLeod, Bianca Baker, and Victor Ndaw.

Next, I'd like to thank my family who have been incredibly helpful over the years. First, my mom, Konjit Eskender, who selflessly raised me and was the first person in my corner. To my dad, Dr. Abebayehu Tegene, who always believed in me and always pushed me to strive for more. To my stepmom, Dr. Misrak Gezmu, who always encouraged me and was a great source of guidance. Having grown up in Ethiopia and moved to the United States on their own, my parents have always served as great examples of perseverance.

Lastly, my biggest thanks goes to my wife, Mary Catherine. She has been my biggest source of encouragement, support, consolation, and overall help. In addition to staying at home and raising our boys (which alone warrants its own paragraph), she cheers me up when things don't go my way (as they often do in science) and celebrates with me at the noteworthy moments. I say this because it is incredibly true but I could not have done any of this without her.

Table of Contents

List of Figures

List of Abbreviations

1,1,1,3,3,3-hexafluoro-2-proponol (HFP)

α -Cyano-4-hydroxycinnamic acid (CHC)

Bone marrow derived mast cells (BMMC)

Bovine serum albumin (BSA)

complete RPMI 1640 (cRPMI)

Connective tissue mast cells (CTMC)

Dimethyl sulfoxide (DMSO)

Dinitrophenol-conjugated albumin (DNP)

Extracellular Matrix (ECM)

Foreign body response (FBR)

Hypoxia-inducible factor (HIF)

Human Skin Mast cells (SkMC)

Human Umbilical Vein Endothelial Cells (HUVEC)

Immunoreceptor tyrosine-based activation motif (ITAM)

Immunoreceptor tyrosine-based inhibition motif (ITIM)

Lactic acid (LA)

leukotriene B_4 receptor 2 (BLT2)

Linker for activation of T cells (LAT)

Lipopolysaccharide (LPS)

Monocarboxylate transporter (MCT)

microRNA (miRNA or miR)

Mucosal mast cells (MMC)

Paraformaldehyde (PFA)

Passive Systemic anaphylaxis (PSA)

Peritoneal Mast Cells (PMCs)

Quantitative PCR (qPCR)

Sodium Lactate (NaLA)

Stem Cell Factor (SCF)

Small interfering RNA (siRNA)

Skin Mast Cell (SkMC)

TGFβ-1-activated kinase 1 (TAK1)

Abstract

MODULATING THE INNATE IMMUNE RESPONSE TO ELECTROSPUN SCAFFOLDS AND POLYMER DEGRADATIVE BYPRODUCTS

By Daniel Abebayehu, B.S.

A dissertation submitted in partial fulfillment of the requirements for the degree of Doctor of Philosophy in Biomedical Engineering at Virginia Commonwealth University.

Virginia Commonwealth University, 2017

Director: JOHN J. RYAN, PH.D.
Professor, Biology

Implanted biomaterials often induce inflammation that frequently leads to the foreign body response, fibrosis, and the failure of the implant. Thus, it is important to evaluate how cells interact with materials to promote a more regenerative response. It is critical to determine how to modulate the response of tissue resident innate immune cells, as they are among the first cells to interact with implanted materials. Among tissue resident innate immune cells are mast cells, which are inflammatory sentinels that degranulate and orchestrate the fate of other cell populations, such as monocytes/macrophages and

lymphocytes. Mast cells have also been reported to play a vital role in the foreign body response of implanted biomaterials as well as angiogenesis. The goal of this study was to determine how to modulate mast cell responses to electrospun scaffolds by altering scaffold architecture and composition to promote anti-inflammatory and regenerative cell-scaffold interactions. Scaffold architecture was manipulated by changing either fiber diameter or pore diameter and mast cell responses were mediated by endogenous and exogenous DAMPs (i.e. IL-33 and LPS, respectively). Particularly in response to IL-33, scaffolds with increased fiber and pore diameter promoted less inflammatory cytokine and chemokine release while increasing angiogenic cytokine release. Additionally, taking scaffolds that promoted increased inflammatory cytokine expression and increasing the pore diameter alone dampened inflammatory cytokine expression. The next question we wanted to answer was how might the degradative byproducts of scaffolds alter mast cell inflammatory responses. Given the widespread use of polylactic acid, we decided to investigate this question using lactic acid as a degradative byproduct. In the presence of physiologically relevant levels of lactic acid, IL-33- and IgE-mediated inflammatory cytokines and chemokines are suppressed, while angiogenic cytokines are enhanced. This response was shown to be pH- and MCT1-dependent and was recapitulated in primary human skin mast cells as well as *in vivo*. In summary, scaffold architecture and the presence of select polymer degradative byproducts have the potential of selectively suppressing inflammatory cytokines and enhancing angiogenic cytokines.

CHAPTER I: INTRODUCTION

I.1 HISTORICAL OVERVIEW

The stories of immunology and regenerative medicine are inextricably linked, dating back to ancient civilizations, where people used therapies that promoted healing and repair without knowing that these interventions manipulated the immune response. For example, people in ancient Egypt used honey as a wound dressing because it accelerated healing of burns and various dermal wounds, which is partially due to honey's ability to enhance neutrophil infiltration, lymphocyte proliferation, MMP activation, and growth of granulation tissue (1). In 2500 BC, Suśrata, widely considered the father of Surgery, operated on patients with autologous gluteal skin grafts, which would have had a higher rate of rejection by the immune system had they not been autografts. The Mayans were noted to have used nacre shell as a dental implant, which requires a balance of enhancing sufficient bone formation and reducing activity of osteoclasts, bone-resident macrophages (2). Interestingly, one of the most noteworthy pieces of art within the context of tissue engineering is the Healing of Justinian, which features an early portrayal of homograft transplantation (2-4).

Moving forward in history, immunology and regenerative medicine can also trace their common history back to the age of the Enlightenment, when the observable world was no longer explained exclusively by spiritual or metaphysical truths but by empirical observations. Many of these observations were early discoveries that led to the development of the Cell Theory. In 1665, while looking at cross-sections under a microscope, Robert Hooke first coined the term "cell" or *cella*, which is latin for "small room". While his seminal work *Micrographia* is widely considered to be the advent of microscopy, it is also considered to be the genesis of cell biology (5). From there,

German botanist Matthias Schleiden and German physiologist Theodor Schwann made two critical observations in 1838 and 1839 that would serve as the foundation of Cell Theory: 1) all living organisms are made of cells and 2) the cell is the basic unit of all living organisms (6). The final tenet of Cell Theory was provided by Rudolf Virchow, who in 1858 published a work entitled *Cellular Pathology* where he wrote *omnis cellula e cellula*, "every cell comes from another cell". Virchow's critical observation that cells only come from preexisting cells is critical to cell biology, and particularly for fields such as hematology and stem cell biology (7, 8). The early findings that formulated the Cell Theory lay the foundation for all the following work done in the fields of immunology and regenerative medicine.

An important note to make is that while the success of early therapies that promoted healing and tissue growth can be partially attributed to the immune response, so are many failures. While the two fields have similar origin stories, it is worth taking a closer look at each of their respective histories to better appreciate their current states and what the future holds.

I.3 HISTORY OF IMMUNOLOGY

Since early civilizations, people have acknowledged that exposure to pathogens like smallpox conferred protection against subsequent exposures, though not in those words. Those who had survived smallpox were called upon to nurse the afflicted. As awareness grew of the propensity of previously affected individuals to be protected from further infection, some started to inoculate themselves with the smallpox virus. They would give themselves nasal or subcutaneous exposures to smallpox with fluid from the

blisters of infected individuals. This crude form of vaccination was largely effective, but the dawn of vaccination came with Edward Jenner. As an apprentice to a town surgeon and during his time as a physician, Jenner noticed that milkmaids who had previously contracted cowpox were resistant to becoming infected with smallpox. Based on his observations, Jenner hypothesized that cowpox could confer protection against smallpox, which he proved to be true by vaccinating a young boy with fluid from the blisters a milkmaid who had just contracted cowpox. Jenner then subsequently exposed the boy to smallpox, and ten days later the boy had no infection. A second challenge occurred two months later with smallpox and the boy had developed no disease (9).

This work was advanced further by the contributions of Louis Pasteur, who noticed similar responses among chickens with fowl cholera. But his contributions to vaccinations came to fruition when he began to expand his work to develop a vaccination for anthrax. Interestingly, after reporting his discovery of a vaccine against anthrax for cattle, Pasteur was challenged to treat cattle before a crowd of people. Of course, he accepted. Each of the cattle that received the vaccine with the attenuated bacteria survived subsequent active anthrax challenge, while all the cattle in the control group died. His work also led to the development of a vaccine against rabies, discrediting the spontaneous generation theory based on his work with fermentation, and developing the germ theory to explain infection disease (10).

While Pasteur's work garnered him the title as the "father of immunology", the arrival of the 20th century brought with it the discoveries that comprise modern immunology. The next person to push the field of vaccines and immunization further was Paul Ehrlich. He was the first to bring together different observations and conceptualize

active and passive immunization. He pioneered many different techniques within the field of histology and used those new methods in staining to be the first to identify mast cells, basophils, eosinophils, and neutrophils. And if all of that was not impressive enough, Ehrlich postulated the "side chain theory", which consisted of a hypothesis that receptors were present that would bind specific toxins on cells and could also be released and bind toxins as an antitoxin, or an antibody. This theory would be the last piece of Ehrlich's body of work that helped him win the 1908 Nobel Prize in medicine (11-13).

Ehrlich shared his award with Elie Metchnikoff, a Russian scientist who proposed an alternative theory to characterize immunology. While Ehrlich proposed that immunology entailed antitoxins and responses to specific toxins, Metchnikoff proposed that host defense consisted of phagocytic cells ingesting invading pathogens (14). Interestingly, Ehrlich's theory became the basis for adaptive immunity, while Metchnikoff's phagocytic cell theory is the basis of innate immunity. Figure 1.1 shows the two arms of the immune system that these two men hypothesized over a century ago. The ability of the immune system to recognize foreign antigens and non-self tissue, as well as phagocytize those foreign substances, has had major repercussions on different fields but particularly on organ and tissue transplantation. Interestingly, organ and tissue transplantations were the early forms of tissue engineering. The introduction of tissue engineering was meant to help address the rising need for more organ and tissue donors, with no changes in the supply. Throughout history, the idea to engineer new organs and tissue was always present but did not fully materialize until the late 20th century.

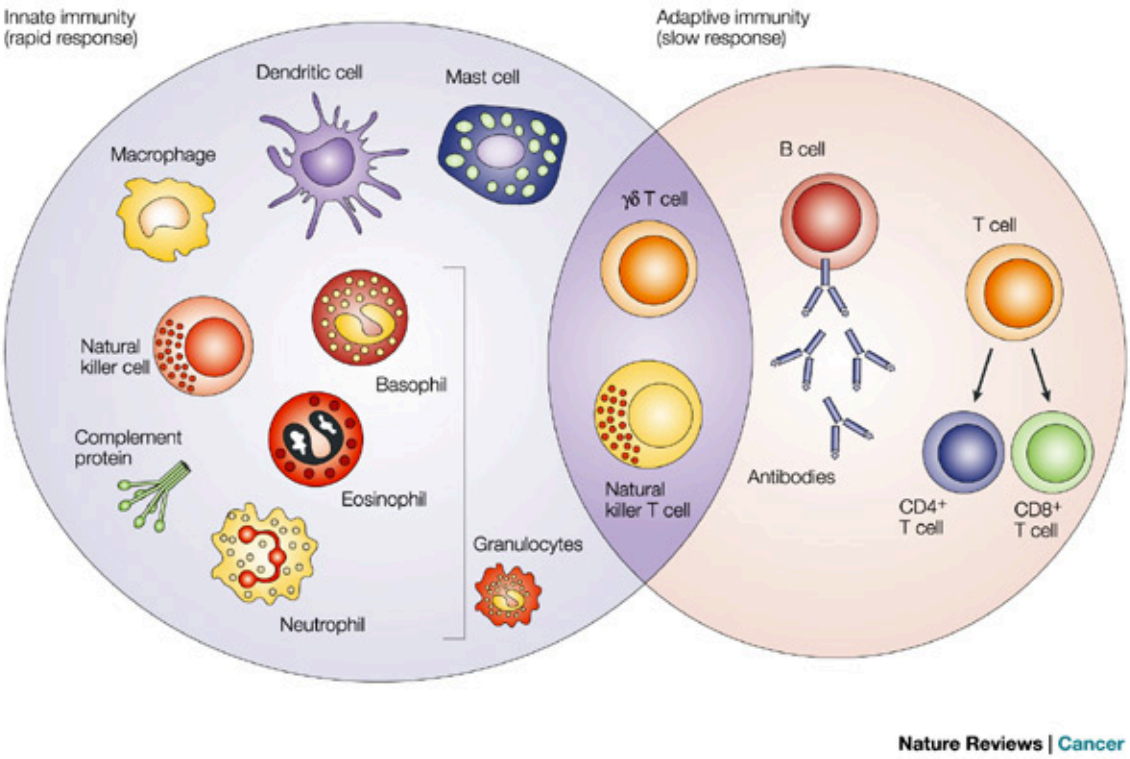

FIGURE 1.1 Adaptive and Innate Immunity (15) The innate immune system consists of various granulocytes, such as basophils, eosinophils, and neutrophils, as well as macrophages, dendritic cells, macrophages, and mast cells. The adaptive immune response consists of antibody producing B cells and key effector T cells. There also exists a group of adaptive immune cells that bear non-specific characteristics that make them innate-like lymphocytes, such as γδ T cells and NK T cells.

I.3 HISTORY OF TISSUE ENGINEERING & REGENERATIVE MEDICINE

While the use of the terms "tissue engineering" and "regenerative medicine" only sprang up in the 20th century, the concepts have existed for much longer. Dating back to Ancient Greece, the legend of Prometheus tells of a man whose liver would undergo regeneration on a daily basis (2). In the book of Genesis in the Old Testament, we read that Eve was made, or "engineered", from a rib taken from the side of Adam (3). Lastly, we read in Mary Shelley's 1818 novel *Frankenstein* the story of a scientist who engineers a living creature out of tissues from corpses (4). Each of these stories demonstrates a historical precedent for our fascination with the regeneration of human tissues.

While the above stories are fictional, biblical, or mythological, the early forms of tissue engineering and regenerative medicine in reality were pioneering studies and observations in tissue grafting (e.g. autologous and allograft), and organ transplantation. One of the key early studies that demonstrated real regeneration was done by Abraham Trembley, who in 1744 reported the ability of severed polyps to totally regenerate after resecting samples into different lengths and numbers of pieces. In 1817, Christian Pander proposed a critical relationship between cells and the microenvironment they inhabit (2). Around this same time, some of the earliest studies investigating skin graft transplantation were underway. Johann Friedrich Dieffenbach wrote a doctoral thesis entitled *Nonnulla de Regeneratione et Transplantatione* (meaning "some of regeneration and transplantation") that explored suitable skin grafts from various sources on birds and mammals. His work failed once he switched to the human system, but others who followed in his footsteps, including Heinrich Christian Bünger, Jaques Reverdin, and

Karl Thiersch, expounded on Dieffenbach's findings and helped us to better understand skin graft transplantation in humans (4).

In 1910, Ross Harrison was the first to accomplish *ex vivo* tissue growth. However, his discovery was furthered by Alexis Carrel, who designed a tissue culture system for expanding large numbers of *ex vivo* cells. This work is the foundation for modern tissue culture techniques today. Carrel continued to press on and worked with the famous aviator Charles Lindbergh to develop a perfusion pump (i.e. the Lindbergh Pump) that kept *ex vivo* tissue viable for 1-2 months after harvesting. This pump would become a monumental contribution to whole organ transplantation and open-heart surgery (2). Much of early tissue engineering was focused on facilitating tissue and organ transplantation. Due to limitations on sourcing, there arose a need for an alternative to patients waiting for tissues and organs to become available. This need led to the advent of modern tissue engineering.

Early modern tissue engineering history brings us into the mid-20th century, where Dr. James Till and colleagues discovered that there existed hematopoietic cells that could differentiate into various lineages in the spleen (16). These findings served as the introduction into stem cells and stem cell biology. Nearly concurrent with the discovery of stem cells, Judah Folkman at Harvard's Children's Hospital was making great strides in tissue differentiation and organization, and his most notable work in tumor angiogenesis. This had great bearing on our understanding of the vascularization of nearly all tissues. One of Judah Folkman's trainees would later go on to study the interplay between cells and stem cells and their response to mediators that would promote new tissue formation on engineered substrates. That trainee was Robert Langer, who in

collaboration with Joseph Vacanti from Massachusetts General Hospital published the seminal 1993 paper that first introduced the term "tissue engineering" (17). Interestingly, that was not the first time the term "tissue engineering" was used. A paper investigating the outcome of corneal prosthetics first published the term describing the importance of prosthetic integration with native tissue via the formation of a new, integrating membrane (18). However, the Langer and Vacanti paper popularized the term and established the paradigm for the field.

Tissue engineered therapies consist largely of some combination of these three elements:

1) Cells, whether progenitor/stem cells or fully differentiated, that will be the basis for the desired tissue
2) Growth factors or other mediators that help inform how tissue develops
3) Scaffolds or some structure that either provides the architecture for the desired tissue or is simply a delivery mechanism (17).

In addition to laying out the principles of tissue engineering, Vacanti later published a strikingly unforgettable example of how successful tissue engineering therapies can be when they employ some combination of the principles mentioned above. Briefly, a polyglycolyic acid polymer structure was designed in the shape of a 3-year-old patient's outer ear, the structure was then seeded with chondrocytes, and then implanted subcutaneously in athymic mice. In short, the implant produced new cartilage formation subcutaneously, maintained its structure throughout the implantation period, and closely resembled the histological properties of a native ear. This work produced what has now

been dubbed the “Vacanti mouse”, which is illustrated in Figure 1.2 (19). Ever since the Langer and Vacanti paper, scientists have been engineering therapies for nearly every major tissue imaginable. As new avenues are explored and new questions posed, new obstacles arise. One obstacle that is nearly a ubiquitous problem throughout all of tissue engineering and biomaterial design is overcoming the initial immune response and the subsequent inflammation becoming chronic. Therefore it is important to better understand the mediators present in response to initial tissue injury, the phases of wound healing, and what biomaterials should be doing in that context.

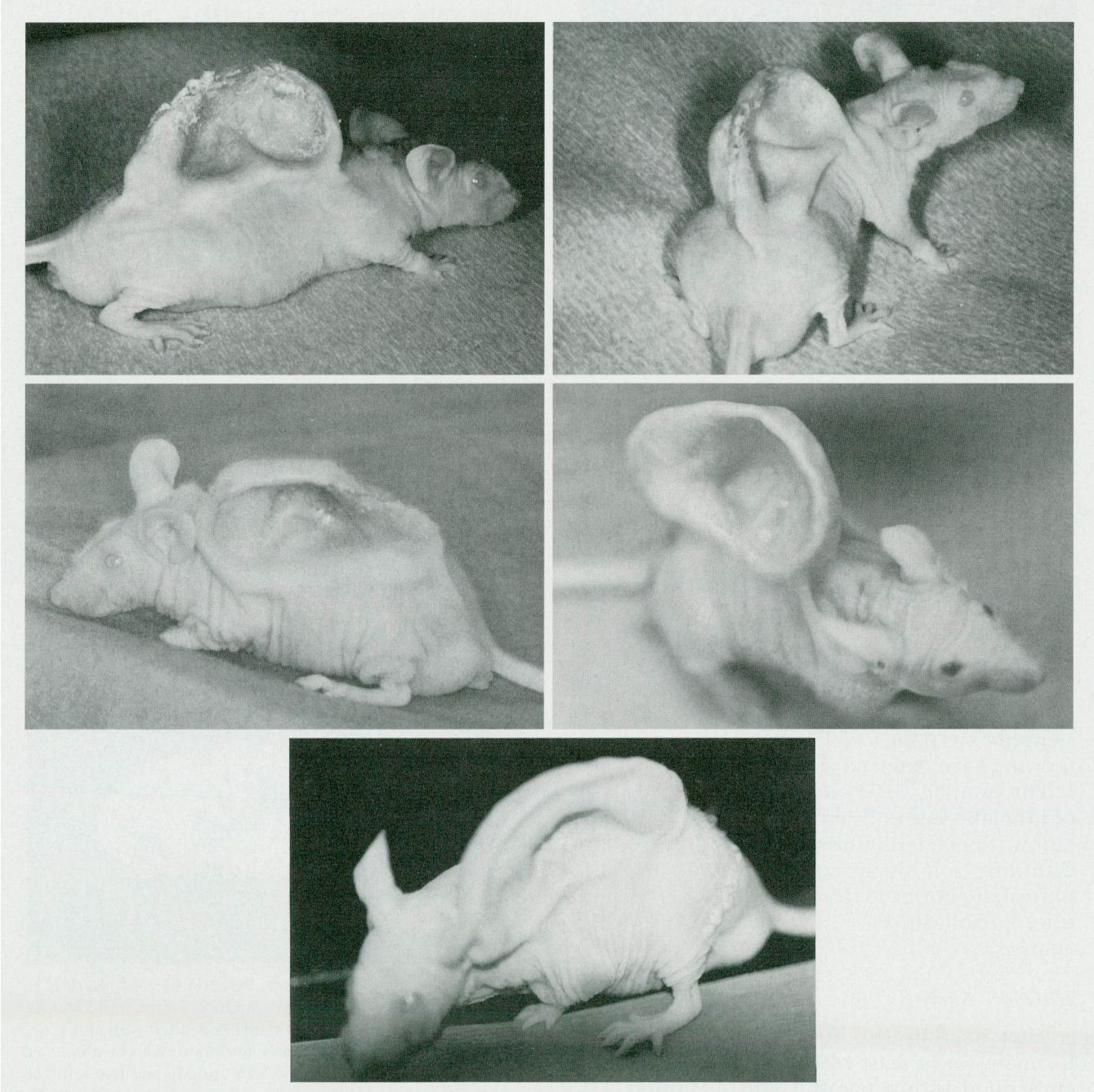

FIGURE 1.2 The "Vacanti mouse" (19) In this seminal study, synthetic polymer scaffolds were fabricated in the shape of the human outer ear, seeded with chondrocytes, and then implanted subcutaneously into athymic nude mice. This was a key study demonstrating the potential of tissue engineered therapies.

I.4 TISSUE INJURY AND RESPONSE TO BIOMATERIALS

In order to better understand how to improve healing, it is critical to understand what occurs during injury. The mediators that are released in response to tissue injury or are required for healing include factors unique to certain tissues, however, much of the steps that take place are common to many tissues, as displayed in Figure 1.3. In response to tissue damage or simply the implantation of a biomaterial, there are initial interactions with the blood that prompt protein adsorption to the surface of the implant. Next, platelet aggregation occurs causing coagulation and the formation of a provisional fibrin matrix. This matrix serves as an early endogenous scaffold that mediates cell migration as well as biochemical signals (20). The source of the biochemical signals present on the provisional matrix is platelets, which release the contents of their granules when aggregated. The contents of platelet granules consist of von Willebrand factor (vWf), transforming growth factor β-1 (TGF β-1), platelet derived growth factor (PDGF), fibronectin, vascular endothelial growth factor (VEGF), basic fibroblast growth factor (bFGF), stromal cell-derived factor-1α (SDF-1α), IL-10, monocyte chemotactic protein-1 (MCP-1), macrophage inflammatory protein-1 (MIP-1α), tumor necrosis factor (TNF), and IL-1β (21, 22). Simultaneous to the formation of a provisional matrix, tissue damage elicits the release of several different endogenous mediators in the tissue microenvironment (TME), which include, but are not limited to, IL-33, high mobility group box 1 (HMGB1), IL-1α, heat shock proteins (HSP), and reactive oxygen species. Exogenous signals include pathogen associated molecular patterns (PAMPs), such as lipopolysaccharide (LPS) (23). IL-33, HMGB1, IL-1α, and heat shock proteins (HSP)

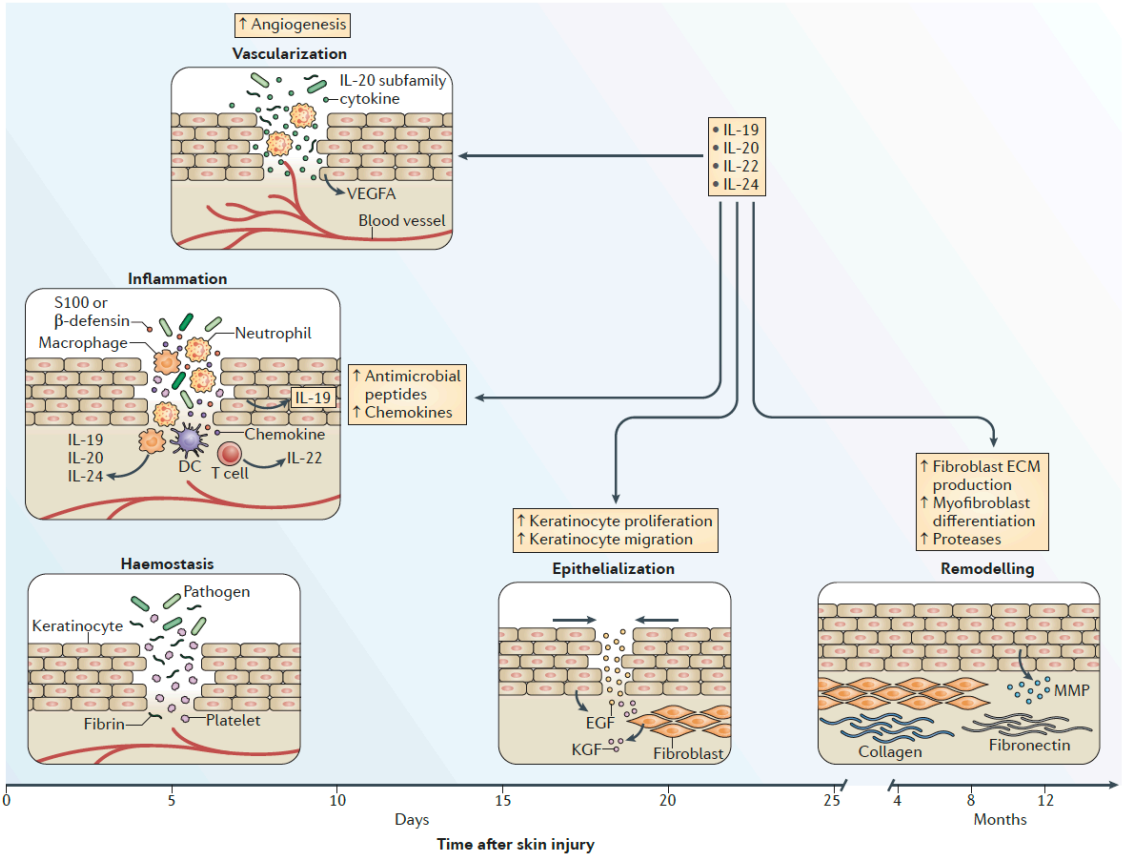

FIGURE 1.3 Tissue Injury and Wound Healing (24) The wound healing cascade is a spatio- and temporally-controlled process that includes early phases of hemostasis and recruitment of innate immune cells that dictate local inflammation. In response to factors released by platelets, macrophages, and mast cells, granulation tissue arises to revascularize and restructure the local environment. Controlled inflammation and ECM deposition promotes healing, whereas chronic inflammation and aberrant ECM deposition leads to poor healing and scarring.

serve as alarmins that signal the occurrence of tissue damage and prompt robust inflammatory signaling (25). The cells that respond to these newly present alarmins are tissue-resident innate immune cells, which chiefly consist of macrophages and mast cells. Macrophages and mast cells are innate immune cells that mature once they migrate into the peripheral tissue and carry out various functions. Macrophages play a significant role in responding to intracellular pathogens, microbial products, and perform phagocytosis. Mast cells are critical sentinel cells that respond to parasitic infections and are critical in atopic disease. While distinct in those various functions, both cell populations respond to damage signals. In response to the milieu of factors now present, tissue-resident innate immune cells release a myriad of inflammatory factors.

It is important to take a moment and acknowledge how macrophages and mast cells respond to these different stimuli. Upon activation, macrophages can commit to a polarized state, either M1 or M2. The anti-inflammatory M2 phenotype, which was traditionally defined by their IL-4 and IL-13 induction (now referred to as M2a), has recently been further expanded to include more subsets, depending on the stimulus. The other stimuli that can prompt one of the M2 subsets (i.e. M2b, M2c, or M2d) are IL-10, glucocorticoids, immune complexes, TGFβ-1, and IL-6. The inflammatory M1 phenotype is triggered in the presence of TNF, lipopolysaccharide (LPS), or interferon-γ (IFNγ). Figure 1.4 illustrates the different macrophage phenotypes, what initiates their polarization, and the factors they produce. Many of these polarizing signals become present shortly after tissue injury or biomaterial implantation. It is important to note that macrophages do not permanently commit to one of the polarized states, and that the local macrophage population does not homogenously commit to one polarization. More

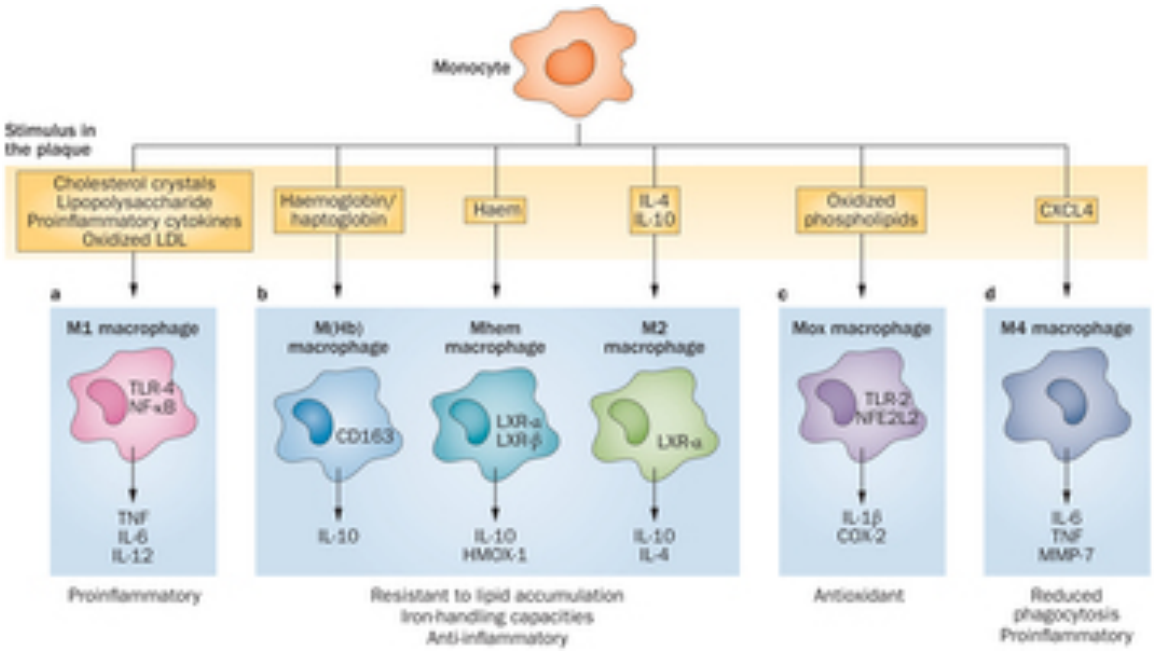

FIGURE 1.4 Macrophage polarization (26) Naïve macrophages undergo polarization depending on the factors present in the local microenvironment. Macrophage polarization is both plastic and exists on a spectrum, where each phenotype plays a key role in various context and pathologies. While the human system is not totally analogous to murine macrophage polarization, the key phenotypes of M2 macrophages being anti-inflammatory and M1 macrophages being pro-inflammatory holds true.

inflammatory conditions will promote more M1 macrophages, and conditions that are resolving inflammation and promoting repair will have a greater M2 macrophage presence. Interventions should be focused on changing the balance of macrophage polarization (26). While our work is not focused on determining macrophage responsiveness and polarization, this process is critically important for tissue homeostasis and resolving inflammation (27, 28). Interestingly, the alarmins and mediators released during hemostasis can trigger some of these macrophage-polarizing factors to be released via mast cell activation.

Previous work has demonstrated that a key mast cell activating agent in the context of cell injury is IL-33 (23). It was not until 2005 that the receptor for IL-33 was discovered to be ST2, before which ST2 was referred to as an orphan receptor (29). Despite the fairly recent pairing of IL-33 and ST2, there has been study of IL-33 activation in mast cells. In response to IL-33 ST2 signal transduction elicits release of various pro-inflammatory cytokines, chemokines, and eicosanoids (30). The IL-33 signaling pathway is illustrated in Figure 1.5. IL-33 also promotes mast cell survival, adhesion, and maturation (31-34). Prior to pairing IL-33 with ST2, it was previously referred to as nuclear factor-high endothelial venules and is largely expressed at the protein level in the nucleus of structural cell populations, such as endothelial cells, epithelial cells, fibroblasts, keratinocytes, and airway smooth muscle cells (34). While in the nucleus, IL-33 has surprisingly been shown to be capable of suppressing inflammatory signaling by hindering NF-κB-mediated transcription (35). Despite that anti-inflammatory role, the ability of IL-33 to activate mast cells elicits a strong pro-

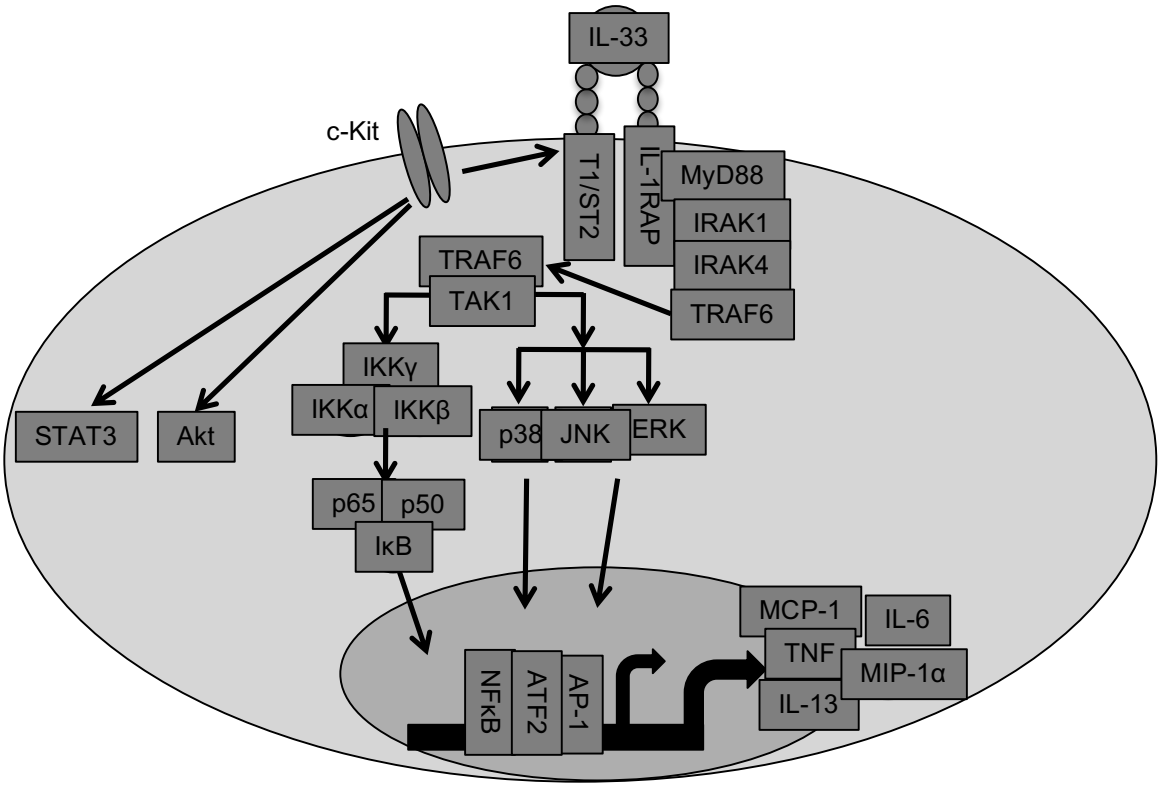

FIGURE 1.5 IL-33 Signaling Pathway in mast cells IL-33 binds to its receptor, ST2, and as a member of the IL-1 family, it's receptor co-associates with IL-1Rap (IL-1 receptor-associated protein. Additionally, ST2 and IL-1Rap co-associate with c-Kit to form a complex upon IL-33 binding ST2, leading to signaling events downstream of c-Kit that have been shown to be critical for IL-33 signaling. IL-33 activation leads to downstream phosphorylation of MAPK and NF-ϰB, leading to transcription and production of inflammatory cytokines and chemokines.

inflammatory response. Mast cell activation by IL-33 has also been shown to promote TNF-mediated neutrophil recruitment (36).

After the responses of tissue-resident cells, neutrophils are among the first cell populations recruited to the injury or implanted biomaterial. Their role as currently understood involves clearing debris, releasing matrix metalloproteinases (MMP) and inflammatory reactive oxygen species (ROS), and releasing chemoattractants that mediate the recruitment of other cells (20). Among the cells that neutrophils recruit are more macrophages that can be polarized to M1 or M2 phenotypes. As macrophages, neutrophils, and mast cells secrete factors altering innate immune cell recruitment, their response, coupled with platelet activation also promotes fibroblast and endothelial cell recruitment. As the proteases that have been released clear space for cell recruitment, fibroblasts begin laying down new collagen while endothelial cells strive to revascularize the area, creating granulation tissue (20, 37).

It is at this point that two divergent fates emerge. The favorable fate consists of sufficient vascularization of the local microenvironment, implant integration with the local tissue, deposition of new ECM proteins that resemble the native tissue, and production of the necessary factors unique to that tissue for *de novo* functional tissue formation. The pathological fate, which is the case for many implanted biomaterials, consists of aberrant collagen deposition and myofibroblast differentiation, indicative of a fibrotic response. Next, the inability of macrophages to engulf the material can lead to "frustrated phagocytosis", where macrophages begin to fuse together to form multinucleated foreign body giant cells (FBGCs) (38). FBGC development and aberrant collagen production culminate into a collagenous fibrotic capsule closing off the implant

from surrounding tissue, rendering it ineffective and unable to perform the intended function. This foreign body response is of great concern to biomaterial design and requires novel approaches. Recent work has shown that biomaterials implanted into mast cell-deficient animals were subjected to a more severe foreign body response than the wild type mouse, indicating a role for mast cells to be explored in addressing this pathology (39). There is a need to better understand how early signals from mast cells can control inflammation to prevent chronic inflammation and fibrosis. More specifically, based on the work showing that IL-33 is the primary activating mediator of mast cells during cell injury, more work needs to be done investigating how IL-33 activation of mast cells can be modulated in response to biomaterials and their various features.

CHAPTER II: ALTERED STRUCTURE OF ELECTROSPUN SCAFFOLDS PROMOTES DIFFERENT PHENOTYPES OF INNATE IMMUNE CELLS

II.1 ABSTRACT

Implanted scaffolds often induce inflammation that frequently leads to the foreign body response (FBR), fibrosis, and the failure of the scaffold. Thus, it is important to evaluate how cells interact with the scaffolds to promote a more regenerative response. Our group has recently demonstrated that macrophage phenotype can be modulated by the fiber diameter and pore size of an electrospun scaffold. However, it is critical to determine how to modulate the response of other tissue resident innate immune cells. Mast cells are inflammatory sentinels that degranulate and orchestrate the fate of other cell populations, such as monocytes/macrophages and lymphocytes. Mast cells have also been reported to play a vital role in the FBR of implanted biomaterials as well as angiogenesis (39-47). The goal of this study was to determine how to modulate mast cell responses to electrospun scaffolds of varying fiber diameter and porosity in order to promote anti-inflammatory and regenerative cell-scaffold interactions. Murine bone marrow-derived mast cells (BMMC) were cultured on 10mm disks composed of electrospun polydioxanone (PDO) scaffolds. Scaffolds were either made from a 60 mg/mL polydioxanone solution, which yielded a scaffold with a pore diameter of 1.5 μm and fiber diameter of 400 nm, or a 140 mg/mL polydioxanone solution, which yielded a scaffold with a pore diameter of 18 μm and fiber diameter of 2.4 μm. Scaffolds were coated with fibronectin to promote mast cell adhesion and incubated with mast cells for 48 hours, followed by IL-33- or LPS-mediated activation. Relative to the 60 mg/mL scaffold, the 140 mg/mL scaffold promoted significantly less inflammatory cytokines to be released, while enhancing VEGF secretion. This corroborates the previous findings with macrophages, showing that altering scaffold structure alone is capable of altering

innate immune cell interactions. The changes in cytokine levels were also present at the mRNA level as well. When pore size was increased on the 60 mg/mL scaffold using an air-flow mandrel, inflammatory cytokine production went down. Surprisingly, decreasing the pore size of the 140 mg/mL scaffold only partially elevated inflammatory cytokine production, indicating a possible role for fiber diameter in addition to pore size in altering innate immune cell interactions. All together, this demonstrates that LPS- and IL-33-mediated mast cell responses to electrospun scaffolds can be modulated by altering scaffold architecture.

II.2 INTRODUCTION

Biomaterials are characterized as materials engineered for therapeutic or diagnostic purposes by interacting with living organisms (20). For any implanted biomaterial, an important limitation to consider is the immune response and how to mitigate inflammation. Upon implantation, a cascade of events is initiated that often leads to unresolved inflammation, frustrated phagocytosis, and macrophage fusion to form foreign body giant cells. This leads to fibrosis, with the biomaterial being encapsulated with a fibrotic capsule. This outcome contributes to implant failure and persistent pain among patients (38, 48-51). However, the mechanism by which the immune response can be modulated by polymer scaffold design has yet to be fully determined. Innate immune cells are understood to determine the fate of implanted biomaterials (52). Of innate immune cells, two key tissue-resident populations are macrophages and mast cells.

Macrophages are a heterogeneous cell population that plays a major role in innate immunity. Their inactive phenotype (MØ) is converted to a pro-inflammatory (M1) or an

angiogenic/regenerative phenotype (M2) by the microenvironment, with great plasticity (53). Macrophages originate in the bone marrow from the common myeloid progenitor cell, and mature until exiting the marrow as a blood monocyte. Monocytes differentiate to their mature macrophage form upon entering tissues (54). Macrophages are crucial for tissue homeostasis, pathogen clearance, inflammation resolution, angiogenesis, and wound healing (55). Their role as a key phagocytic cell is part of why macrophages play an important part in implant fate. As a phagocyte, macrophages engulf cellular debris during implant-induced tissue remodeling, and directly interact with the implant. The regenerative capacity of a scaffold can be dictated by macrophage phenotype and activity (growth factor/cytokine secretion), especially the ability to promote macrophage-mediated angiogenesis/tissue regeneration (49). Macrophages can also be influenced by the response to an implant from other tissue resident immune cells, such as the mast cell.

Mast cells are another innate immune cell that have been shown to play an essential role in wound healing, inflammation, angiogenesis, tissue remodeling, and the foreign body response (56). Similar to macrophages, mast cells originate in the bone marrow from the common myeloid progenitor, move to the vasculature as a mast cell progenitor, and fully mature in the tissue. Mast cells are widely present throughout the body and have been extensively studied in the context of allergic disease (57, 58). However, recent findings have expanded the importance of mast cells in other contexts, including vascularization (47). When angiogenesis occurs during remodeling, it is preceded or accompanied by macrophage and neutrophil influx that has been shown to be mast cell-mediated (59). Once activated, mast cells produce myriad factors, including transforming growth factor (TGF-β1), fibroblast growth factors (FGF-1 and FGF-2),

interleukin-8 (IL-8), and vascular endothelial growth factor (VEGF) (60). Since mast cells and macrophages clearly play a pivotal role in inflammatory and remodeling/wound healing responses, scaffolds should be engineered to modulate their behavior. Biomaterial implants designed to suppress inflammation and promote wound healing will have a greater capacity for regeneration, yielding improved vascular prosthetics.

One hypothesized way of controlling innate immune cell responses to electrospun scaffolds is to alter the architecture of the implant. There has been considerable work exploring how altering scaffold pore size can influence implant function and success (48). Altering pore size in engineered structures can influence both angiogenesis and macrophage polarization (61). Additionally, scaffold fiber diameter changes affect inflammatory cytokine production (62). Our group has previously published that increasing scaffold pore size and fiber diameter promotes macrophage M2 polarization (38). While the findings with macrophages are important and will help improve biomaterial design, macrophages are not the only immune cell population that need to be studied in relation to scaffold interactions. Very little work has assessed how mast cells respond to scaffolds, despite the important role mast cells play in inflammation, wound healing, and angiogenesis (46, 63, 64). This next chapter describes studies investigating how scaffold structure can alter mast cell responses. Mouse bone marrow-derived mast cells (BMMC) were cultured on scaffolds of varying morphologies and activated with either LPS or IL-33, to mimic mediators present during tissue damage.

II.3 MATERIALS AND METHODS

II.3.1 Electrospinning

Electrospinning was used to create fibrous scaffolds of various morphologies made from polydioxanone (Ethicon Inc.). Polydioxanone was dissolved in 1,1,1,3,3,3, Hexafluoro-2-isopropanol (HFP) at either 60 or 140 mg/mL in a scintillation vial. The polymer solutions were then aspirated into Becton Dickinson 5mL syringes with 18 gauge blunt tip needles. The syringe was then loaded into a KDS 100 Legacy Syringe Pump (KD Scientific) and the polymer solution was dispensed at a 6 mL/hr. Polymer solutions were electrospun across a gap distance of 12 cm onto stainless steel rotating rectangular mandrels (0.5 cm x 3 cm 1.5 cm) or onto a perforated air-flow mandrel with an inlet pressure of 50 kPa. All scaffolds were electrospun with an applied voltage of 25kV and mandrels rotating at a speed of 400 rpm. After electrospinning, scaffold samples were imaged using a JEOL JSM-5610LV scanning electron microscope. Scanning electron micrographs were analyzed to measure fiber diameter and pore diameter using ImageJ.

II.3.2 Reagents

Recombinant mouse IL-3, SCF, and IL-33, as well as mouse IL-6, TNF, and MCP-1 (CCL-2) ELISA kits were purchased from BioLegend (San Diego, CA). Mouse MIP-1α (CCL-3) and VEGF ELISA kits were purchased from PeproTech (Rocky Hill, NJ). Lipopolysaccharide (LPS) from Escherichia coli 055:B5 was purchased from Sigma-Aldrich (cat no. L4524, St. Louis, MO).

II.3.3 Cell culture and cell seeding

Following electrospinning, 10mm disks were produced using biopsy punches and disinfected by soaking in 70% ethanol for 15 minutes and washing twice with 1X PBS. To promote mast adhesion, scaffold disks were incubated in fibronectin at 50 μg/mL for 1 hour at 37°C. After incubation, scaffolds were moved to a new well to avoid residual fibronectin. BMMC were developed by harvesting bone marrow from the tibias and femurs of euthanized C57BL/6 mice. Following harvesting, bone marrow was cultured for 3 weeks in complete RPMI (cRPMI) 1640 medium (Invitrogen Life Technologies, Carlsbad, CA) containing 10% FBS, 2mM L-glutamine, 100 U/ml penicillin, 100 μg/ml streptomycin, 1mM sodium pyruvate, and 1mM HEPES (all from Corning, Corning, NY), supplemented with IL-3-containing supernatant from WEHI-3B cells and SCF-containing supernatant from BHK-MKL cells. The final concentrations of IL-3 and SCF were adjusted to 1.5ng/ml and 15ng/ml, respectively, as measured by ELISA. BMMC were used after 3 weeks of culture, at which point these primary populations were >90% mast cells, based on staining for c-Kit and FcεRI expression. BMMC were seeded at $1x10^6$/mL on fibronectin-coated scaffolds with a cloning ring to concentrate the cells on the scaffold in cRPMI with IL-3 and SCF at 10 ng/mL. After 48-hour incubation on fibronectin-coated scaffolds, IL-33 (100 ng/mL) or LPS (1 μg/mL) was added to activate cells.

II.3.4 qPCR

BMMC were seeded on scaffolds and activated with 100 ng/mL of IL-33 for 6 hours. Scaffolds were then placed in TRIzol reagent (Life Technologies, Grand Island, NY) to extract RNA, which was measured using a Thermo Scientific NanoDrop 1000 UV-vis

Spectrophotometer (Thermo Scientific, Watham, MA). cDNA was produced using qScript cDNA Synthesis Kit from Quanta Biosciences (Gaithersburg, MD), and amplified using PerfeCTa SYBR Green SuperMix (QuantaBio, Gaithersburg, MD) on the Bio Rad CFX96 Touch™ Real-Time PCR Detection System (Bio-Rad, Hercules, CA). The following primers were used: IL-6 forward, 5'-TCCAGTTGCCTTCTTGGGAC-3'; IL-6 reverse, 5'-TCCAGTTGCCTTCTTGGGAC-3'; TNF forward, 5'-AGCACAGAAAGCATCATCCGC-3'; TNF reverse, 5'-TGCCACAAGCAGGAATGAGAAG- 3'; VEGF forward, 5'-GAGGATGTCCTCACTCGGATG-3'; VEGF reverse, 5'-GTCGTGTTTCTGGAAGTGAGCAA-3'; MMP-9 forward, 5'-GCCCTGGAACTCACACGACA-3'; MMP-9 reverse, 5'-TTGGAAACTCACACGCCAGAAG-3'; TGFβ-1 forward, 5'-GTGTGGAGCAACATGTGGAACTCTA-3'; TGFβ-1 reverse, 5'-TTGGTTCAGCCACTGCCGTA-3'; FGF-2 forward, 5'-CCAACCGGTACCTTGCTATG-3'; FGF-2 reverse, 5'-TATGGCCTTCTGTCCAGGTC-3'; β-actin forward, 5'-GATGACGATATCGCTGCGC-3'; β-actin reverse, 5'-CTCGTCACCCACATAGGAGTC-3'.

All primers were purchased from Eurofins MWG Operon (Huntsville, AL).

II.3.5 Statistical Analysis

Data are presented as mean ± SE and analyzed using GraphPad Prism 6 software (GraphPad, La Jolla, CA). Comparisons between two groups were done using unpaired

Student's *t* test and comparisons between multiple groups were done using one-way analysis of variance with Tukey's post-hoc test. All p values <0.05 were deemed significant.

II.4 RESULTS

II.4.1 Fabrication of Electrospun Scaffolds

We first sought to demonstrate the ability to create electrospun scaffolds with varying geometries. Previous work has shown that altering polymer concentration is a feasible approach to changing the architecture of electrospun scaffolds. Therefore we generated electrospun scaffolds with the lowest and highest polymer concentrations possible, using 60 mg/mL and 140 mg/mL of polydioxanone. Polymer concentrations of polydioxanone below 60 mg/mL led to uneven dispersal at the needle tip and failed to produce a usable scaffold. Additionally, concentrations above 140 mg/mL were too viscous to consistently electrospun scaffolds. Figure 2.1 features electron micrographs of electrospun polydioxanone scaffolds from 60 and 140 mg/mL polymer solutions. 60 mg/mL scaffolds featured fibers with a diameter of 400nm and pores with an approximate diameter of 1.5μm, while 140 mg/mL scaffolds contained fibers with a diameter of 2.4μm and pores with a diameter of 18μm. These large variations permitted us to examine how scaffolds architecture alters mast cell inflammatory responses.

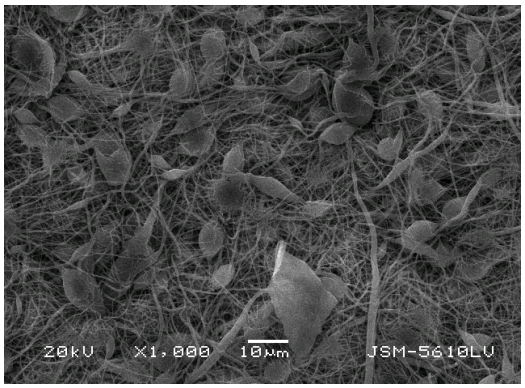

Polydioxanone 60mg/mL

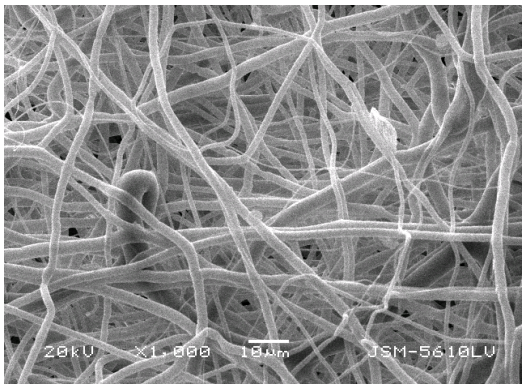

Polydioxanone 140 mg/mL

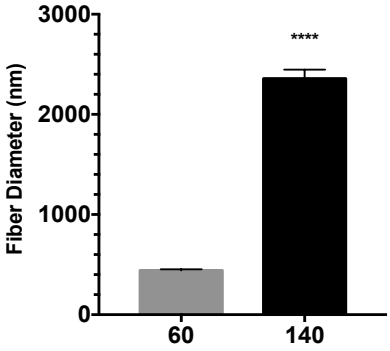

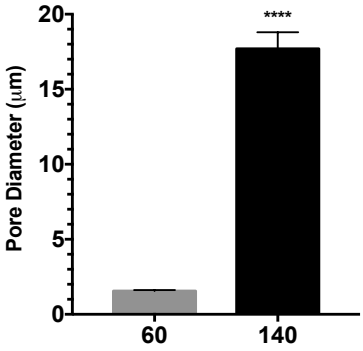

FIGURE 2.1 Electrospun polydioxanone scaffolds Polydioxanone scaffolds of different polymer concentrations were electrospun, yielding scaffolds of different morphologies, as confirmed by scanning electrospun microscopy. Electron micrograpahs were used to characterize fiber and pore diameters of the electrospun scaffolds. . *, p<0.05; **, p<0.01; ***, p<0.001; ****, p<0.0001; NS, not significant.

II.4.2 Altered Mast Cell Cytokine Production on Scaffolds of Varying Morphologies

Over the last decade, studies of macrophage responses, including our own, have shown scaffold capacity to modulate inflammation, promote angiogenesis, and control tissue remodeling (38, 65-67). The ethos of tissue engineering and regenerative medicine over the last decade has largely been that if implants or therapies can elicit an M2 phenotype from macrophages, then the fate of the implant or therapy will be favorable (68). There is certainly credibility to that outlook, since macrophages are a critical tissue-resident population of innate immune cells present throughout the body. Even though macrophages in various tissues bear different names (e.g. Kuppfer cells, Langerhans cells, osteoclasts, and microglia), macrophages are nonetheless nearly ubiquitously present. However, they do not exist or operate independently of other tissue-resident innate immune cells. Therefore, there is a need to explore the role and responses of other innate immune cells in regard to tissue engineering therapies.

Our group has shown that mast cells adhere to fibronectin-coated polydioxanone scaffolds (69). Additionally, mast cells are not activated by the scaffold architecture alone, allowing us to test various stimuli. In the context of tissue damage, IL-33 and LPS, endogenous and exogenous cell injury signals respectively (23), should be abundant. Therefore, we examined how fibronectin-coated scaffolds with varying morphologies altered IL-33- and LPS-mediated mast cell cytokine production.

After electrospinning, 10mm diameter segments of scaffolds were coated with fibronectin and held in place with 8mm cloning rings to help concentrate cells onto the membrane. BMMC were seeded and 48 hours later subsequently activated with IL-33, LPS, or neither. Supernatants were collected after 16 hours and analyzed via ELISA.

Figure 2.2 shows that in response to IL-33 or LPS, mast cells on 140 mg/mL scaffolds secreted less IL-6 than cells cultured on 60mg/ml membranes. This was also true of TNF secretion but only in response to IL-33 activation. This demonstrated that altering scaffold structure is able to suppress IL-33- and LPS-mediated inflammatory cytokine secretion. Moreover, this effect appears to be selective, since chemokine production was unchanged by scaffold structure (Figure 2.3). Moreover, VEGF secretion was significantly enhanced among IL-33-stimulated BMMC on 140 mg/mL scaffolds (Figure 2.4). All together, these data demonstrate that relative to 60 mg/mL scaffolds, the 140 mg/mL scaffolds, which have larger fiber and pore diameters, reduce inflammatory cytokines and enhance pro-angiogenic cytokines. This indicates that our group's earlier findings of altered macrophage phenotype on scaffolds has a parallel in the mast cell response (38).

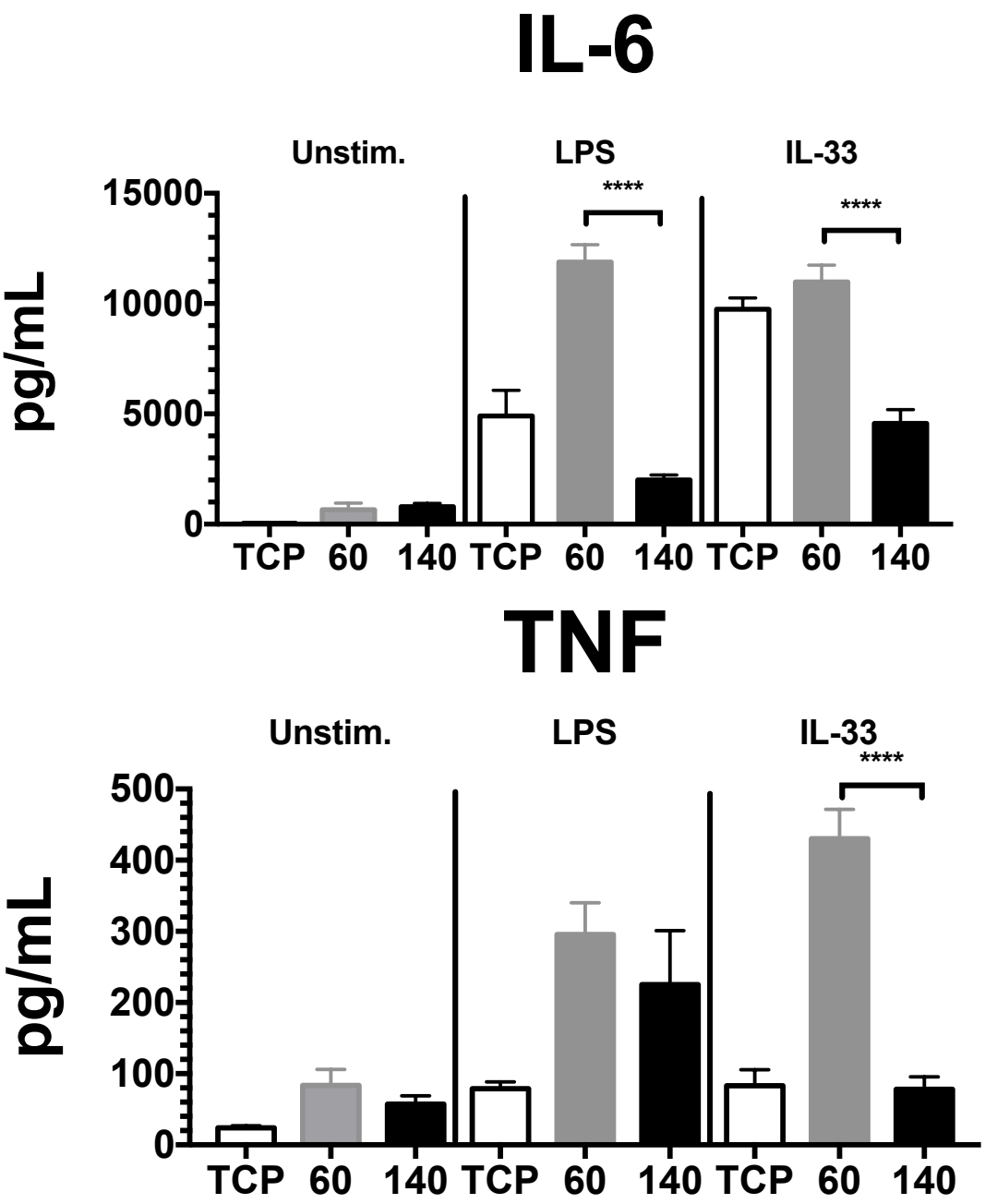

FIGURE 2.2 Mast cell IL-6 and TNF production is altered on scaffolds of different morphologies BMMC were seeded on fibronectin-coated electrospun scaffolds for 48 hours and then activated with LPS (1 μg/mL) or IL-33 (100 ng/mL). Supernatants were collected 16 hours later and analyzed via ELISA for IL-6 and TNF. Results are presented as mean ± SEM. Figures are 3 indpendent experiments conducted in triplicate. . *, p<0.05; **, p<0.01; ***, p<0.001; ****, p<0.0001; NS, not significant.

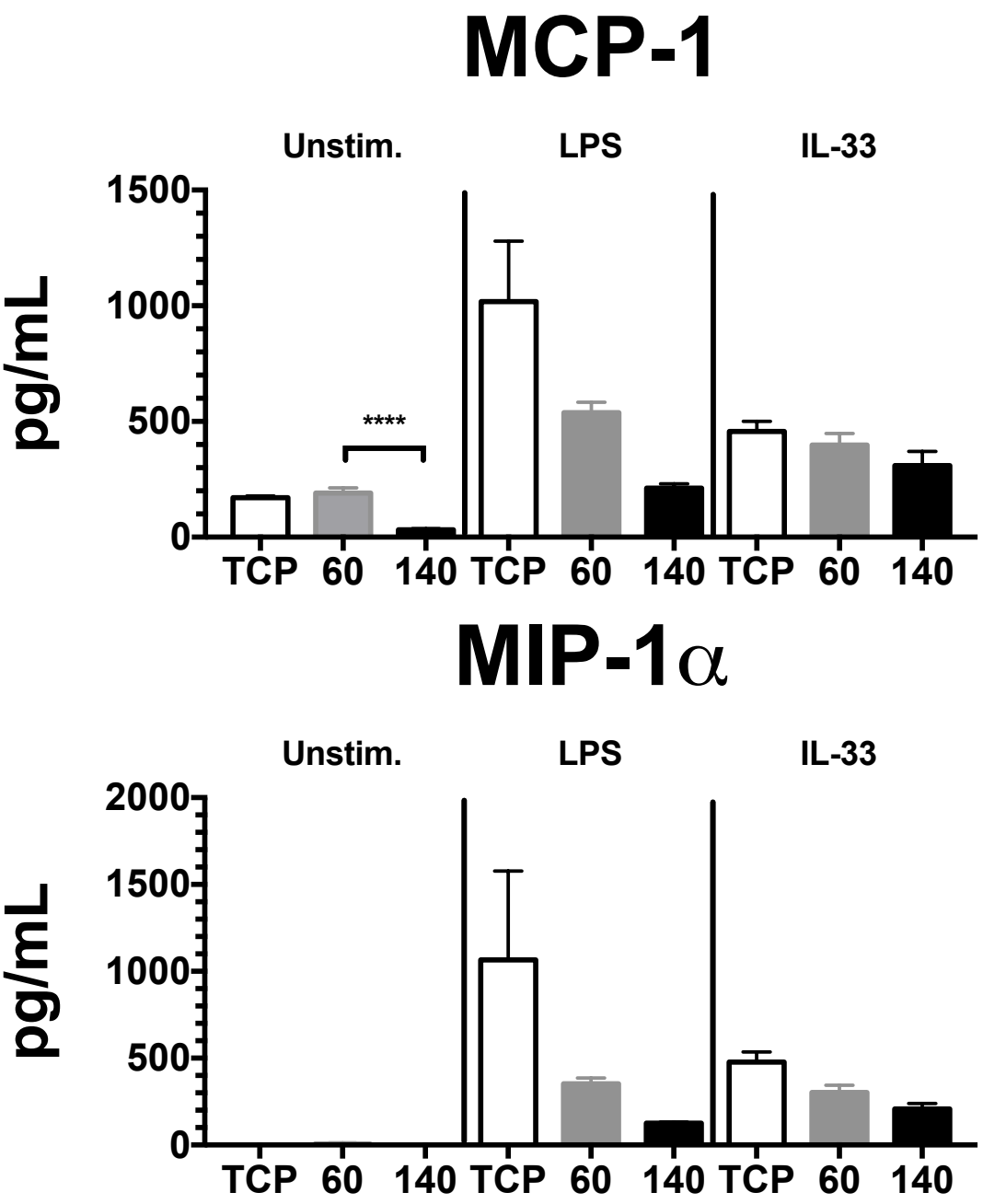

FIGURE 2.3 Mast cell MCP-1 and MIP-1α production is altered on scaffolds of different morphologies BMMC were seeded on fibronectin-coated electrospun scaffolds for 48 hours and then activated with LPS (1 μg/mL) or IL-33 (100 ng/mL). Supernatants were collected 16 hours later and analyzed via ELISA for MCP-1 and MIP-1α. Results are presented as mean ± SEM. Figures are 3 indpendent experiments conducted in triplicate. . *, $p<0.05$; **, $p<0.01$; ***, $p<0.001$; ****, $p<0.0001$; NS, not significant.

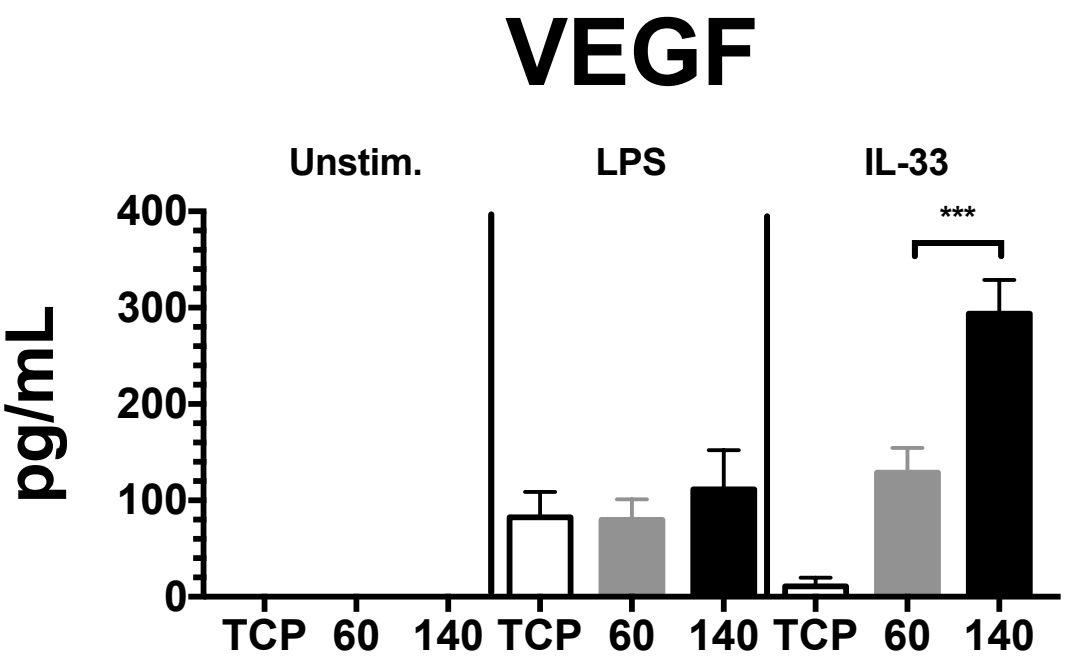

FIGURE 2.4 Mast cell VEGF production is altered on scaffolds of different morphologies BMMC were seeded on fibronectin-coated electrospun scaffolds for 48 hours and then activated with LPS (1 μg/mL) or IL-33 (100 ng/mL). Supernatants were collected 16 hours later and analyzed via ELISA for VEGF. Results are presented as mean ± SEM. Figures are 3 indpendent experiments conducted in triplicate. . *, $p<0.05$; **, $p<0.01$; ***, $p<0.001$; ****, $p<0.0001$; NS, not significant.

II.4.3 Scaffold Morphology Alters Mast Cell Cytokine mRNA Expression

While Figure 2.2 demonstrated a trend among cytokines that matched a phenotype described in earlier work, there was a variable that needed to be addressed. The scaffolds were coated with fibronectin, which contains a growth factor-binding domain (70). It is possible that the changes in cytokine detection could be attributed to sequestration at the scaffold surface via fibronectin binding. Therefore, cytokines mRNAs were measured. BMMC were seeded on fibronectin-coated 60 and 140 mg/mL polydioxanone scaffolds. To streamline the work, BMMC were activated only with IL-33, due to consistent suppression of IL-33-mediated inflammatory cytokine secretion and enhancement of VEGF. As observed at the protein level, 140 mg/mL polydioxanone scaffolds enhanced IL-33-mediated expression of VEGF mRNA (Figure 2.5). Additionally, 140 mg/mL scaffolds significantly enhanced IL-33-mediated production of MMP-9 mRNA. MMP-9 has been shown to play a critical role in angiogenesis, which further confirms the pro-angiogenic mast cell phenotype promoted by the 140 mg/mL scaffold (71).

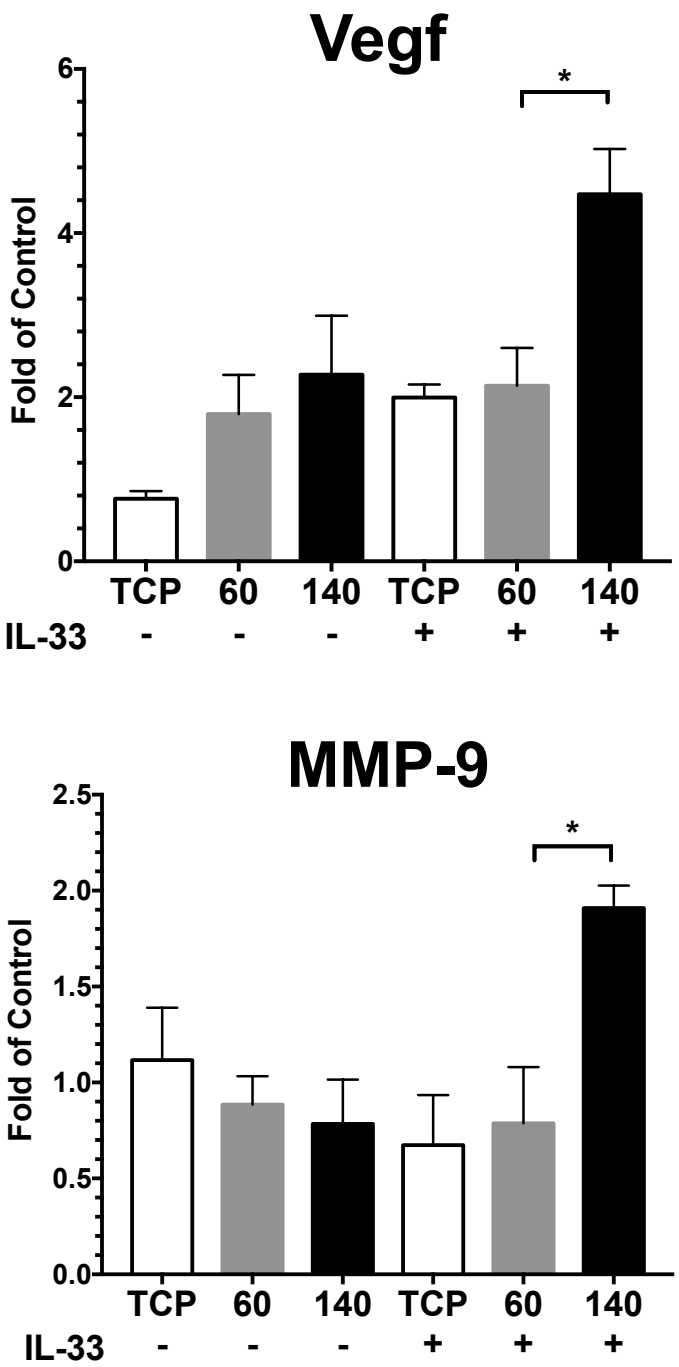

FIGURE 2.5 Mast cell cytokine and protease expression is altered on scaffolds of different morphologies at the mRNA level BMMC were seeded on fibronectin-coated electrospun scaffolds for 48 hours and then activated with IL-33 (100 ng/mL). RNA was harvested 3 hours later and analyzed via qPCR for VEGF and MMP-9. Results are presented as mean ± SEM. Figures are 2 indpendent experiments conducted in triplicate. . *, $p<0.05$; **, $p<0.01$; ***, $p<0.001$; ****, $p<0.0001$; NS, not significant.

II.4.4 Increased Pore Size of 60 mg/mL Polydioxanone Scaffolds

While 60 mg/mL and 140 mg/mL scaffolds elicit very different responses from mast cells, the two scaffolds are different in two ways, fiber diameter and pore size. Therefore these two variables need to be acknowledged and accounted for. It is feasible to create scaffolds with the same fiber diameters but different pore sizes. We first focused on the 60 mg/mL scaffold, attempting to generate a scaffold with the same small fiber diameter, but with increased pore sizes.

In 2012, Michael McClure and colleagues published a method for increasing electrospun scaffold pore size without changing fiber diameter (72). In place of the standard solid, closed-surfaced rotating mandrel, they fabricated a hollow mandrel with perforations throughout the surface. One end of the mandrel is connected to tubing that forces air through the perforations, generating regions with large pore sizes. The inlet pressure is entirely controllable, though the previous work done by McClure and colleagues determined that the optimal inlet pressure was 50 kPa. When the inlet pressure is at between 50 and 100 kPa, there is increased scaffold pore size and permeability. However, as the inlet pressure exceeds 100 kPa, the pressurized air striking the closed end of the mandrel causes a balloon-like structure to form at that end of the mandrel. Therefore, we used 50 kPa as our inlet pressure. While the areas directly above the perforations have larger pore sizes, the pore sizes throughout the structure are larger as well. Therefore, we employed this method to create 60 mg/mL scaffolds with larger pore sizes but the same fiber diameters as a 60 mg/mL scaffold electrospun onto a solid mandrel.

Figures 2.6A and 2.6B show electron micrographs of 60 mg/mL scaffolds electrospun onto solid mandrel (60) and air-flow mandrels (60AF). The images illustrate the differences in their respective morphologies, which was quantified in Figure 2.6C. Additionally, Figure 2.6B shows images of the air-flow mandrel and a low magnification electron micrograph of the regions with larger pore sizes. Figure 2.6C shows that the 60 mg/mL scaffold electrospun onto the air-flow mandrel contains significantly larger pore sizes, approximately 4 μm in diameter compared to 1.5 μm in diameter for the 60 mg/mL scaffold from the solid mandrel. However, there is no difference in fiber diameter between the two scaffolds. Therefore, differences observed in mast cell responses to the two scaffolds can be attributed to their different pore sizes.

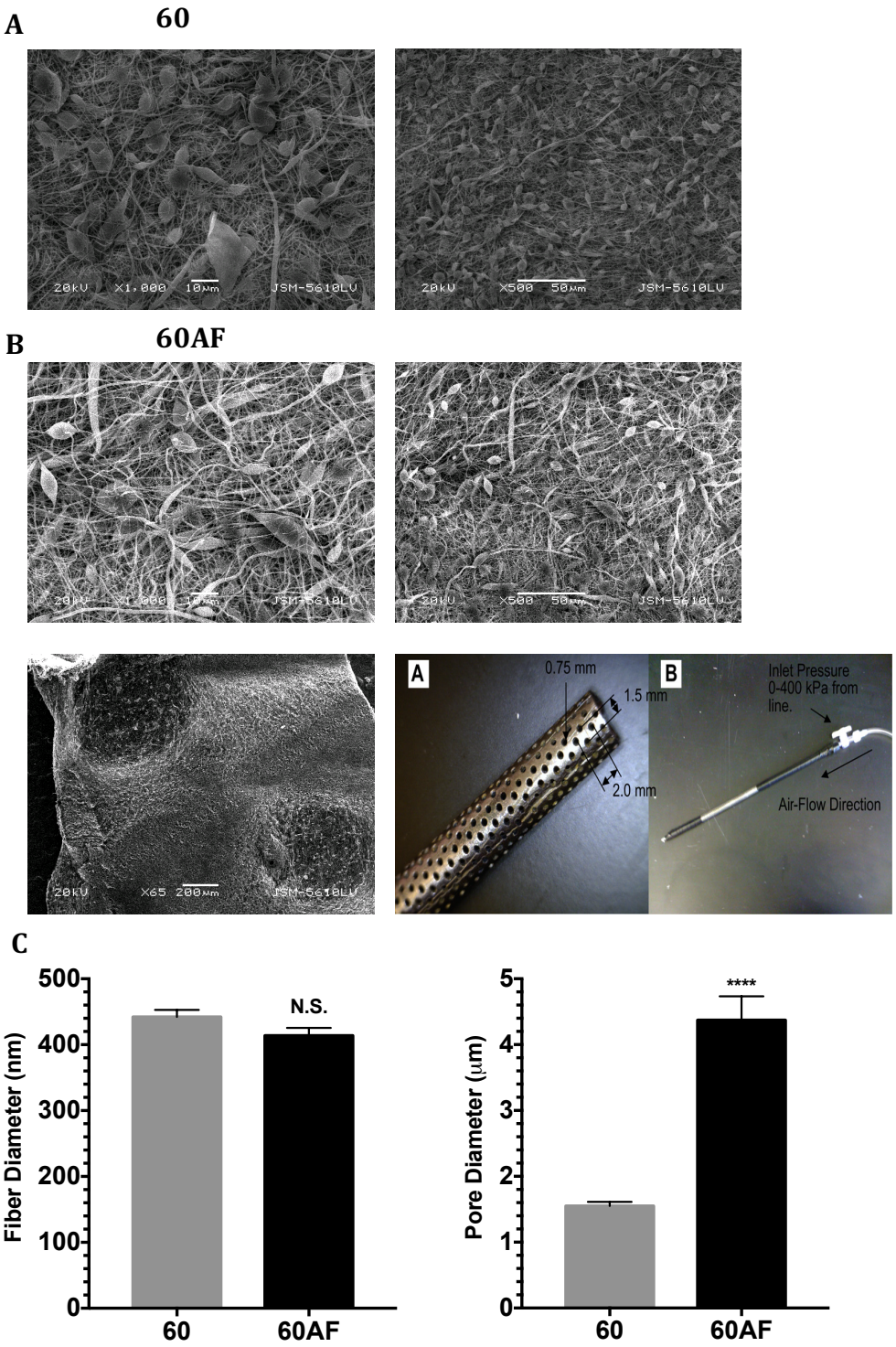

FIGURE 2.6 Increasing pore size of 60 mg/mL electrospun scaffolds. Electron micrographs of 60 mg/mL polydioxanone scaffolds electrospun on A) a solid mandrel and B) air-flow mandrel. B) also features an image of the air-flow mandrel (72). C) Fiber and Pore diameter were measured using ImageJ to analyze scaffold morphology. *, p<0.05; **, p<0.01; ***, p<0.001; ****, p<0.0001; NS, not significant.

II.4.5 Altered Mast Cell Cytokine Secretion on 60 vs 60AF Scaffolds

In order to determine if increasing scaffold pore size alone alters mast cell cytokine secretion, mast cells were seeded on 60 mg/mL scaffolds from the solid mandrel and the air-flow mandrel. Similar to before, BMMC were seeded onto fibronectin-coated scaffolds and activated with IL-33, LPS, or neither. 16 hours later, supernatants were collected and analyzed via ELISA. Figure 2.7 shows that scaffolds from the air-flow mandrel with larger pore sizes were able to significantly reduce IL-6 and TNF secretion from BMMC activated with IL-33 or LPS, compared to the scaffolds from the solid mandrel. This demonstrates that even between scaffolds with the same fiber diameter, changing pore size can greatly alter inflammatory cytokine secretion.

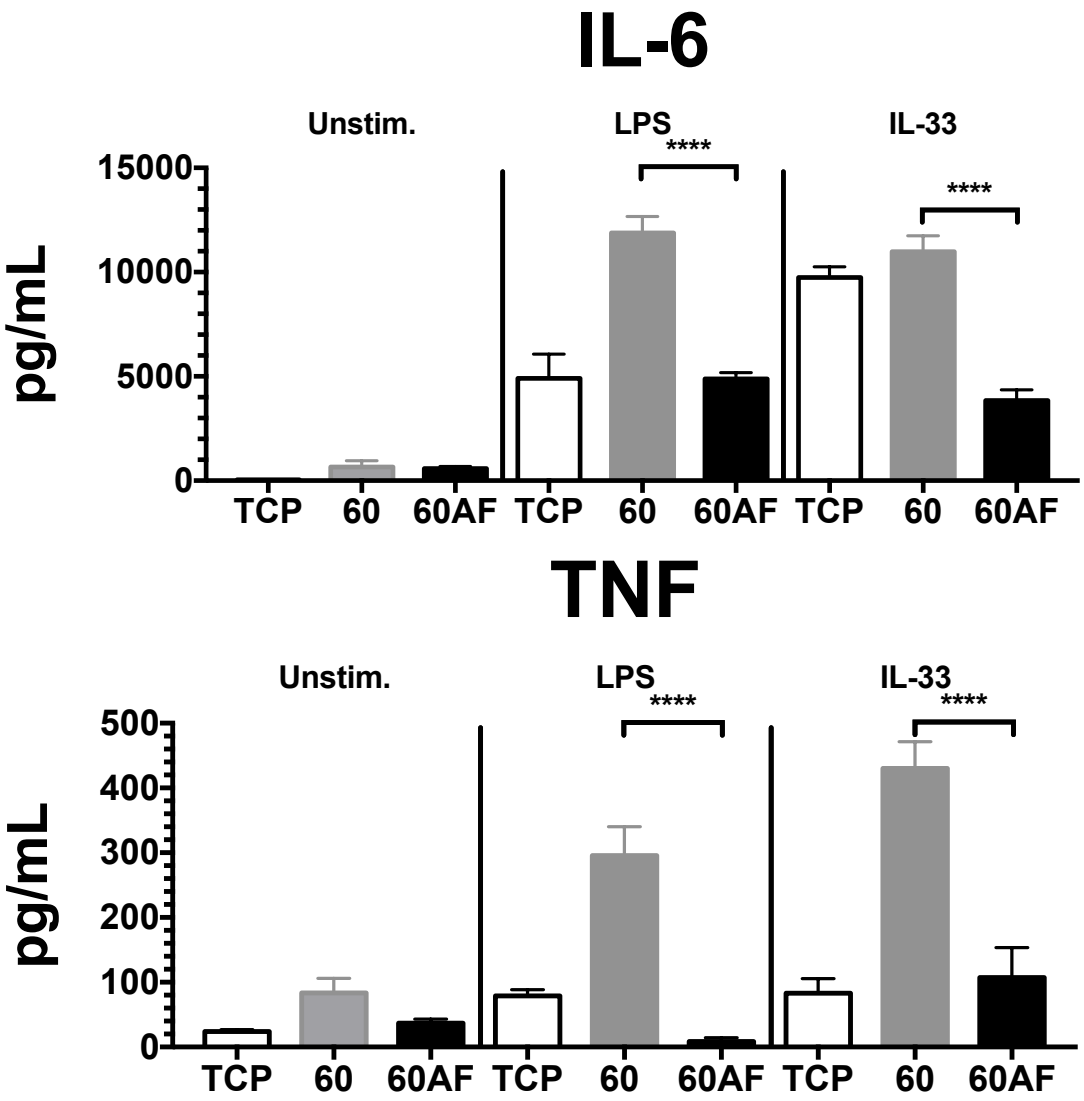

FIGURE 2.7 Mast cell cytokine secretion on 60 and 60AF scaffolds BMMC were seeded on fibronectin-coated 60 and 60 AF electrospun scaffolds for 48 hours and then activated with LPS (1 μg/mL) or IL-33 (100 ng/mL). Supernatants were collected 16 hours later and analyzed via ELISA for IL-6 and TNF. Results are presented as mean ± SEM. Figures are 3 indpendent experiments conducted in triplicate. . *, $p<0.05$; **, $p<0.01$; ***, $p<0.001$; ****, $p<0.0001$; NS, not significant.

II.4.6 Reduced Pore Size of 140 mg/mL Polydioxanone Scaffolds

To complement the air mandrel studies using 60 mg/ml membranes, we next altered pore size on the 140 mg/ml scaffolds. We showed earlier that these membranes, with larger diameter fibers and pores, elicit less inflammatory cytokine production from BMMC when compared to the 60 mg/ml scaffolds. Therefore, we determined if reducing the pore size of 140 mg/mL scaffolds enhances inflammatory cytokine secretion. Scaffolds were compressed using a hydraulic press that provided a uniform pressure across the scaffold. To ensure that the amount of pressure applied was consistent from sample to sample, the arm to close the clamp on the sample was fully swung each time. Scanning electron micrographs were used to measure pore size and fiber diameter. As shown in Figure 2.8, there is a clear visual difference in the morphology of 140 mg/mL polydioxanone scaffolds before (140) and after (140C) compression, but no changes in fiber diameter. The 140 scaffold had an approximate pore diameter of 18 μm, while the 140C scaffold pores were reduced to 6 μm. Both scaffolds had a fiber diameter of approximately 2.4 μm. Thus we selectively reduced pore size without changing fiber diameter.

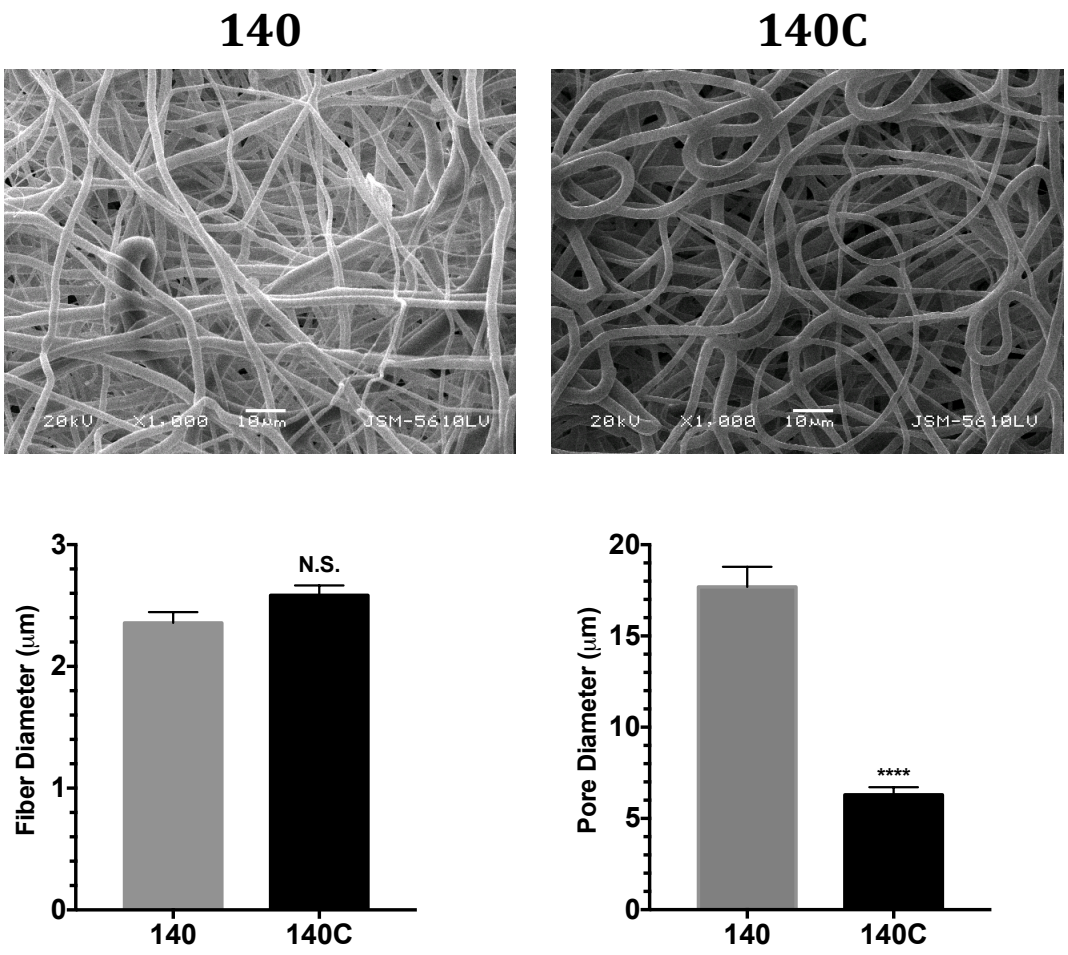

FIGURE 2.8 Decreasing pore size of 140 mg/mL electrospun scaffolds Electron micrographs of electrospun 140 mg/mL polydioxanone scaffolds that are either unaltered or have been compressed to reduce pore size. Fiber and Pore diameter were measured using ImageJ to analyze scaffold morphology. *, $p<0.05$; **, $p<0.01$; ***, $p<0.001$; ****, $p<0.0001$; NS, not significant.

II.4.7 Mast Cell Cytokine Secretion on 140 vs 140C electrospun scaffolds

Using the scaffolds shown in Figure 2.8, we determined if reducing pore size without changing fiber diameter could increase inflammatory cytokine secretion from mast cells. BMMC were seeded onto 140 or 140C scaffolds and activated with IL-33, LPS, or neither. 16 hours later supernatants were collected and analyzed via ELISA. As shown in Figure 2.9, LPS-induced IL-6 and TNF secretion was unchanged on the 140C scaffolds. Moreover, IL-33-induced cytokines were inconsistent. TNF production was reduced below detectable levels when BMMC were cultured on 140C membranes – but IL-6 production surprisingly increased. One conclusion may be that with fiber diameters on the micron scale, pore sizes are not critical. However, that seems unlikely given previous work demonstrating reduced M2 macrophage polarization on scaffolds with micron fiber diamters and reduced pore size (38). An alternative explanation may be that since the pore diameter of the140C scaffolds is approximately 6 μm, that size may be sufficient to elicit a response from BMMC that suppresses inflammatory cytokines. That pore diameter resembles the 60AF scaffold (4μm) that suppressed IL-33-mediated mast cell inflammatory cytokine secretion, despite the sub-micron fiber diameters. Perhaps a scaffold geometry with pore sizes of 6 μm is on the verge of being sufficiently different from scaffolds with pore sizes of 18 μm to alter inflammatory cytokine secretion. Mast cells have an approximate diameter of 10 μm, which may explain why scaffolds with pore sizes of 6 μm vs. 18 μm might not elicit different inflammatory responses (73). Mast cells may still be able to engage with a scaffold that has 6 μm pores as it does with a scaffold with 18 μm pores. This will require further investigation where the pore sizes of compressed 140 mg/mL scaffolds are further reduced to approximately 3 μm. We

conclude that in the presence of large fibers, reducing pore size to 6 μm does not consistently increase inflammatory cytokine secretion from mast cells.

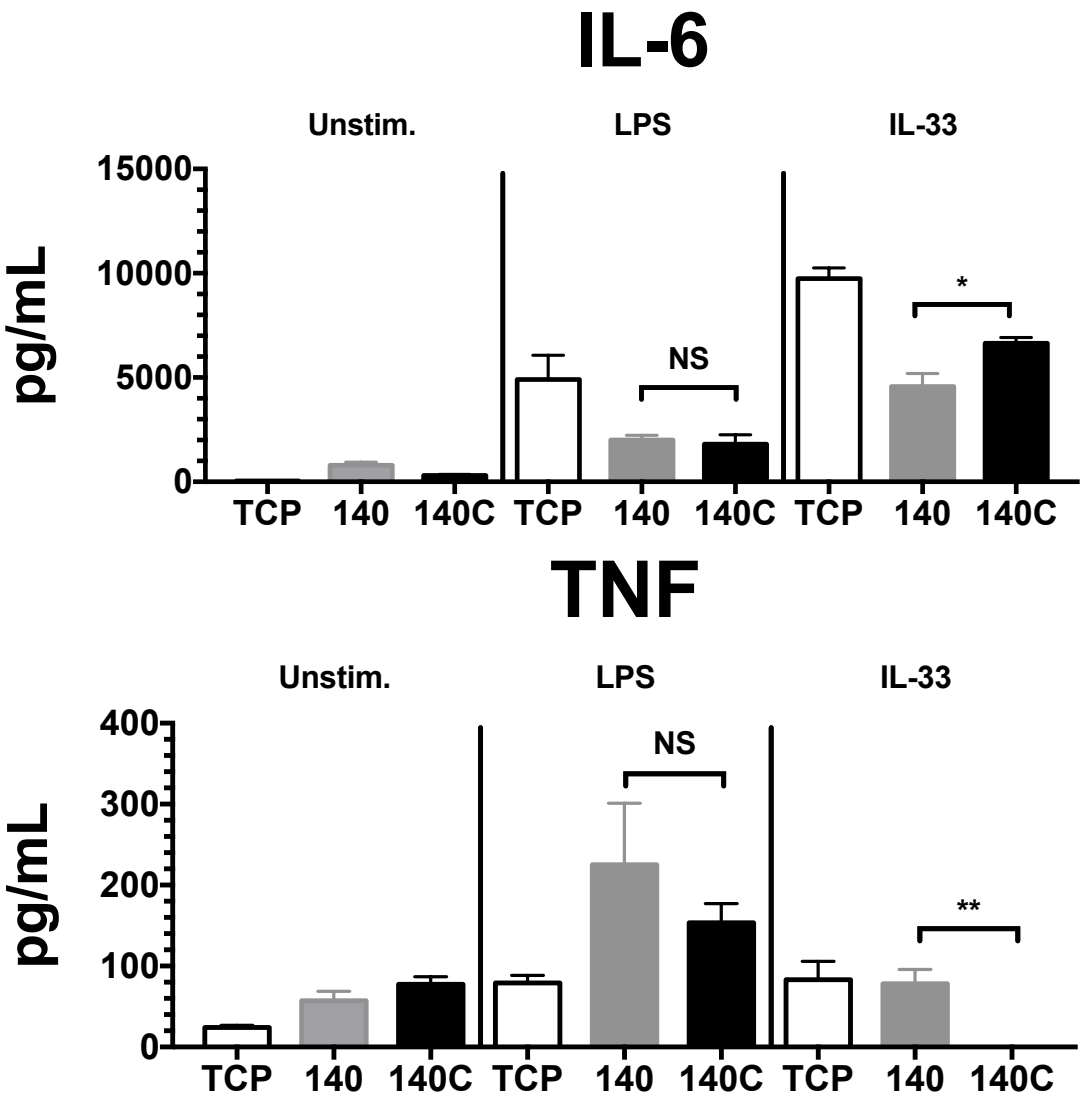

FIGURE 2.9 Mast cell cytokine secretion on 140 and 140C scaffolds BMMC were seeded on fibronectin-coated 140 and 140C electrospun scaffolds for 48 hours and then activated with LPS (1 μg/mL) or IL-33 (100 ng/mL). Supernatants were collected 16 hours later and analyzed via ELISA for IL-6 and TNF. Results are presented as mean ± SEM. Figures are 3 indpendent experiments conducted in triplicate. . *, $p<0.05$; **, $p<0.01$; ***, $p<0.001$; ****, $p<0.0001$; NS, not significant.

II.5 DISCUSSION

Electrospinning offers great promise as a method for fabricating synthetic grafts that are inexpensive, have the potential to be bioresorbable, and have off-the-shelf availability. Additionally, the sub-micron fiber diameters of electrospun scaffolds allow it to mimic the structure and function of the native extracellular matrix (ECM) (74). However, one major limitation of electrospinning is the inability to finely control scaffold porosity. Scaffold porosity is the design focus that is most vital for promoting healing, transmural angiogenesis (i.e. capillary in-growth through the walls of the implant), and cellular infiltration for tissue growth. Sufficient endothelialization is one major limitation of many vascular prosthetics and can be addressed by increasing porosity throughout an implant by facilitating transmural angiogenesis (75). Currently, clinically used synthetic grafts undergo transanastomotic endothelialization (i.e. endothelium growth from the adjacent vessel into graft), however, this phenomenon provides extremely limited endothelium growth. Therefore, the solution would be to promote capillary in-growth throughout the walls of the implant (76). Beyond endothelial growth, fibroblast migration into the implant is important for tissue remodeling. Both of these issues can be facilitated by increasing the porosity of the implant. The success of electrospun scaffolds has been limited due to the inability to directly control pore size due to the tight packing of the fibers (77). Therefore it is imperative to find ways to alter scaffold structure to improve functionality.

Another variable that can dictate the fate of any implanted biomaterial is the initial interaction with the immune system. If the response elicited by introduced scaffolds from innate immune cells is inflammatory, it can lead to scaffold rejection,

capsule formation, and failure (51). Addressing this variable was the over-arching goal of this work. In the present study we sought to determine if changing electrospun scaffold geometry could alter the response from innate immune cell populations. Our group has previously published that increasing pore and fiber diameter promoted an M2 polarization of macrophages cultured on these scaffolds. While the macrophage response to these scaffolds is important, macrophages do not respond to these materials independently of other cells, nor do they exist in the tissue independently. Therefore it is important to characterize the response of other innate immune cells that reside in the peripheral tissue with macrophages. This is why we characterized the mast cell response to electrospun scaffolds.

Since it is critical to improve the pore size of electrospun scaffolds and mitigate the inflammatory response from the tissue resident innate immune cells, this work sought to unite the two topics of study by examining how altering scaffold structure might modulate the response from mast cells. We demonstrated in this chapter that scaffold pore size could be increased in response to increasing fiber diameter, which is achieved by increasing polymer concentration during electrospinning. However, the pitfall with this method is losing the sub-micron fiber diameters that closely mimic the structure of the native ECM. Therefore there was a need to maintain sub-micron fiber diameters while increasing scaffold pore size. Previous work has shown that while scaffolds like our 60 mg/mL polydioxanone scaffold have sub-micron fiber diameters, the dense morphology of these polymers promote inflammatory responses. Macrophages will fuse together to form multinucleated foreign body giant cells (FBGCs) when met with a material they cannot infiltrate nor engulf, such as an electrospun scaffold with low fiber and pore

diameter. In this scenario, FBGCs will begin to release highly inflammatory reactive oxygen species in an attempt to break down the material (38). This points towards a relationship between implant architecture and mediating inflammatory responses. So the explicit goal is to create a scaffold with sub-micron fiber diameters that have increased scaffold pore size. This was accomplished with the introduction of the air-flow mandrel. While we demonstrated that the 140 mg/mL scaffold prompted BMMC to release less inflammatory cytokines than the 60 mg/mL scaffold in response to IL-33 and LPS, the 140 mg/mL scaffold does not offer desirable fiber diameters. However, when 60 mg/mL scaffolds were electrospun onto the air-flow mandrel and seeded with BMMC, the 60AF scaffold promoted significantly less mast cell inflammatory cytokine production in response to IL-33 and LPS. This demonstrates a way to make electrospun scaffolds with fiber diameters that still mimic the native ECM, but with larger pore sizes. We also demonstrate how the changes in scaffold pore size promote an anti-inflammatory and pro-angiogenic phenotype. This work corroborates previous findings and helps to address a pressing need in the field of biomaterial design.

One point worth making is that while macrophages do not require scaffolds to be coated with an adhesion-promoting protein, mast cells do, as reported in our earlier study (69). In this work, scaffolds were coated with fibronectin prior to mast cell seeding. While this does not initially seem to mimic normal physiology, previous work has demonstrated the role of plasma fibronectin on scaffold fate and the foreign body response. When biomaterials were implanted in mice deficient in plasma fibronectin, fibrotic capsules were thicker and more foreign body giant cells were present. This indicates a critical role for plasma fibronectin in mitigating inflammatory responses to

biomaterials (78). This is by no means a reason to coat each implanted biomaterial with fibronectin, but suggests that coating electrospun scaffolds with fibronectin may have physiological relevance. All together, this work provides another perspective on how biomaterials should be designed to mitigate inflammatory responses.

II.6 CONCLUSION

In this study we demonstrate that LPS- and IL-33-mediated mast cell responses to electrospun scaffolds can be modulated with scaffold structure. When comparing the 60 mg/mL polydioxanone scaffold to the 140 mg/mL, which had larger pore and fiber diameters, the latter elicited less inflammatory cytokine and more VEGF secretion. Further, by increasing the pore size of the 60 mg/mL scaffold, mast cells secreted less inflammatory cytokines. These findings provide helpful information that is necessary in biomaterial design when considering parameters meant to mitigate inflammation. As the importance of managing inflammation and innate immune responses to biomaterials rises, studies such as this will provide a better understanding in how to do so.

CHAPTER III: LACTIC ACID SUPPRESSES IL-33-MEDIATED MAST CELL INFLAMMATORY RESPONSES VIA HYPOXIA INDUCIBLE FACTOR (HIF)-1α-DEPENDENT miR-155 SUPPRESSION

III.1 ABSTRACT

Lactic acid (LA) is elevated in tumors, the asthmatic lung, and wound healing, environments with elevated IL-33 and mast cell infiltration. LA is also a degradative byproduct of poly-lactic acid breakdown (PLA). PLA is a widely used synthetic polymer in biomaterial design. While IL-33 is a potent mast cell activator, how LA affects IL-33-mediated mast cell function is unknown. To investigate this, mouse bone marrow-derived mast cells (BMMC) were cultured with or without LA and activated with IL-33. LA reduced IL-33-mediated cytokine and chemokine production, yet enhanced VEGF. Using inhibitors for monocarboxylate transporters (MCT) or replacing LA with sodium lactate revealed that LA effects are MCT-1- and pH-dependent. LA selectively altered IL-33 signaling, suppressing TAK1, JNK, ERK, and NFκB phosphorylation, but not p38 phosphorylation, and enhanced Akt phosphorylation. We connected the enhancement of VEGF production and Akt phosphorylation by showing that IL-33-mediated VEGF production requires Akt1 expression. LA effects in other contexts have been linked to HIF-1α, which was enhanced in BMMC treated with LA. Since HIF-1α has been shown to regulate the microRNA miR-155 in other systems, LA effects on miR-155-5p and -3p species were measured. In fact, LA selectively suppressed miR-155-5p in a HIF-1α-dependent manner. Moreover, overexpressing miR-155-5p, but not miR-155-3p, abolished LA effects on IL-33-induced cytokine production. These in vitro effects of reducing cytokines were consistent in vivo, since LA injected intraperitoneally into C57BL/6 mice suppressed IL-33-induced plasma cytokine levels. Lastly, IL-33 effects on primary human mast cells were suppressed by LA in an MCT-

dependent manner. Our data demonstrate that LA, present in inflammatory and malignant microenvironments, can alter mast cell behavior to suppress inflammation.

III.2 INTRODUCTION

In the previous chapter, scaffold architecture was explored as a variable that can alter mast cell responses. Another critical factor that can alter the fate of implanted biomaterials is the response from tissue resident innate immune cells to the byproducts of the material. While materials degradation rates vary, all biomaterials secrete byproducts into the local microenvironment, presenting an additional variable to consider in designing biomaterials.

One of the most widely used synthetic polymers in biomaterials is polylactic acid (PLA). Part of the appeal of using PLA is that it is an FDA approved polymer, has been well studied, widely applied, and the degradative byproduct is lactic acid, which can be metabolized and excreted as carbon dioxide and water (79, 80). PLA was first approved by the FDA for use as a suture, but has been applied in many other ways, from use as an orthopedic implant, drug delivery system, electrospun scaffold, and even food storage (81). PLA is a thermoplastic polymer in the polyester class, which possess an ester linkage in their backbone susceptible to hydrolytic degradation (82). Lactate is a chiral molecule and comes in two forms, L-lactate and D-lactate. Unsurprisingly, PLA also comes in two forms, poly-L-lactic acid (PLLA) and poly-D-lactic acid (PDLA). Both PLLA and PDLA are crystalline polymers that undergo bulk erosion via hydrolysis (83). The hydrolytic degradation of these polymers happens over the course of approximately two years, however, it does lead to the local accumulation of lactic acid in the tissue

microenvironment (TME) (84). Therefore, it is critical to understand how the build up of byproducts like lactic acid can alter the fate of an implanted biomaterial, particularly how tissue resident immune cells respond. In light of this, the next chapter will explore how mast cells, a tissue resident immune cell, respond to lactic acid exposure.

Mast cells are sentinels of the innate immune system, guarding the body against select bacterial and parasitic infections. However, mast cells are best known for the major role they play in allergies and allergic asthma. The interaction of allergen with mast cell-bound IgE and subsequent signaling through the IgE receptor, FcεRI, result in a signaling cascade provoking release of early and late phase mediators (58, 85-88). The early phase mediators, released within minutes of activation, include tryptases, chymases, histamine, prostaglandins, leukotrienes and platelet-activating factor, whereas the late phase mediators, released hours later, consist of cytokines and chemokines, including IL-1β, IL-4, IL-5, IL-6, IL-10, IL-13, TNF, MIP-1α, and MCP-1. These factors yield the clinical symptoms of immediate hypersensitivity, including the wheal-and-flare response, itching, and vasodilation/edema. Mast cells can also promote chronic diseases such as asthma upon repeated antigen exposure, which results in airway remodeling due to sustained inflammation (58, 85-88).

While IgE crosslinking is the best-studied form of mast cell activation, many stimuli elicit a mast cell response. IL-33 is a recently discovered alarmin in the IL-1 family. Produced by endothelial cells, epithelial cells, fibroblasts, mast cells, and keratinocytes in response to damage or stress, IL-33 promotes a T_H2 response (89-92). IL-33 binding to the ST2/IL-1RacP receptor complex on mast cells results in the release of cytokines, chemokines and lipid mediators (89, 90). IL-33 has also been shown to

promote mast cell survival, maturation and adhesion (33, 91). While it is a poor inducer of degranulation, IL-33 augments degranulation triggered through the IgE receptor (89, 90). IL-33 has beneficial effects in atherosclerosis, cardiac remodeling and helminth infection (91). However, it has been linked to asthma, rheumatoid arthritis, multiple sclerosis, Type I diabetes, and skin inflammation (90).

Inflammation causes important changes in the cellular microenvironment, which can be beneficial if temporally and spatially controlled, but pathological when chronic. A well-known example of chronic inflammation is the TME. Tumors are known to preferentially undergo anaerobic glycolysis, even in the presence of sufficient oxygen, resulting in a hypoxic microenvironment with high (40mM) lactic acid (LA) concentrations (93-101). These unique environmental factors can alter cellular responses, allowing tumors to escape immune surveillance (98, 101-103). There is evidence that the TME uses LA to promote tumor-associated macrophages (TAM) to take on an M2 phenotype, which is anti-inflammatory and has reduced antigen presentation ability (94, 101). Tumor-derived LA has also been shown to inhibit dendritic cell function, resulting in decreased proliferation and reduced antigen presentation (96). Among cytotoxic T cells, LA decreases proliferation and inhibits their cytotoxic function (98). Other examples of altered microenvironments that have increased lactate levels are obesity, hypertension, and Type II diabetes, as well as tissues suffering injury, infection, or ischemia (102-105).

Since LA is known to alter cellular responses in inflammatory environments, we tested the effects of physiological LA concentrations on mast cell function. LA exposure for 24 hours was sufficient to suppress IL-33-mediated cytokine secretion, effects that

were pH- and monocarboxylate transporter-1 (MCT-1)-dependent. Suppression of IL-33-induced inflammatory cytokine and chemokine secretion was accompanied by reduced activation of several signaling intermediates. Expectedly, LA treatment enhanced HIF-1α expression. This correlated with a decrease in pro-inflammatory miR-155-5p, which was reversed by HIF-1α blockade. miR-155-5p overexpression abolished LA suppressive effects, demonstrating the critical nature of the HIF-1α-miR-155 cascade. These results provide insight into microenvironmental effects during wound healing, chronic inflammation, and tumorigenesis.

III.3 MATERIALS AND METHODS

III.3.1 Animals

C57BL/6 male and female mice were purchased from The Jackson Laboratory (Bar Harbor, ME) and used at a minimum of 6 weeks old, with approval from the Virginia Commonwealth University institutional animal care and use committee (IACUC).

III.3.2 Mouse Mast Cell Cultures

BMMC were derived by harvesting bone marrow from C57BL/6 mouse femurs, followed by culture in complete RPMI (cRPMI) 1640 medium (Invitrogen Life Technologies, Carlsbad, CA) containing 10% FBS, 2mM L-glutamine, 100 U/ml penicillin, 100 μg/ml streptomycin, 1mM sodium pyruvate, and 1mM HEPES (all from Corning, Corning, NY), supplemented with IL-3-containing supernatant from WEHI-3B cells and SCF-containing supernatant from BHK-MKL cells. The final concentrations of IL-3 and SCF were adjusted to 1.5ng/ml and 15ng/ml, respectively, as measured by ELISA. BMMC

were used after 3 weeks of culture, at which point these primary populations were >90% mast cells, based on staining for c-Kit and FcεRI expression. Mouse peritoneal mast cells were obtained by collecting peritoneal lavage from C57BL/6J mice, which cultured in cRPMI supplemented with recombinant mouse IL-3 and SCF at 10ng/mL each. Peritoneal mast cells were used after 14 days, at which these *ex vivo* expanded cells were approximately 85% mast cells, based on staining for c-Kit and FcεRI expression.

III.3.3 Cytokines and Reagents

Recombinant mouse IL-3, SCF, and IL-33, recombinant human IL-33, as well as mouse IL-6, TNF, and MCP-1 (CCL-2) ELISA kits were purchased from BioLegend (San Diego, CA). Mouse MIP-1α (CCL-3) and VEGF ELISA kits were purchased from PeproTech (Rocky Hill, NJ). Mouse IL-13 ELISA kits were purchased from eBioscience (San Diego, CA). L-(+)-lactic acid and Sodium L-lactate were purchased from Sigma-Aldrich (St. Louis, MO). Human IL-6, TNF, and MCP-1 ELISA kits were purchased from BD OptEIA (BD Biosciences; Franklin Lakes, NJ).

III.3.4 Cell Culture Conditions

For IL-33 activation, BMMC ($2x10^6$ cells/mL) were cultured in 20ng/mL of IL-3 and SCF in cRPMI. An equal volume of 25mM LA in cRPMI was added to the cell suspension, resulting in a final cell concentration of $1x10^6$ cells/ml, 10ng/mL of IL-3 and SCF, and 12.5mM LA. Control conditions received cRPMI in place of LA. After 24 hours of pretreatment in LA media, cells then received 100ng/mL of IL-33 for 16 hours,

after which supernatants were collected. pH was measured for media alone, lactic acid, and lactate-conditioned media using the Beckman Phi 45 pH meter.

III.3.5 Intracellular Staining with Flow Cytometry

Cells were first treated with 12.5 mM LA and activated with IL-33 (100 ng/mL). 90 minutes after activation, cells were given Monensin (5 μM) for 6 hours to promote cytokines accumulation in the Golgi complex, and incubated at 37°C. Cells were washed twice with PBS and fixed with 4% paraformaldehyde (PFA) at room temperature for 20 minutes. Cells were then placed in a permeabilizing buffer, which consisted of 500 mL of FACS buffer, 5 mL of HEPES, and 2.5 g of Saponin. After 20 minutes at room temperature in permeabilizing buffer, cells were stained for cytokines, washed twice in PBS, placed back in FACS buffer, and run on a FACSCelesta flow cytometer.

III.3.6 Western Blot Analysis

Cells were cultured at $2x10^6$/ml and lysed in Lysis Buffer (Cell Signaling Technology, Danvers, MA) supplemented with 1.5X ProteaseArrest (G-Biosciences, Maryland Heights, MO). Protein concentration was determined using the Pierce BCA protein assay kit (Thermo Scientific). Proteins were resolved by SDS-PAGE using 30 μg of total protein per sample on 4-20% Mini-Protean TGX Gels (Bio-Rad, Hercules, CA). Transfer was made onto nitrocellulose membranes, which were then blocked for 1 hour at room temperature with 2% BSA in PBS. Membranes were rinsed in PBS and then incubated overnight at 4ºC in PBS-T containing 2% BSA and primary antibody diluted 1:1000. Membranes were probed with antibodies purchased from Cell Signaling Technology

(Danvers, MA), including: anti phospho-TAK1 (Thr-184/187, catalog no. 4508), total TAK1 (catalog no. 5206), phospho-NFκB p65 (Ser-536, catalog no. 13346), total NFκB p65 (catalog no. 4764), phospho-JNK (Thr-183/Tyr-185, catalog no. 9251), total JNK (catalog no. 9258), phospho-p38 (Thr-180/Tyr-182, catalog no. 9216), total p38 (catalog no. 9212), phospho-Akt (Ser473, catalog no. 4060), total Akt (catalog no. 4685), total Akt1 (catalog no.2938), total Akt2 (catalog no. 2964), phospho-ERK1/2 (Thr-202/Tyr-204, catalog no. 9101), total ERK1/2 (catalog no. 4695), and GAPDH (catalog no. 2118). Membranes were washed the next day with PBS-T every 5 minutes for a total of 30 minutes, then incubated with a 1:15,000 dilution of either goat anti-rabbit DyLight800 (catalog no. 5151) or goat anti-mouse DyLight680 (catalog no. 5470) infrared-labeled secondary antibodies (Cell Signaling Technology, Danvers, MA). Membranes were rinsed a final time before being analyzed with an Odyssey CLx infrared scanner (Li-Cor, Lincoln, Nebraska). Normalization was done using Image Studio 4.0 software (Li-Cor, Lincoln, Nebraska).

III.3.7 Inhibitors

TAK1 inhibitor (5Z)-7-Oxozeanol (5 μM; Tocris Bioscience, Bristol, UK), JNK inhibitor SP600125 (10 μM; EMD Millipore, Billerica, MA), NFκB inhibitor BAY 11-7085 (2 μM; Tocris Bioscience, Bristol, UK), Akt inhibitor Akt Inhibitor IV (EMD Millipore, Billerica, MA), ERK inhibitor FR180204 (25 μM; Cayman Chemical, Ann Arbor, MI) and monocarboxylate transporter (MCT) inhibitors α-cyano-4-hydroxycinnamic acid (CHC; 5 mM; Sigma Aldrich, St. Louis, MO) and AR-C155858 (100 nM; Tocris Bioscience, Bristol, UK), were solubilized in dimethyl sulfoxide (DMSO). Under the

conditions used, none of these inhibitors caused significant cell death. Inhibitors were added to culture one hour prior to activation with IL-33 (100 ng/mL). Supernatants were collected 16 hours later, and ELISAs used to determine cytokine production.

III.3.8 mRNA and microRNA qPCR

After BMMC were treated in 12.5mM LA, total RNA was extracted with TRIzol reagent (Life Technologies, Grand Island, NY) and later measured using the Thermo Scientific NanoDrop™ 1000 UV–vis Spectrophotometer (Thermo Scientific, Waltham, MA) according to the manufacturer's recommended protocol. For RNA extraction used to measure microRNA expression, polyadenylation was done prior to cDNA synthesis using the qScript microRNA cDNA synthesis kit (Quanta Biosciences, Gaithersburg, MD). For samples used to measure mRNA expression, cDNA was synthesized using the qScript cDNA Synthesis Kit (Quanta Biosciences, Gaithersburg, MD) following the manufacturer's protocol. qPCR analysis was performed with Bio Rad CFX96 Touch™ Real-Time PCR Detection System (Hercules, CA) and SYBR® Green detection using a relative Livak Method (106). Each reaction was performed according to the manufacturer's protocol using 10ng of sample cDNA, with the following primers: mmu-miR-155-5p, 5'-UUAAUGCUAAUUGUGAUAGGGGU-3' (cat no. MMIR-0155, Quanta Biosciences); mmu-miR-155-3p, 5'-CUCCUACCUGUUAGCAUUAAC-3' (cat no. MMIR-0155*, Quanta Biosciences); HIF-1α forward, 5'-TGAGGCTCACCATCAGTTAT – 3'; HIF-1α reverse, 5'-TAACCCCATGTATTTGTTC-3'; MCT-1 forward, 5'-GCTGGAGGTCCTATCAGCAG-3'; MCT-1 reverse, 5'-

CGGACAGCTTTTCTCCTTTG-3'; MCT-2 forward, 5'-TTACCGTATCTGGGCCTTTG-3'; MCT-2 reverse, 5'-CCAAAGCAGTTTCGAAGGAG-3'; GAPDH forward, 5'-GATGACATCAAGAAGGTGGTG-3'; GAPDH reverse, 5'-GCTGTAGCCAAATTCGTTGTC-3'; SOCS1 forward, 5'-CAGGTGGCAGCCGACAATGCGATC-3'; SOCS1 reverse, 5'-CGTAGTGCTCCAGCAGCTCGAAAA-3'; SHIP-1 forward, 5'-GGTGGTACGGTTTGGAGAGA-3'; SHIP-1 reverse, 5'-ATGCTGAGCCTCTGTGGTCT-3';

SNORD47, 5'-GUGAUGAUUCUGCCAAAUGAUACAAAGUGAUAUCACCUUUAAACCGUUCAUUUUAUUUCUGAGG-3' (cat no. MM-SNORD47, Quanta Biosciences); β-Actin forward, 5'-GATGACGATATCGCTGCGC-3'; and β-Actin reverse, 5'-CTCGTCACCCACATAGGAGT-3'. Primers for microRNAs were purchased from Quanta Biosciences (Gaithersburg, MD) and all other primers were purchased from Eurofins MWG Operon (Huntsville, AL). Amplification conditions for microRNA detection were set to heat-activation at 95 °C for 2 min followed by 40 cycles of denaturation at 95 °C for 5s, annealing at 60 °C for 15s, and extension at 70 °C for 15s. All other reactions consisted of a heat-activation step at 95 °C for 10 min followed by 40 cycles of 95 °C for 15s, 55 °C for 30s and 60 °C for 1 min. Fluorescence data were collected during the extension step of the reaction.

III.3.9 siRNA and miR-mimic Transfection

BMMC were transfected with 100nM HIF-1α siRNA (cat no. GS15251), SOCS1 siRNA (cat no. GS12703), Akt1 siRNA (cat no. GS11651), Akt2 siRNA (cat no. GS11652), or scrambled FlexiTube siRNA (cat no. 1027280) from Qiagen (Valencia, CA). miR-155-5p (cat no. 470919), miR-155-3p (cat no. 471999), and negative control/mock (cat no. 479903) microRNA mimics were transfected at 50nM and purchased from Exiqon (Woburn, MA). Transfections were done with the Amaxa Nucleofactor from Lonza (Allendale, NJ) using program T5 in the following transfection media: Dulbecco's modified Eagle's medium (DMEM), 20% FBS, and 50 mM HEPES Buffer. BMMC were incubated in IL-3 and SCF (10ng/mL each) and used 48 hours after transfection.

III.310 Intraperitoneal Injections

C57BL/6J mice (12-16 weeks old) were first injected with 1mg/kg of ketoprofen from Spectrum Chemical (New Brunswick, NJ) for pain relief, then 30 minutes later injected with 4mg/kg of 4%(w/v) LA. 16 hours later, mice were injected with 1μg of recombinant mouse IL-33 from eBioscience (San Diego, CA). Four hours later, mice were euthanized and blood was collected via cardiac puncture and plasma prepared from collected blood. All animal protocols were approved by the VCU Institutional Animal Care and Use Committee.

III.3.11 Human Skin Mast Cell Culture

As approved by the Internal Review Board at the University of South Carolina, surgical skin samples were collected from the Cooperative Human Tissue Network of the National Cancer Institute. Skin mast cells were harvested and cultured from 5 human

donors as previously described (107). After 6-10 weeks, mast cells were used, at which time purity was nearly 100%, as confirmed with toluidine blue staining.

III.3.12 Statistical Analysis

Data are presented as mean ± SE and analyzed using GraphPad Prism 6 software (GraphPad, La Jolla, CA). Comparisons between two groups were done using unpaired Student's *t* test and comparisons between multiple groups were done using one-way analysis of variance with Tukey's post-hoc test. All p values <0.05 were deemed significant.

III.4 RESULTS

III.4.1Kinetics of Lactic Acid Auppressing IL-33-mediated Mast Cell Cytokine Production

In a normal physiological state, LA is present in peripheral tissue at 1-2 mM (108), whereas in pathological conditions LA concentrations often exceed 10 mM (101, 109). Elevated levels of LA are present in tissues where pathological conditions also promote mast cell infiltration and IL-33 expression (90, 95, 96, 110). Therefore, we investigated how LA alters IL-33-mediated mast cell activation by measuring the impact on cytokine secretion. The timing and dose of LA treatment were determined by measuring changes in IL-33-induced cytokine and chemokine production. LA exposure reduced IL-33-mediated IL-6 secretion by approximately 50%, with maximal effects at 6-24 hours of pre-exposure. Adding LA simultaneously or 48 hours prior to IL-33 yielded no inhibition (Figure 3.1A).

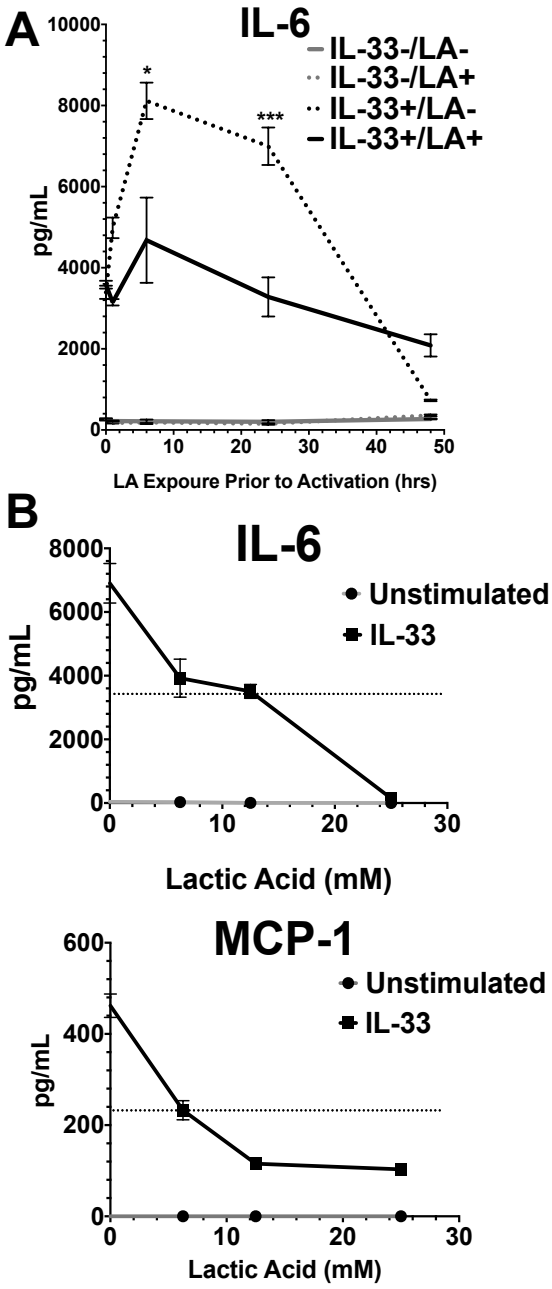

FIGURE 3.1 Kinetics of Lactic acid suppressing IL-33-mediated mast cell cytokine secretion. Mast cells were pretreated with 12.5 mM lactic acid prior to IL-33 activation. Supernatants were collected 16 hrs after IL-33 activation. A) Time-course and B) dose-response experiments were done to determine kinetics of lactic acid effects on BMMC cytokine production. 24 hours and 12.5mM were the optimal conditions for lactic acid pretreatment. Dotted line indicates 50% inhibition, used to calculate IC_{50}. Supernatants were analyzed by ELISA. Results are representative of three independent experiments using 3 BMMC populations each, and expressed as mean ±SEM. *, $p<0.05$; **, $p<0.01$; ***, $p<0.001$; ****, $p<0.0001$; NS, not significant.

Based on this time-course analysis, 24 hours of LA pre-exposure was determined to be optimal. In order to determine the effective concentration of LA, BMMC were treated with varying amounts prior to IL-33 activation. An IC_{50} between 6-12.5 mM was observed for inhibiting IL-6 and MCP-1 secretion (Figure 3.1B). While 25 mM LA yielded further inhibition of some cytokines, it also resulted in approximately 30% cell death. Hence, we employed 12.5 mM LA, which elicited no changes in cell viability.

III.4.2 Lactic acid suppresses IL-33-mediated mast cell inflammatory cytokine production

We next sought to expand on the cytokines we measured and investigate if LA alters the secretion of other cytokines and chemokines under the same conditions. BMMC were treated with 12.5 mM of LA for 24 hours prior to IL-33 activation, after which supernatants were collected to measure cytokines and chemokines via ELISA. The inhibitory effect of LA was consistent among pro-inflammatory cytokines, since BMMC pretreated with LA showed significantly decreased IL-33-mediated IL-6, TNF, MCP-1, MIP-1α, and IL-13 production, yet increased VEGF production (Figure 3.2). This phenotype, where there is selective control of inflammatory versus anti-inflammatory cytokines, agrees with a recent paper describing LA effects on macrophage polarization (101).

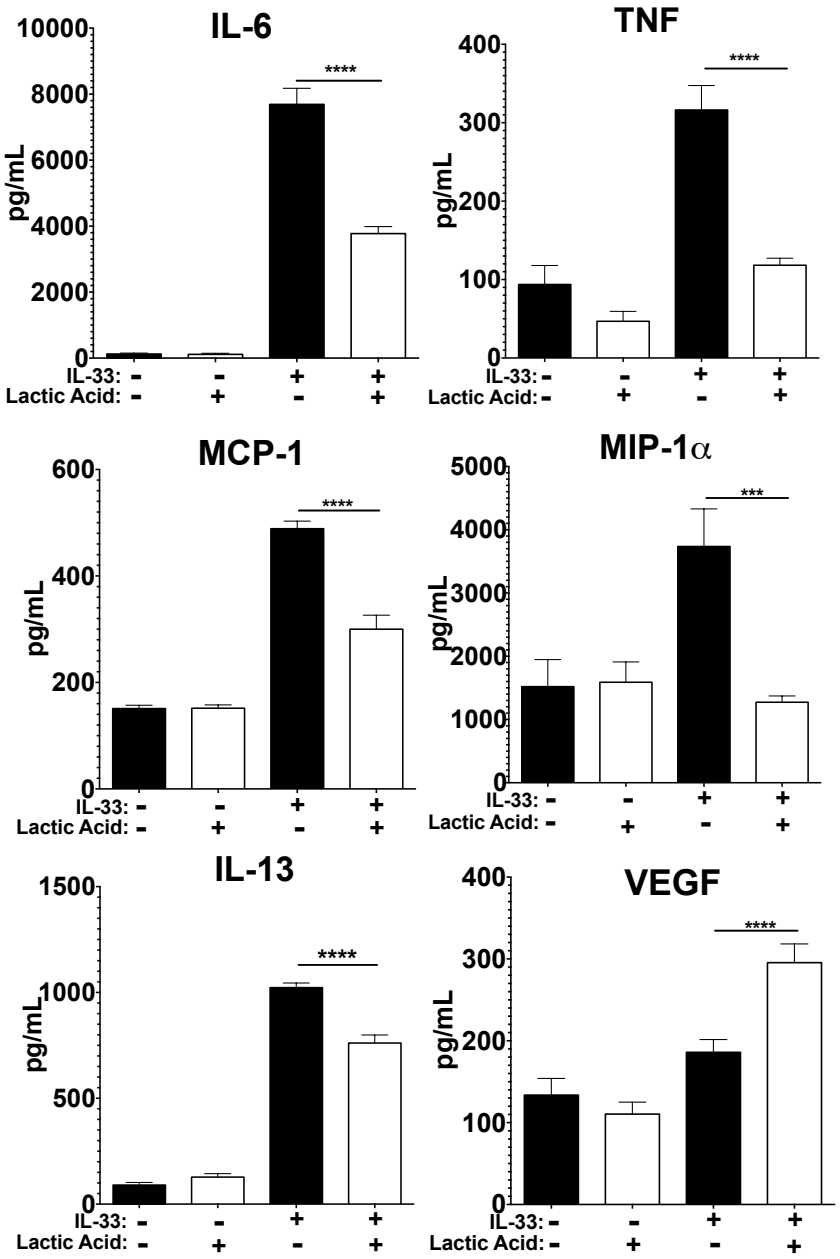

FIGURE 3.2 Lactic acid suppresses IL-33-mediated inflammatory cytokine secretion in mast cells. BMMC were treated as described in Figure 3.1, and supernatants assessed by ELISA. Results are expressed are representative of three independent experiments using 3 BMMC populations each, expressed as mean ±SEM. *, $p<0.05$; **, $p<0.01$; ***, $p<0.001$; ****, $p<0.0001$; NS, not significant.

III.4.3 Lactic Acid Suppresses IL-33-mediated Peritoneal Mast Cell Cytokine Secretion

To determine if LA would also suppress IL-33-mediated cytokine secretion from *ex vivo* derived mast cells, peritoneal mast cells were harvested from C57BL/6 mice via peritoneal lavage and expanded for 2 weeks. Cells were then pretreated with LA and activated with IL-33. As shown in Figure 3.3, LA significantly suppressed the IL-33-induced production of IL-6, MIP-1α, and MCP-1 by peritoneal mast cells as well. These findings demonstrate that LA can selectively suppress inflammatory cytokines from *in vitro* differentiated as well as *ex vivo* expanded primary mast cells.

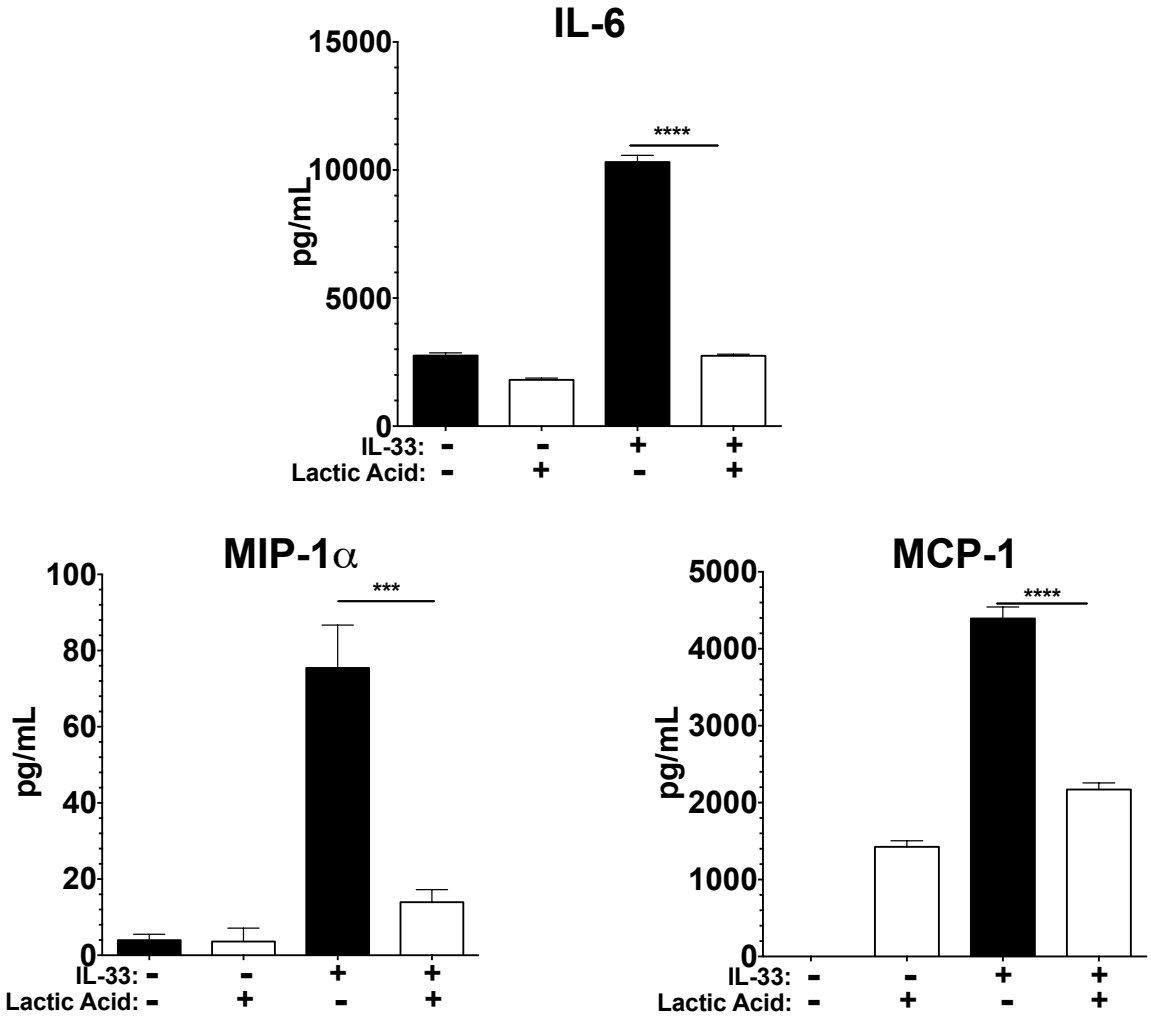

FIGURE 3.3 Lactic acid suppresses IL-33-mediated peritoneal mast cell cytokine secretion. Peritoneal mast cells harvested from C57BL/6 mice were treated with 12.5 mM lactic acid for 24 hours, then activated with IL-33 for 16 hours. Supernatants were analyzed by ELISA. Results are expressed as mean ±SEM. Results are representative of three independent experiments conducted in triplicate. *, $p<0.05$; **, $p<0.01$; ***, $p<0.001$; ****, $p<0.0001$; NS, not significant.

III.4.4 Intracellular staining for cytokine production

To determine whether the altered levels of cytokines and chemokines were due to changes in production or secretion, we stained for cytokine proteins intracellularly via flow cytometry. BMMC were treated with LA for 24 hours and activated with IL-33, as in Figure 3.1. However, here we added monensin as a golgi antagonist to inhibit the cytokine transport, leading to their accumulation in the golgi. Several hours after IL-33 activation, cells were fixed, permeabilized, and stained. In response to LA treatment, Figure 3.4 shows that IL-33-mediated production of IL-1β and MIP-1α is suppressed. These data indicate that LA suppresses cytokine production, but do not rule out antagonistic effects on secretion.

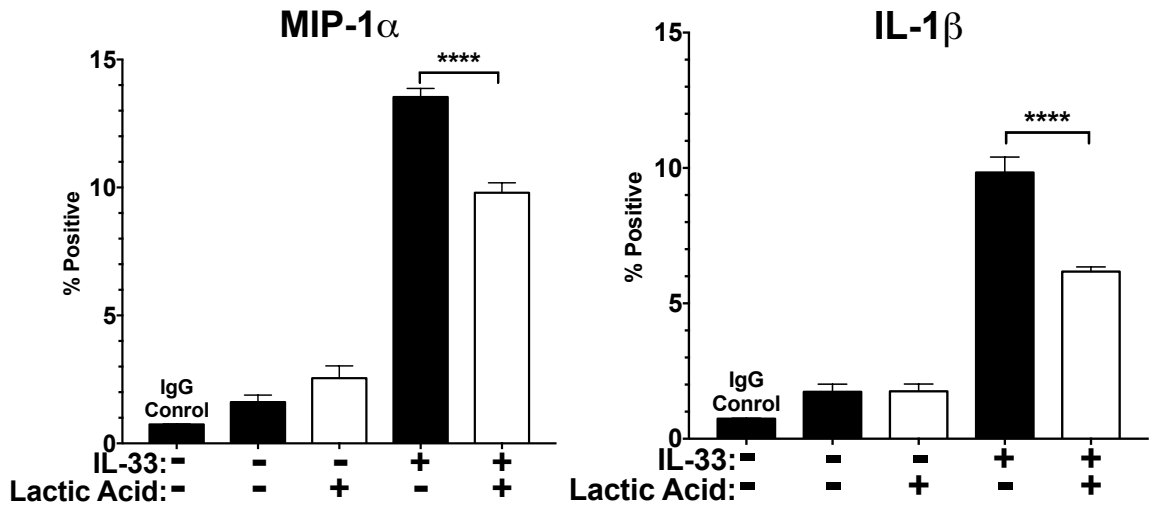

FIGURE 3.4 Lactic acid suppresses IL-33-mediated Intracellular accumulation of cytokines in mast cells. BMMC were pre-treated with 12.5 mM LA for 24 hours and then activated with 100 ng/mL of IL-33. 90 minutes after activation, 10 μM of monensin was added as a golgi stop to promote the accumulation of cytokines. 6 hours later, BMMC were fixed with paraformaldehyde, permeabilized with a Saponin buffer, and stained for MIP-1α and IL-1β. Staining was measured using FACS. *, $p<0.05$; **, $p<0.01$; ***, $p<0.001$; ****, $p<0.0001$; NS, not significant.

III.4.5 LA-mediated suppression of cytokines is pH-dependent

Previous papers have demonstrated that pH plays a critical role in LA effects on cellular function. For example, LA has been shown to suppress LPS-induced TNF secretion and delay NFκB activation in monocytes, while promoting an anti-inflammatory M2 phenotype in macrophages (101, 111, 112). However, lactate, the salt form of LA which does not lower pH, enhances LPS-mediated inflammatory responses in macrophages (103). We noted that media pH decreased to 6.5 immediately after adding LA, and returned to 7.2 within 6-8 hours (data not shown). To investigate the importance of pH on LA effects in mast cells, BMMC were cultured in 12.5 mM LA or sodium lactate for 24 hours prior to IL-33 activation. The results showed a clear difference, as LA suppressed IL-33-mediated IL-6, TNF, IL-13, and MCP-1 production, while sodium lactate had no effect (Figure 3.5), indicating the importance of pH on cytokine production.

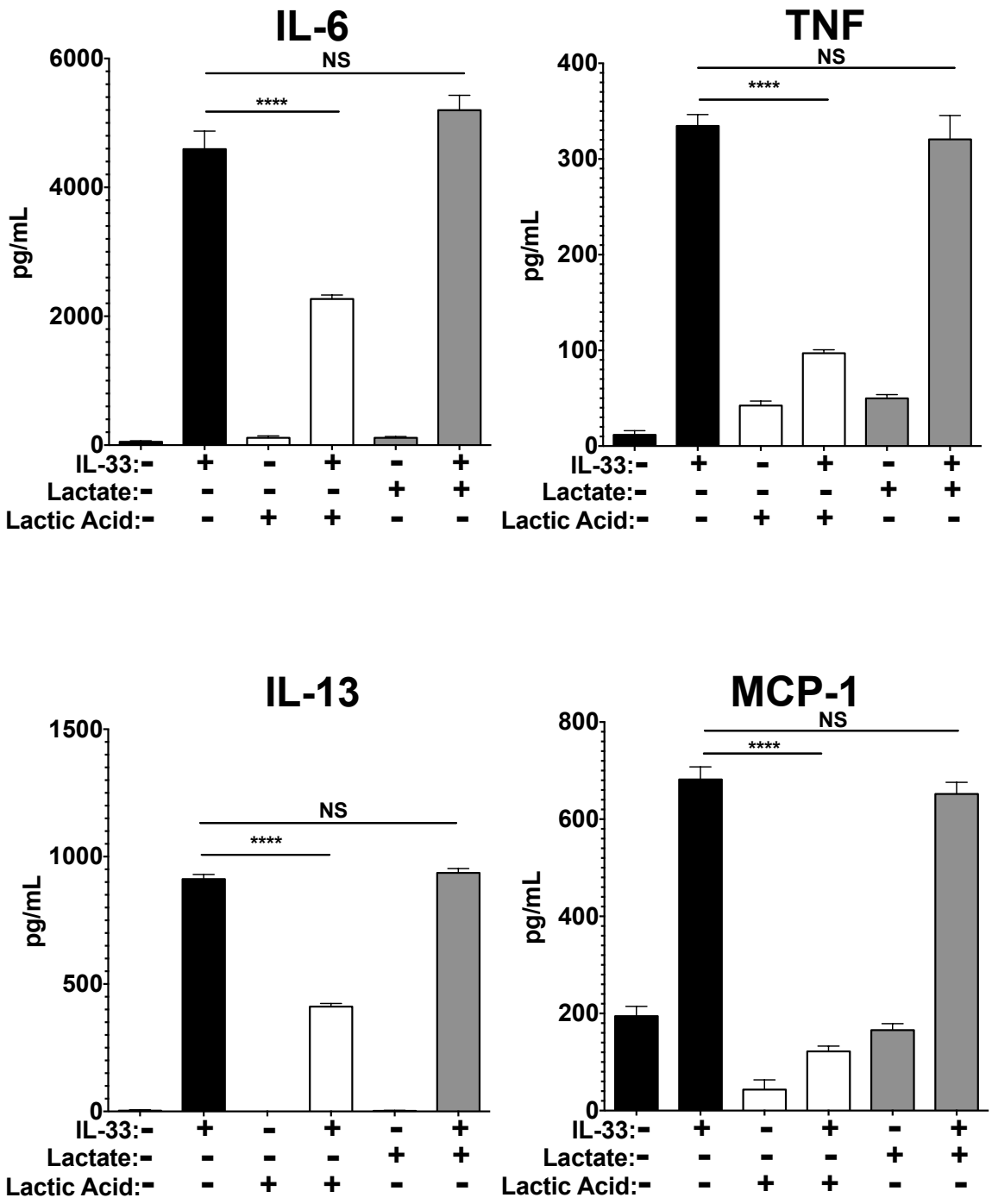

FIGURE 3.5 LA effects are pH-dependent. BMMC were cultured in media alone, 12.5 mM lactic acid, or 12.5 mM sodium lactate for 24 hours prior to IL-33 activation. ELISA was used to measure IL-6, TNF, IL-13, and MCP-1 in culture supernatants. Results are representative of three independent experiments using 3 BMMC populations each, and expressed as mean ±SEM.. *, p<0.05; **, p<0.01; ***, p<0.001; ****, p<0.0001; NS, not significant.

III.4.6 LA-mediated cytokine suppression is MCT-1-dependent

Other work has demonstrated that cellular entry and egress of LA is controlled by monocarboxylate transporters (MCT), a group of proteins within the solute carrier family (SLC16). MCT-1 and -2 can transport lactate into the cell (113-115). While MCT-2 expression is largely restricted to the testis, heart, and brain, MCT-1 is widely expressed including in hematopoietic cells (113, 116, 117). To determine if MCT-1 is important for LA effects on mast cells, we treated BMMC with two different MCT inhibitors, α-cyano-4-hydroxycinnamic acid (CHC; a pan-MCT inhibitor) and AR-C155858 (an MCT-1 & -2 inhibitor), and measured IL-33-induced cytokine production. In the presence of these inhibitors, LA did not suppress IL-33-mediated IL-6 production (Figure 3.6A). To determine MCT-1 and -2 expression in mast cells, RNA was harvested from BMMC and analyzed via qPCR. Functionality of MCT-1 and -2 primers were confirmed by using kidney tissue cDNA with these primers (data not shown). While MCT-1 transcripts were easily detected in BMMC within 40 cycles, MCT-2 transcripts were not detectable at all (Figure 3.6B). Thus these data demonstrate that LA effects on IL-33 activation are likely dependent upon acid pH- and the MCT-1 carrier.

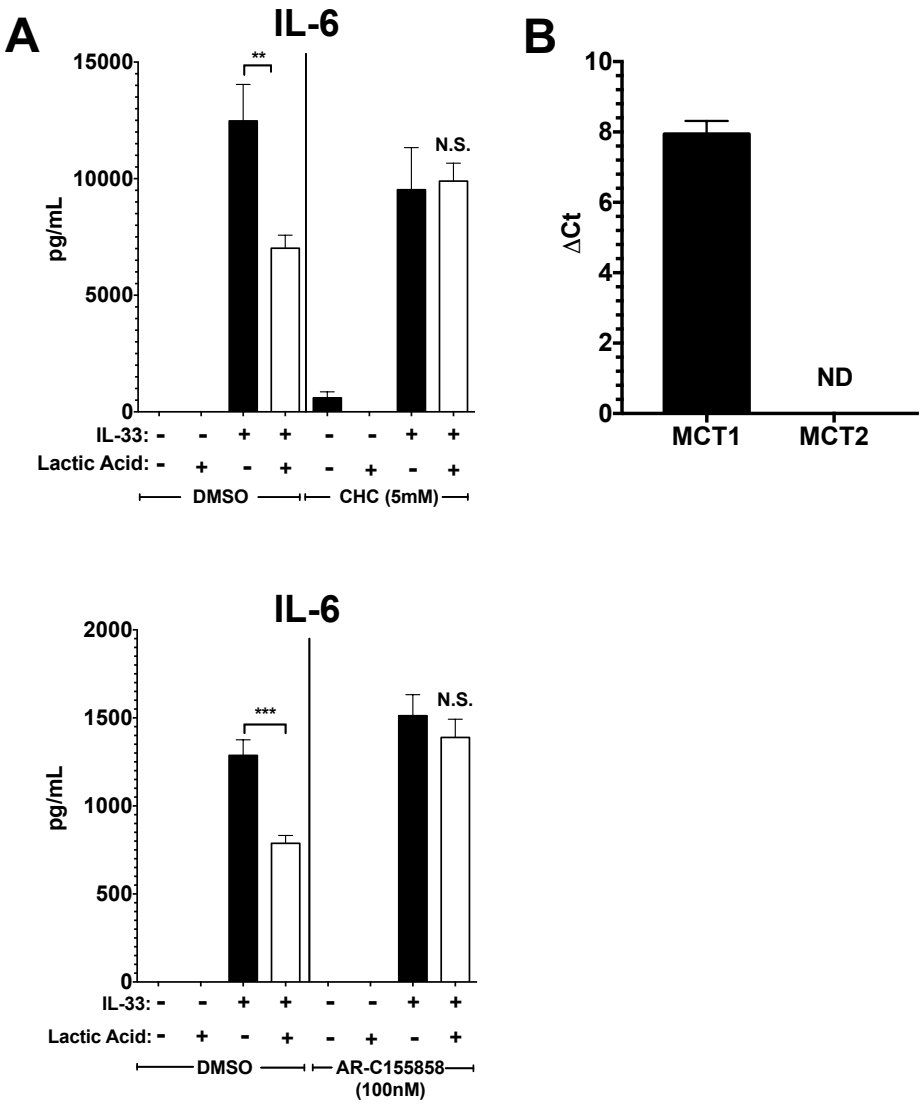

FIGURE 3.6 LA effects are MCT-1 dependent. A) BMMC were treated with either vehicle (DMSO) or the indicated MCT inhibitors, α-cyano-4-hydroxycinnamic acid (CHC) or AR-C155858 for 1 hour prior to lactic acid or media treatment for 24 hours. Cells were then activated with 100ng/mL of IL-33 for 16 hours, supernatants collected, and IL-6 measured using ELISA. B) MCT-1 and MCT-2 expression was measured during 40 cycles of RT-qPCR using RNA harvested from BMMC. β-actin was used as the housekeeping gene for MCT-1 and GAPDH for MCT-2, based on primer optimization and melting point similarities. ND means "not detectable". Results are representative of three independent experiments using 3 BMMC populations each, and expressed as mean ±SEM. *, $p<0.05$; **, $p<0.01$; ***, $p<0.001$; ****, $p<0.0001$; NS, not significant.

III.4.7 Lactic acid selectively alters IL-33 signaling

We next sought to elucidate how LA alters IL-33 signaling. Flow cytometry revealed a modest (approximately 17%) decrease in surface ST2 expression after 24 hours of LA treatment, which seemed unlikely to explain the inhibitory effects (data not shown). Therefore we examined LA-mediated alterations in downstream signaling events. BMMC were pretreated in 12.5 mM LA for 24 hours and activated with IL-33 before lysis. These lysates were then used to assess changes in TAK1, JNK, p38, NFκB p65, Akt, and ERK phosphorylation, pathways shown to be important for IL-33-mediated mast cell function (118). LA suppressed IL-33-induced activation of NFκB p65, JNK, ERK, and TAK1, did not change p38 phosphorylation, and elevated Akt phosphorylation (Figure 3.7). To determine if blocking these pathways alone is sufficient to mimic LA effects, we treated BMMC with JNK, TAK1, ERK, or NFκB chemical inhibitors. While the JNK inhibitor did not reproduce the same level of suppression, TAK1, NFκB, or ERK inhibition completely abolished IL-33-mediated cytokine production, mimicking LA effects (Figure 3.8). Thus LA inhibits multiple IL-33 signaling cascades, yielding redundant suppression of the pro-inflammatory stimulus.

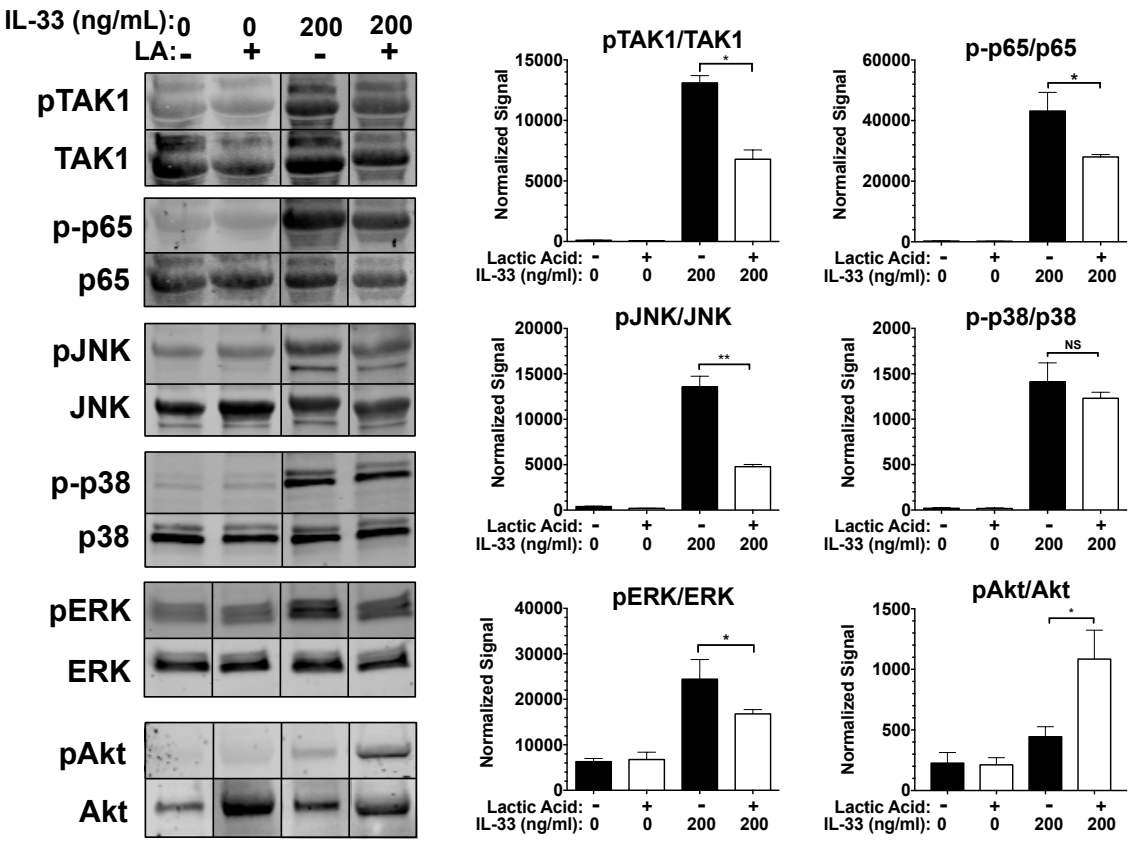

FIGURE 3.7 IL-33 signaling is suppressed by lactic acid treatment. BMMC were pretreated with media or lactic acid then activated with IL-33. Lysates were analyzed by Western blotting to measure expression and phosphorylation of the indicated proteins. Representative blots are shown on the left, while bar charts show mean ± SEM of phospho-protein:total protein ratios calculated using the LI-Cor Odyssey software Image Studio 4.0. Results shown are representative of three experiments done in triplicate. *, $p<0.05$; **, $p<0.01$; ***, $p<0.001$; ****, $p<0.0001$; NS, not significant.

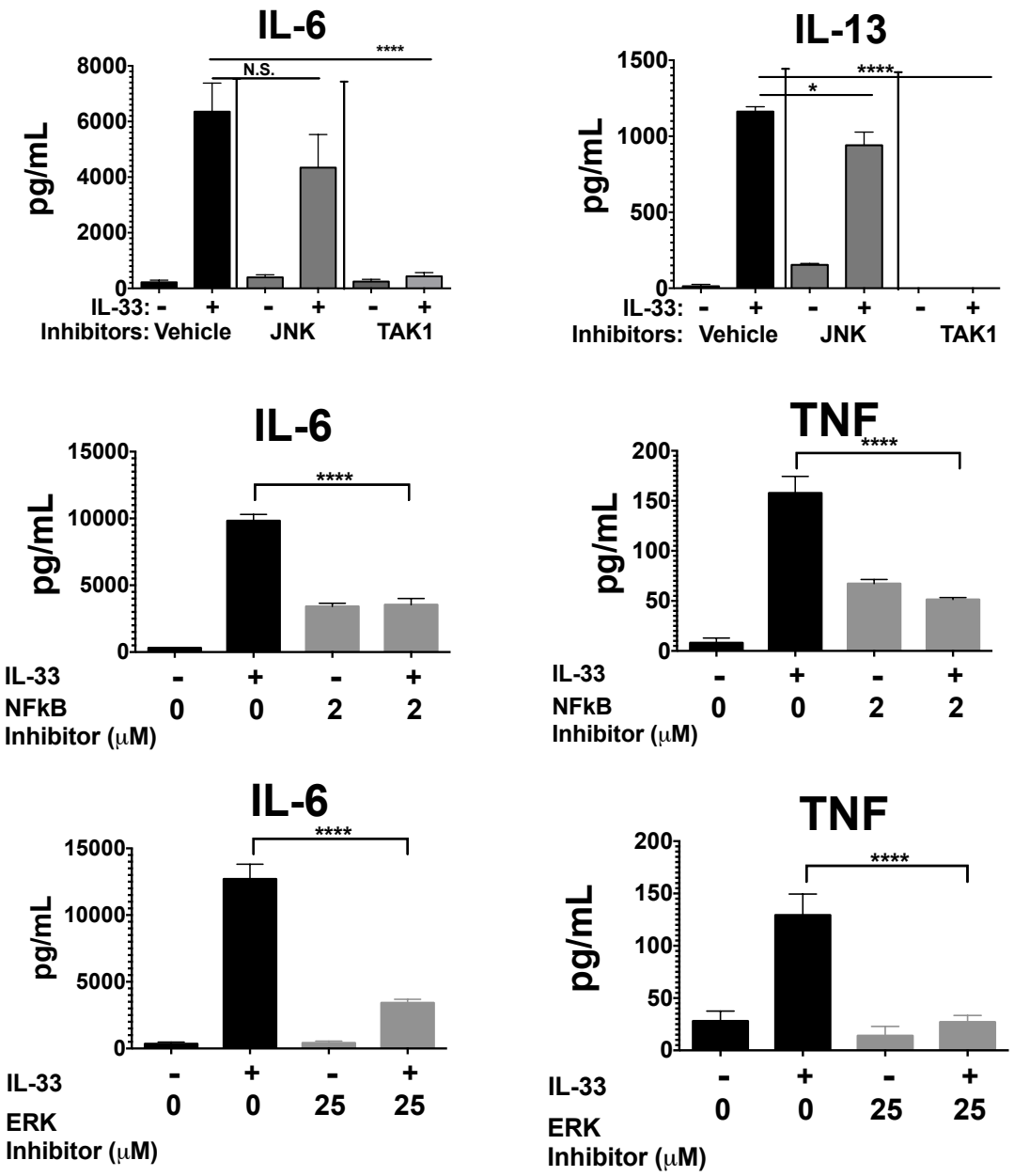

FIGURE 3.8 Signal transduction inhibitors reproduce lactic acid-mediated suppression. BMMC were pretreated for 1 hour with inhibitors of selected signaling pathways (JNK: SP600125, 10 μM; TAK1: (5Z)-7-Oxozeaenol, 5 μM; NFκB: BAY 11-7085, 2 μM; ERK: FR180204, 25 μM). After exposure to the inhibitor, cells were then activated with IL-33 for 16 hours, and supernatants were collected and analyzed via ELISA. These data are shown as mean ± SEM of three independent experiments conducted in triplicate. *, $p<0.05$; **, $p<0.01$; ***, $p<0.001$; ****, $p<0.0001$; NS, not significant.

III.4.8 LA-mediated VEGF enhancement is Akt-dependent

Work in different cell populations has demonstrated a relationship between Akt activation and VEGF expression (119, 120). Thus the enhancement of IL-33-mediated Akt phosphorylation in the presence of LA was noteworthy, because VEGF was the only cytokine studied whose expression was increased by LA. Therefore, we determined if the LA-mediated enhancement of VEGF was Akt-dependent. Prior to LA treatment, BMMC were exposed to an Akt inhibitor for 1 hour, then given LA for 24 hours, followed by IL-33 activation. While in the vehicle alone condition, LA enhanced VEGF production in response to IL-33 activation, the introduction of an Akt inhibitor abolished LA-mediated enhancement of VEGF production (Figure 3.9). This demonstrates that the ability of LA to enhance VEGF secretion is Akt-dependent. However, this experiment also revealed a more complicated relationship, as IL-33 only induced VEGF secretion in the presence of the Akt inhibitor. On balance, our results suggest that Akt represses IL-33-mediated VEGF production, but has a positive impact on LA effects.

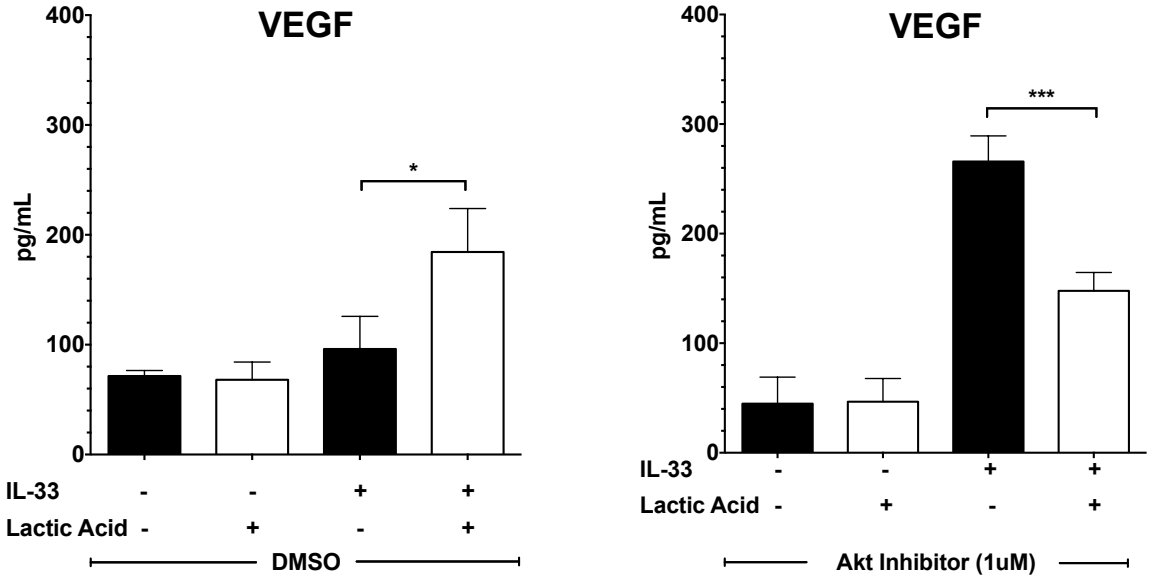

FIGURE 3.9 VEGF enhancement is Akt-dependent. BMMC were pretreated for 1 hours with inhibitors (JNK: SP600125, 10 μM; TAK1: (5Z)-7-Oxozeaenol, 5 μM; NFκB: BAY 11-7085, 2 μM; ERK: FR180204, 25 μM), then activated with IL-33 for 16 hours. Supernatants were collected and analyzed via ELISA. These data are shown as mean ± SEM of three independent experiments conducted in triplicate. *, $p<0.05$; **, $p<0.01$; ***, $p<0.001$; ****, $p<0.0001$; NS, not significant.

III.4.9 LA-mediated enhancement of VEGF is specifically Akt1-dependent

While Figure 3.9 showed that VEGF enhancement in response to LA treatment and IL-33 activation is Akt-dependent, a risk with using chemical inhibitors is the possibility of off-target effects. Therefore we corroborated these findings using siRNA targeting specific Akt isoforms. Using the Jackson Phenome Database, we were able to rule out Akt3 as a target, since myeloid cells did not express this isoform. Therefore, we targeted Akt1 and Akt2 to determine if either is necessary for the enhancement of VEGF in response to LA and IL-33. siRNA was transfected into BMMC using AMAXA Nucleofector Technology from Lonza. There were four groups that received siRNA transfection: negative control, Akt1, Akt2, and Akt1+Akt2. Cells were incubated for 48 hours after transfection before being treated with LA for 24 hours, and activated with IL-33 for 16 hours. Supernatants were analyzed by ELISA. Figure 3.10 shows that while LA enhanced VEGF secretion in cells transfected with control or Akt2-targeting siRNA, the group transfected with siRNA against Akt1 was resistant to LA effects. Similarly, the group with siRNAs against both Akt1 and Akt2 were not able to enhance VEGF with LA treatment. This confirms the chemical inhibitor data from Figure 3.9, and specifically identifies the Akt1 isoform as being required for LA to enhance VEGF secretion.

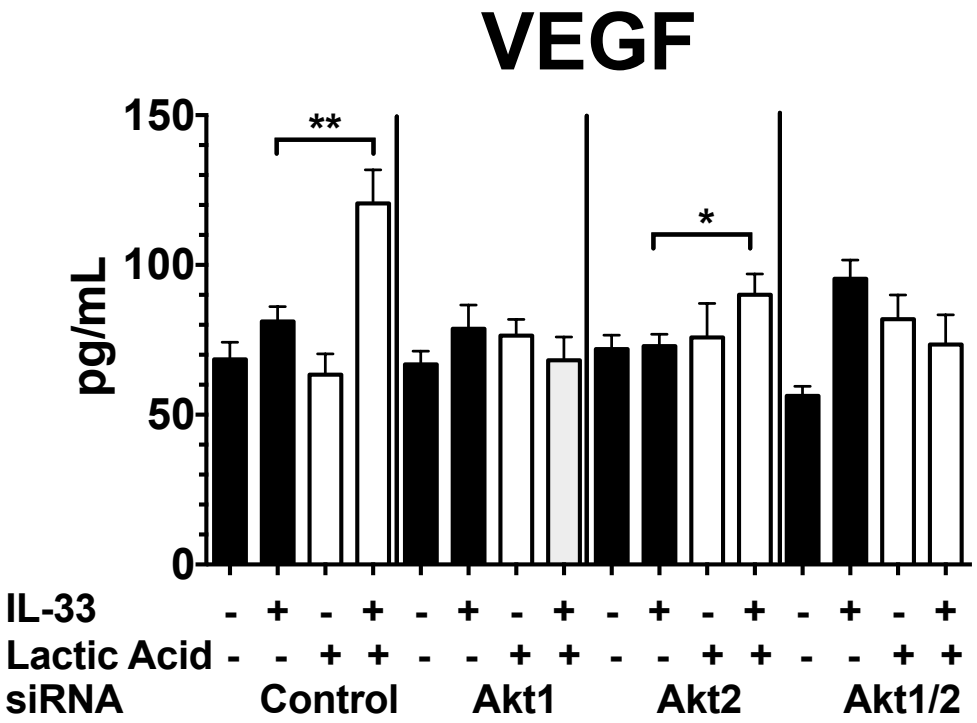

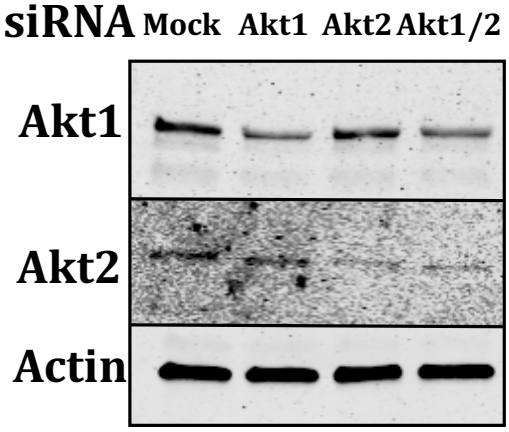

FIGURE 3.10 VEGF enhancement is specifically Akt1-dependent. BMMC were transfected with negative control, Akt1, Akt2, or Akt1+Akt2 siRNA, then treated with LA for 24 hours. Cells were then activated with IL-33 for 16 hours, and supernatants were collected and analyzed via ELISA. These data are representative of three independent experiments conducted in triplicate and are shown as mean ± SEM. *, $p<0.05$; **, $p<0.01$; ***, $p<0.001$; ****, $p<0.0001$; NS, not significant.

III.4.10 LA enhances HIF-1α expression while selectively suppressing miR-155-5p

The microRNA miR-155 has recently emerged as a powerful pro-inflammatory regulator, by virtue of its ability to target and suppress inhibitory proteins (121). Since LA is known to promote HIF-1α production (101, 122, 123) and HIF-1α can control miR-155 expression (124-126), we hypothesized that LA-induced HIF-1α might suppress miR-155, yielding a net negative effect on IL-33 signaling. After 6 hours of LA treatment, HIF-1α mRNA increased nearly 3-fold, while miR-155-5p was suppressed >50% in BMMC. Interestingly, the miR-155-3p species was unaffected, indicating selectivity of these effects (Figure 3.11).

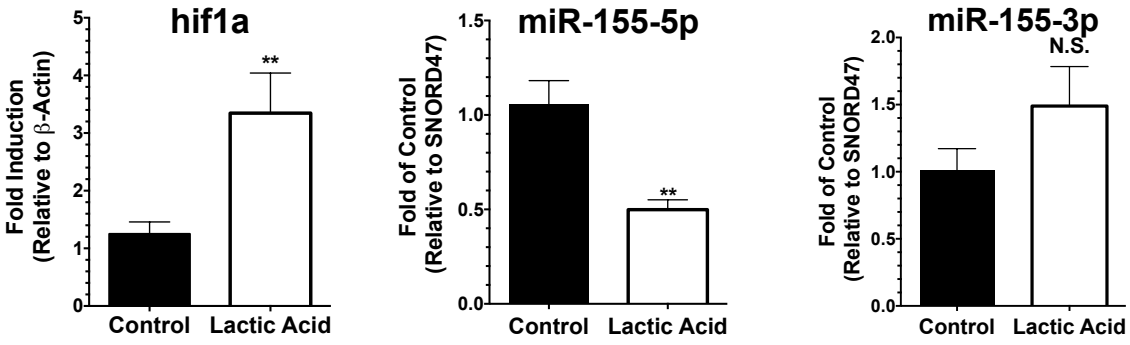

FIGURE 3.11 Lactic acid enhances HIF-1α and suppresses miR-155-5p BMMC were treated with lactic acid for 6 hours, after which RNA was to measure levels of HIF-1α or miR-155 expression. Results are expressed as mean ±SEM. HIF-1α results are from 3 independent experiments conducted in triplicate, while other data are representative of 2 independent experiments done in triplicate. *, $p<0.05$; **, $p<0.01$; ***, $p<0.001$; ****, $p<0.0001$; NS, not significant.

III.4.11 Suppression of miR-155-5p is HIF-1α-dependent

In an effort to determine if HIF-1α negatively regulates miR-155-5p expression, BMMC were transfected with a control or HIF-1α-targeting siRNA. After 24 hours of incubation, cells were treated with LA for 24 hours and then RNA was extracted to measure miR-155-5p and HIF-1α. Figure 3.12 shows that HIF-1α transfection prevented LA-mediated miR-155-5p suppression, demonstrating that this process is HIF-1 ✔-dependent. Measuring HIF-1α via qPCR confirmed knockdown. Now knowing how miR-155-5p suppression occurs, the next step was to determine if miR-155-5p suppression is required for LA effects on inflammatory cytokine production.

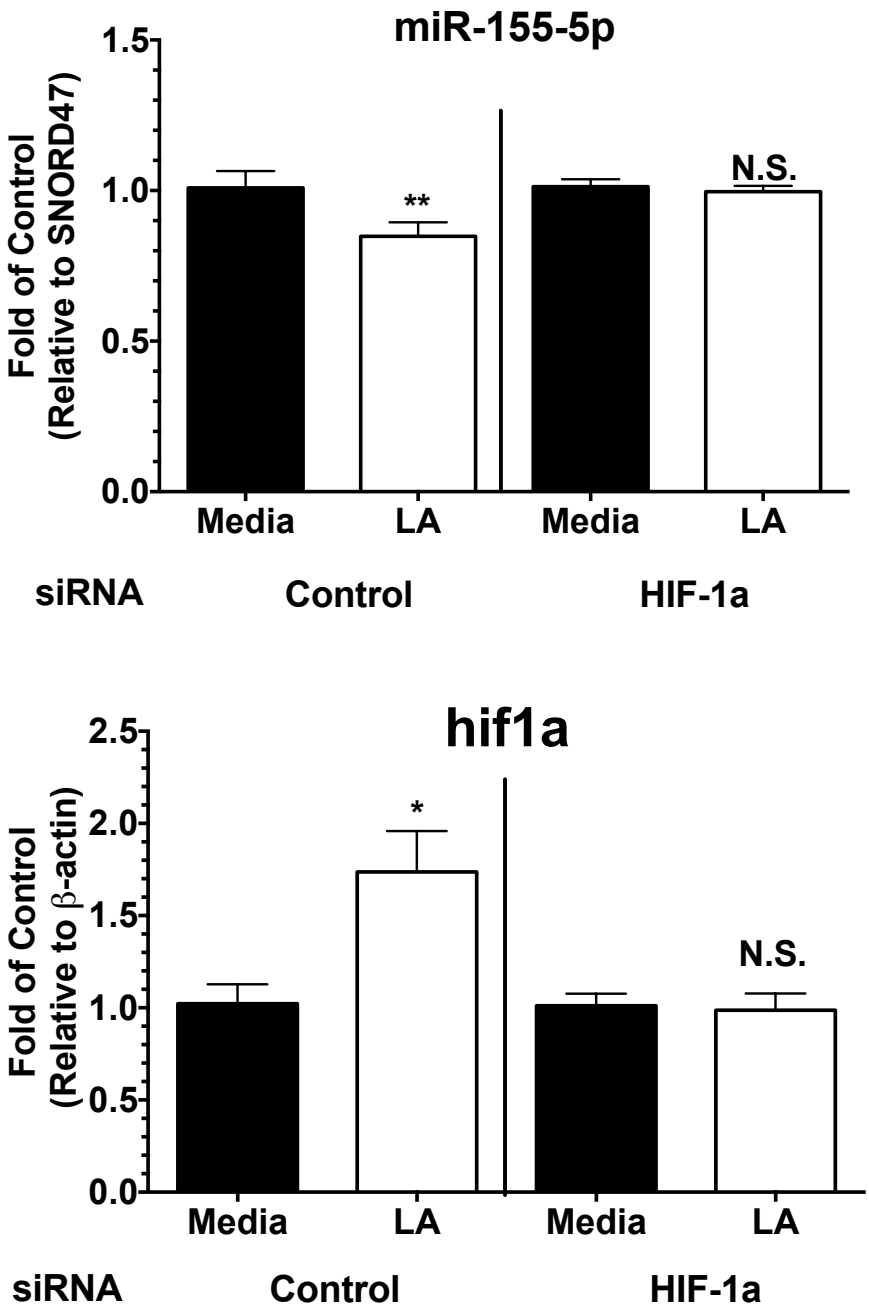

FIGURE 3.12 HIF-1α suppression reduces LA effects on miR-155-5p-dependent Cells were transfected with HIF-1α siRNA using the Amaxa Nucleofector, incubated for 24 hours, treated with lactic acid for 6 hours, and then microRNA and mRNA were collected to measure miR-155-5p, as well as HIF-1α to confirm knockdown. Results are representative of 2 independent experiments done in triplicate. *, p<0.05; **, p<0.01; ***, p<0.001; ****, p<0.0001; NS, not significant.

III.4.12 miR-155-5p blockade is required for LA-mediated suppression

To test the functional importance of miR-155-5p suppression, BMMC were transfected with miR-155-5p or miR-155-3p mimics. BMMC transfected with a miR-155-3p mimic, the species of miR-155 not affected by LA, still showed suppression of IL-33-induced cytokine production in response to LA treatment (Figure 3.13). However, transfecting the miR-155-5p mimic eliminated LA-mediated suppression, suggesting that miR-155-5p downregulation is critical for LA effects (Figure 3.14).

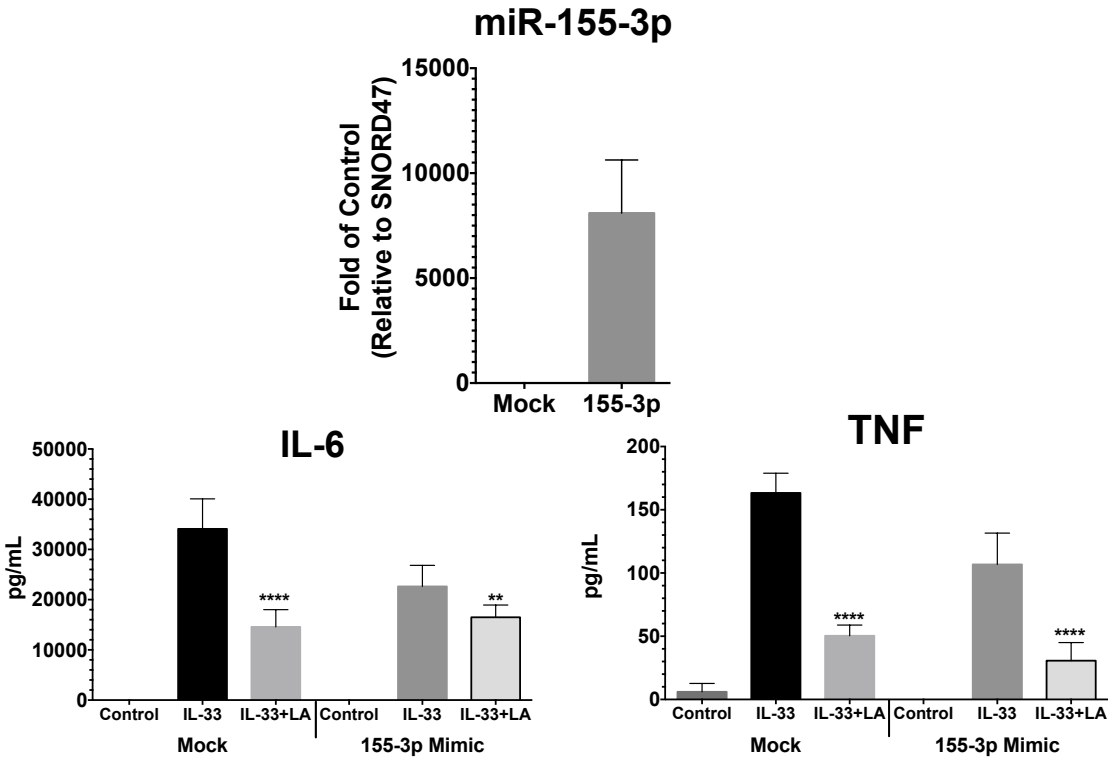

FIGURE 3.13 miR-155-3p overexpression doe not reverse LA effects. BMMC were transfected with either a miR-155-3p mimic or a control/Mock transcript. Following 48 hours of culture, cells were treated with 12.5 mM lactic acid for 24 hours, then activated with IL-33. Cytokines were measured in culture supernatants via ELISA. Results are representative of 2 independent experiments done in triplicate. *, $p<0.05$; **, $p<0.01$; ***, $p<0.001$; ****, $p<0.0001$; NS, not significant.

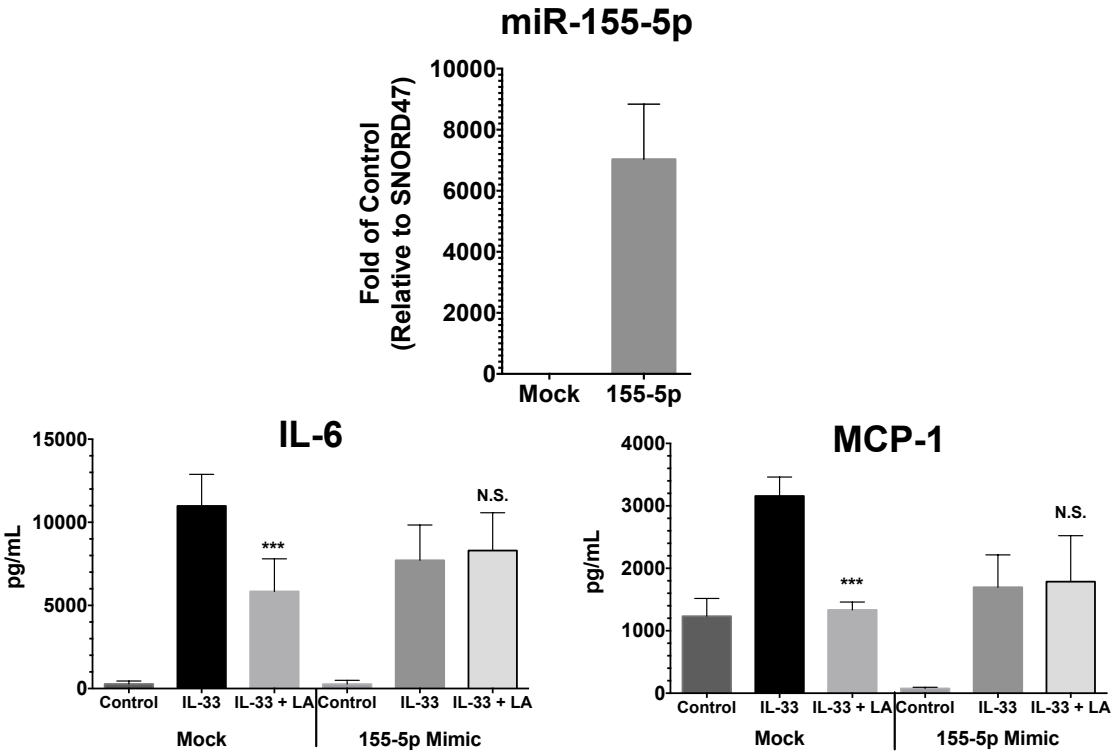

FIGURE 3.14 miR-155-5p overexpression reverses LA effects on IL-33-induced cytokine production. BMMC were transfected with either a miR-155-5p mimic or a control/Mock transcript. Following 48 hours of culture, cells were treated with 12.5 mM lactic acid for 24 hours, then activated with IL-33. Cytokines were measured in culture supernatants via ELISA. Results are representative of 2 independent experiments done in triplicate. *, $p<0.05$; **, $p<0.01$; ***, $p<0.001$; ****, $p<0.0001$; NS, not significant.

III.4.13 Lactic acid suppresses SOCS1, but SOCS1 is not required for cytokine suppression

Based on the importance of miR-155-5p on the ability of LA to suppress inflammatory cytokine production, it became clear how critical it was to determine what miR-155-5p was targeting. Two of the most characterized targets of miR-155 are SOCS1 and SHIP-1 (127). Therefore, we measured the expression of SOCS1 and SHIP-1 in response to LA treatment. After BMMC were treated for 6 hours with LA, RNA was extracted and used to measure SOCS1 and SHIP-1 expression. As shown in Figure 3.15, LA enhanced SOCS1 mRNA expression, while there was no change in SHIP-1. To determine if SOCS1 enhancement is required for cytokine suppression in response to LA, SOCS1 was knocked down in BMMC using siRNA. After siRNA transfection, cells were treated with LA for 24 hours, activated with IL-33, and supernatants were collected 16 hours later and analyzed via ELISA. Interestingly, Figure 3.15 shows that SOCS1 knockdown did not restore cytokine levels in the presence of LA. Therefore, SOCS1 enhancement is not required for suppression of IL-33-mediated inflammatory cytokines in the presence of LA.

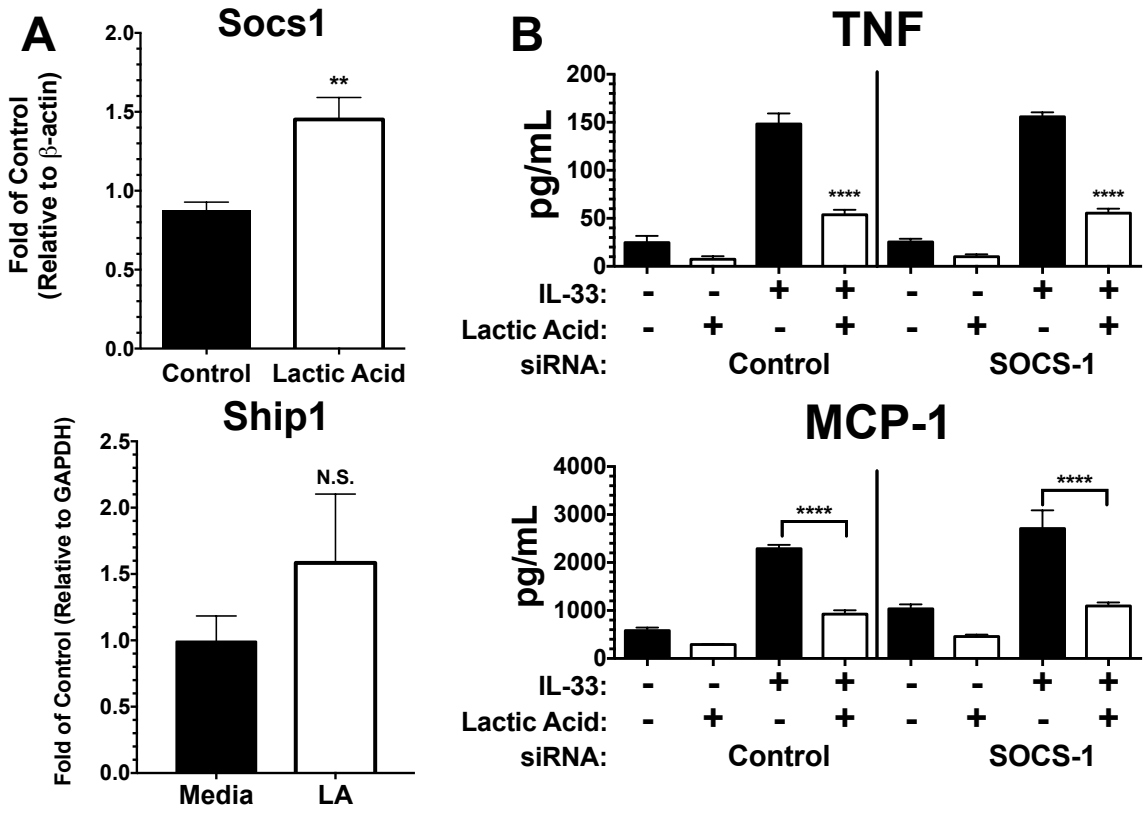

FIGURE 3.15 Lactic acid suppresses SOCS1, but SOCS1 is not required for cytokine suppression A) BMMC were treated with 12.5 mM LA for 24 hours. Following LA treatment, RNA was harvested and analyzed via qPCR to measure expression of key inhibitory molecules, SOCS1 and SHIP-1 at the mRNA level. Expression was normalized to media control group. B) BMMC were transfected with 75 nM of siRNA for either SOCS-1 or negative control and incubated in IL-3 and SCF for 48 hours. BMMC were then treated with 12. 5 mM LA for 24 hours and then activated with 100 ng/mL IL-33. Supernatants were collected 16 hours later and analyzed via ELISA. *, $p<0.05$; **, $p<0.01$; ***, $p<0.001$; ****, $p<0.0001$; NS, not significant.

III.4.14 Lactic acid suppresses IL-33-mediated inflammatory responses in vivo

Thus far, we have shown that LA suppresses IL-33-mediated mast cell inflammatory responses *in vitro* and *ex vivo*. We next broadened this to an *in vivo* model. Intraperitoneal IL-33 injection elicits mast systemic cytokine production, likely from many ST2-expressing cells (36). Mice were first injected intraperitoneally with LA, then 16 hours later injected with IL-33. IL-33 greatly elevated plasma MCP-1 and IL-13 levels, an effect that was nearly completely reversed by LA pretreatment (Figure 3.16). Thus LA antagonizes the pro-inflammatory effects of IL-33 *in vivo* as well as *in vitro*.

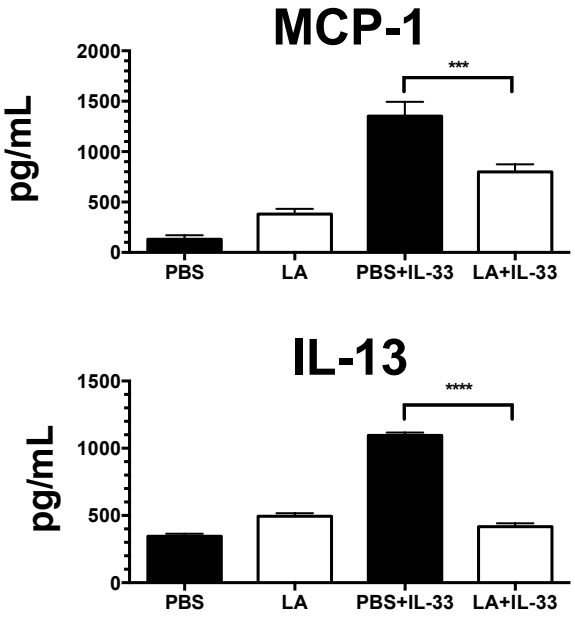

FIGURE 3.16 Lactic acid suppresses IL-33-mediated inflammation *in vivo*. C57BL/6J mice were first injected subcutaneously with ketoprofen (1mg/kg in PBS), as an analgesic. 30 minutes later, mice were injected with either lactic acid (4mg/kg in 4%(w/v) PBS) or PBS alone. 16 hours-post LA injections, mice were injected with either PBS or IL-33. After 4 hours, mice were euthanized, blood was collected via cardiac puncture, and plasma cytokines were measured by ELISA. Results are expressed as mean ±SEM and n=7. *, $p<0.05$; **, $p<0.01$; ***, $p<0.001$; ****, $p<0.0001$.

III.4.15 Lactic acid suppresses primary human skin mast cells in an MCT-dependent manner

In order to determine if our mouse data are consistent in human mast cells, we assessed the effects of LA on IL-33-induced cytokine production using primary human skin mast cells (SkMC). SkMC from 5 healthy donors were harvested and cultured in the presence of LA for 24 hours. Because SkMC respond poorly to IL-33 alone, we measured IL-33-mediated enhancement of IgE responses (90). LA pretreatment suppressed both IgE-mediated cytokine production and the enhancing effects of IL-33. Furthermore, LA effects were completely or partially reversed by the MCT inhibitor CHC (Figure 3.17). These data suggest that LA consistently suppresses IL-33 signaling, and mediates these effects via MCT transporters in both murine and human mast cells.

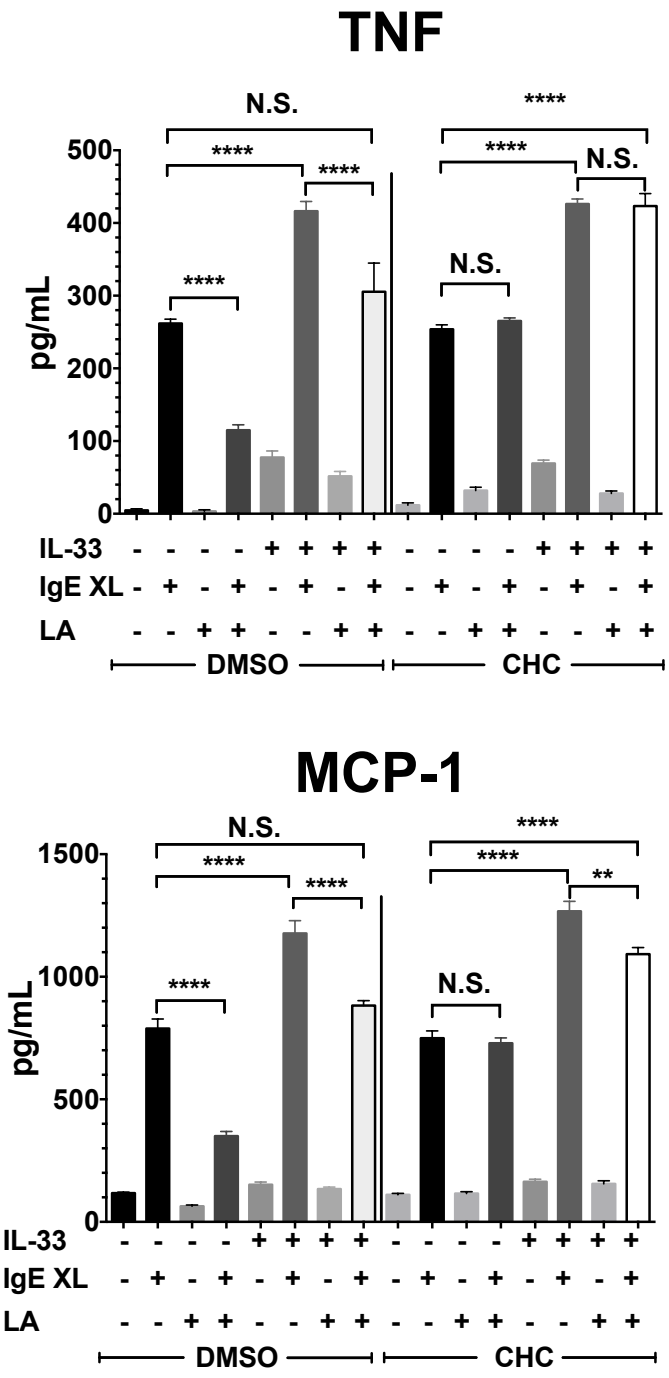

Figure 3.17 Primary human skin mast cell mediator release is decreased by lactic acid in an MCT-dependent manner. Primary human skin mast cells cultured from 5 donors were treated with either DMSO or an MCT inhibitor (CHC; 2.5mM), along with media alone or 12.5 mM lactic acid for 24 hours, then activated with either IL-33, IgE-Ag cross linking (IgE XL), or both. Supernatants were collected 16 hours later and analyzed by ELISA. *, $p<0.05$; **, $p<0.01$; ***, $p<0.001$; ****, $p<0.0001$; N.S., not significant.

III.5 DISCUSSION

PLA is among the most widely used synthetic polymers in biomedical research and in clinical applications (82). In order to better understand how degradative byproducts of scaffolds can alter innate immune responses, treating mast cells with lactic acid was a logical choice. Most of the work to date with respect to polymer degradation has assessed how degradation alters mechanical integrity and capacity for tissue integration (128). There are certainly other feasible options when considering degradative byproducts, but since LA plays a major role in many metabolic and pathological conditions, we chose it as our focus.

LA is a metabolic byproduct of anaerobic glycolysis and is known to be increased in a variety of pathological states including cancer, obesity, type II diabetes and wound healing (102-105). LA concentrations, which are 1-2mM in plasma at rest, can reach 20mM during acute exercise and 40mM at tumor sites (101, 108). While LA has been shown to inhibit cytotoxic T cell-mediated killing, promote M2 macrophage differentiation, and prevent dendritic cell antigen presentation, its effects on mast cell function have not been investigated (96-98, 101). Mast cells are known to participate in allergic disease, parasitic infection, and resistance to bacteria. They have less-defined roles in cancer and wound healing, but are known to participate in both (58, 86-88, 129-132). Our data indicate that LA alters inflammatory cytokine production in mast cells stimulated with IL-33, a cytokine elevated in many pathological conditions. In the context of cancer, this could promote tumor escape from immune surveillance, an effect tumor-derived LA has been argued to have on tumor-associated macrophages (101). In wound healing, LA may prevent a destructive chronic inflammatory response, but might also reduce pathogen clearance.

BMMC exhibited decreased inflammatory cytokine production when exposed to LA prior to IL-33 activation. Similar to reports on other cell types, the inhibitory effects of LA in our assays were tightly linked to acidity (97). While sodium lactate increases NFκB signaling and transcription in macrophages stimulated with LPS (103, 133), LA decreases LPS-mediated signaling in macrophages (111, 112). Sodium lactate is the salt of LA, with the deprotonated carboxyl group linked to sodium via an ionic bond. Our results show that without the decrease in pH, IL-33-induced cytokine and chemokine production was unaltered. Additionally, we demonstrated that the MCT-1 transporter is critical for LA-mediated suppression. Others have shown that MCT-1 employs proton co-transport with lactate (134), suggesting an explanation for the importance of acidity in our assays. Interestingly, MCT-1 was recently shown to require a chaperone protein, CD147, for its function (114). This warrants further investigation of mast cell CD147 expression and how this protein contributes to LA effects.

LA has been shown to suppress TLR4-mediated signaling and cytokine production (111, 112). IL-33 signaling is still being unraveled, but shares common molecular pathways with TLRs. IL-33 activates the MAP3K TAK1 as an apical kinase, with resulting downstream activation of MAP kinases, NFκB, and AP-1 in mast cells (30). Our data show that while p38 phosphorylation is not affected, TAK1, NFκB p65, ERK and JNK phosphorylation were significantly diminished, and this correlated with decreased cytokine production. Chemical inhibitors of TAK1, ERK, or NFκB each mimicked LA effects on IL-33 signaling, while JNK inhibition had no effect. Whether LA effects on multiple signaling proteins are simply due to apical TAK1 blockade yielding multiple downstream consequences, and how LA inhibits phosphorylation are issues that require further study.

In response to LA treatment, HIF-1α expression was elevated in mast cells, as predicted by previous studies (101, 122, 123). A known molecule targeted by HIF-1α in other systems is miR-155, which is pro-inflammatory in many lineages (125). Studies show that miR-155 possesses a hypoxia response element in its promoter region, further connecting HIF-1α and miR-155 (135). We demonstrated that LA specifically suppresses miR-155-5p, while leaving miR-155-3p unaltered. This selectivity appears consequential, since miR-155-5p but not -3p overexpression reversed LA effects. Despite originating from the same transcribed pri-miRNA, it is not unusual for 5p and 3p strands from the same pri-miRNA to be expressed differently in mature form in response to different stimuli. By nature of being complimentary to one another, 3p and 5p strands can have very different targets, eliciting effects with negative or positive feedback on the degradation of these strands (136-138). Additionally, HIF-1α silencing restored miR-155-5p levels, indicating that in mast cells, HIF-1α negatively regulates miR-155-5p expression. This is another example of lineage-restricted effects, since HIF-1α induces miR-155 in populations such as epithelial cells (135). Clearly our understanding of hypoxia and tissue acidity will need to account for variations in lineage, allowing for nuanced effects.

The functional relevance of these findings is supported by consistent effects in vivo and on primary human mast cells. Several features of these experiments warrant further discussion and investigation. First, a recent paper showed that reduced pH enhances IgE-mediated mouse mast cell cytokine production (139). We incidentally noted the opposite while stimulating human mast cells with IgE (Figure 7). The differences between these studies could be due to the acids employed, assay parameters, or species variation. Kamide et al. did not specify the acid they employed. A strong acid might have different effects

than LA (pKa=3.86) and may not be transported by MCT-1. The previous study also employed a 3-hour incubation, whereas we cultured for 24 hours. However, our IL-33 studies showed no enhancing effects on inflammatory cytokines at time points between 0-48 hours. More work should be done to examine the effect of LA on IgE-signaling. It is also important to state that our in vivo assay did not limit LA effects to mast cells, though mast cells are activated by systemic IL-33 (36). A variety of cytokine-producing cells respond to IL-33. This list continues to grow and currently includes mast cells, basophils, eosinophils, ILC2, some Th2 cells, and macrophages (32, 140-143). Therefore our results demonstrate that LA can antagonize IL-33-induced systemic cytokine production in vivo, but do not restrict these effects to a specific lineage. While it is striking to find nearly complete suppression of cytokines in vivo, further study is needed to reveal how LA acts on various lineages.

In conclusion, LA is able to suppress inflammatory responses among IL-33-activated mast cells in a pH- and MCT-1-dependent manner. This suppression requires a HIF-1α-dependent blockade of miR-155-5p. LA's ability to suppress IL-33-mediated inflammatory responses was reproduced *in vivo* and in human mast cells. These data provide fundamental insight into how tissue microenvironments, especially in pathological conditions, can greatly alter mast cell responses. Given our expanding comprehension of myriad activities played by IL-33 and mast cells, understanding and intervening in these signaling cascades is likely to be clinically important.

III.6 CONCLUSION

In this study we demonstrated that LA is able to suppress IL-33-mediated inflammatory cytokine secretion while enhancing VEGF secretion. The suppressive effects of LA on IL-33-mediated inflammatory cytokine secretion were also true of *ex vivo*-derived peritoneal mast cells. LA not only suppressed cytokine secretion but also production, as determined by intracellular staining for cytokines. As illustrated in Figure 3.18, LA effects were pH- and MCT-1-dependent, based on the use of sodium lactate and an MCT-1/2 inhibitor. LA also significantly reduced IL-33-mediated TAK1, p65, ERK, and JNK phosphorylation, while leaving p38 phosphorylation unchanged. Interestingly, Akt phosphorylation was enhanced in the presence of LA, which corresponded to the increase in VEGF. In the presence of an Akt inhibitor, LA was no longer able to enhance VEGF production. To further identify the mechanism of VEGF enhancement, siRNAs were used that specifically knocked down the expression of the different isoforms of Akt, which showed that VEGF enhancement in response to LA and IL-33 was Akt1-dependent. LA treatment enhanced HIF-1α mRNA expression, which negatively regulated miR-155-5p, an activity required for LA effects. In order to determine what miR-155-5p targets are responsible for LA-mediated suppressive effects, we measured SOCS1 and SHIP-1 expression. While SHIP-1 expression was unchanged in response to LA treatment, SOCS1 was elevated. However, when SOCS1 expression was knocked down by siRNA, there were no changes in cytokine production, indicating that SOCS-1 may not be required for LA-mediated suppression. When injected *in vivo* with IL-33, LA suppressed MCP-1 and IL-13 in the systemic circulation. Lastly, when human SkMC were treated with LA, IL-33 enhancement of IgE crosslinking was abolished in the presence of LA, and this suppression was shown to be MCT-dependent. This work

demonstrates the potential of PLA-based materials to alter mast cell behavior in the TME, suppressing inflammatory actviities while promoting angiogenic functions. These data inform our use of PLA scaffolds and offer new insight into how LA may serve as a feeback regulator of inflammatory resposnes in which LA is elevated.

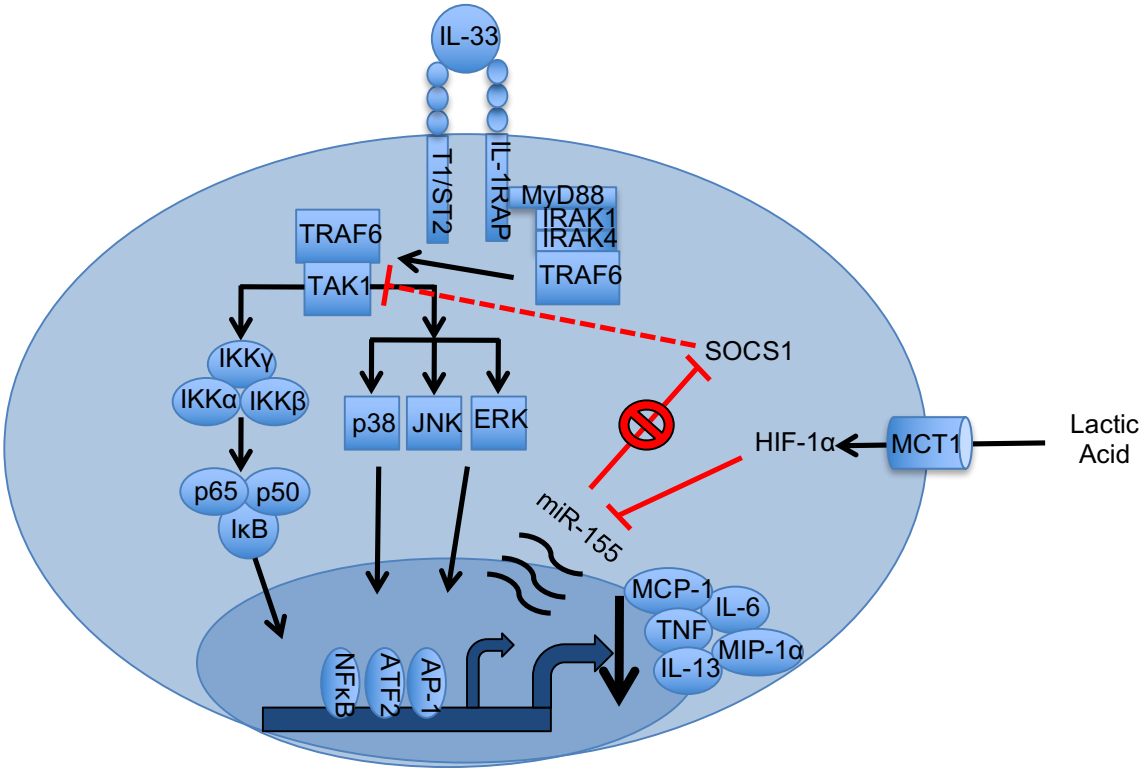

FIGURE 3.18 Model of LA effects on IL-33 activation This model illustrates the mechanism by which LA alters IL-33-mediated mast cell activation.

CHAPTER IV: LACTIC ACID SUPPRESSES IgE-MEDIATED INFLAMMATORY RESPONSES YET PROMOTES MAST CELL-MEDIATED ANGIOGENESIS

II.1 ABSTRACT

IgE crosslinking is a powerful means of activating mast cells and potentiating inflammation and angiogenesis in the local tissue microenvironment. The degradation of PLA-based biomaterials introduces lactic acid into the local tissue, potentially altering IgE-mediated mast cell responses. Therefore, in order to better understand how these degradative byproducts can alter mast cell-mediated inflammation and angiogenesis, BMMC were treated with LA prior to IgE crosslinking. LA enhanced IgE-mediated cytokines and chemokines from BMMC, including VEGF. Conditioned supernatants from IgE crosslinked BMMC in the presence of LA promoted robust tube formation of endothelial cells, confirming the enhancement of angiogenic mediators in response to LA. Interestingly, IgE-mediated cytokine production from human and mouse *ex vivo*-derived mast cells were suppressed in the presence of LA. These mast cells being more physiologically relevant, were used throughout the rest of the work. PMCs pre-treated with LA secreted less inflammatory cytokines in response to IgE crosslinking but enhanced VEGF secretion. Similarly, skin mast cells from human donors secreted less IgE-mediated TNF and MCP-1 in the presence of LA. Using PMCs, the suppression of cytokines in response to LA was shown to be pH- and MCT-1-dependent. Additionally, LA treatment reduced the phosphorylation of Syk, Btk, and ERK, key signaling molecules in the IgE pathway. Lastly, LA injected into mice undergoing passive systemic anaphylaxis reduced the temperature drop, indicating those mice underwent less severe anaphylaxis. All together, this demonstrates that LA suppresses IgE-mediated from *ex vivo* mast cells and mast cell responses *in vivo*.

II.2 INTRODUCTION

While mast cells are responsive to a variety of stimuli, the most well characterized means of activation is by IgE-antigen crosslinking. Mast cells express the high affinity IgE receptor, FcεRI, which binds with an approximate affinity of $K_A = 10^{10} M^{-1}$ (144). In mast cells, FcεRI has a tetrameric structure that consists of an IgE-binding α-chain, a signal-amplifying β-chain, and two disulfinde-linked γ-chains critical for signaling. Both the β-chain and γ-chains bear an immunoreceptor tyrosine-based activation motif (ITAM) that propagates signal transduction FcεRI crosslinking (145).

After FcεRI aggregation, the beta chain-associated Src kinase Lyn phorphorylates ITAMs on their tyrosine residues and promotes the further association of Lyn as well as Fyn, another Src-family kinase, on the β-chain and Syk on the γ-chains. After Syk docks at the SH2 domain of the activated γ-chain ITAM, activated Syk activates the adaptor protein linker for activation of T cells (LAT). LAT activation promotes the assembly of a multimolecular protein complex around LAT, that includes GRB2, SLP76, PLCγ, and GADS. This protein complex leads to downstream activation of MAPKs critical for cytokine production. In addition to LAT activation, another important substrate of Syk is PI3K, which promotes the phosphorylation of PIP2 to PIP3 and subsequent activation of several kinases, including Akt and BTK. Collectively these lead to the activation of transcription factors, including NFκB, AP-1, and Stat5 (145-148), which promote cytokine synthesis and secretion. Additionally, these kinases drive calcium-dependent mast cell degranulation. Figure 4.1 features an illustration of IgE signaling summarizing these proceses. Interestingly, while Lyn serves as an early mediator in the initial wave of IgE signal transduction, it also supports negative feedback regulation of IgE signaling.

Lyn tyrosine phosphorylates a non-canonical beta chain ITAM that promotes recruitment of the phosphatases SHP-1 and SHIP-1 (149, 150). Lyn also phosphorylates C-terminal Src kinase binding protein (CBP), which leads to antagonism of Src kinase activity. These seemingly conflicting events demonstrate the nuanced nature of IgE signaling in mast cells.

Mast cell activation via IgE crosslinking consists of early and late phase responses. The early phase consisting of rapid mast cell degranulation, which introduces a myriad of pre-formed mediators, including histamine, proteases, arachidonic acid metabolites, proteoglycans, and some cytokines (151). This is rapidly followed by release of inflammatory lipids, including arachidonic acid metabolites and sphingosine-1-phosphate. The late phase response consists of de novo cytokine and chemokine synthesis, which can dictate the responses of other cell populations (36, 151). These responses are collectively inflammatory, but anti-inflammatory and pro-angiogenic activities also occur, including synthesis and activation of latent TGFβ–1, and angiogenesis induced by VEGF, tryptase, and chymase (42-45). While most work exploring IgE activation is in the context of allergies, mature mast cells are present in all tissues except blood, mostly at perivascular locations. Hence IgE-mediated mast cell responses offer a unique opportunity to modulate the FcεRI signaling to alter tissue remodeling and blood vessel growth (43, 47, 152).

In evaluating how the degradative byproducts of polylactic acid-based biomaterials can alter mast cell responses, and given the potency of IgE crosslinking in activating mast cells, as well as the potential to modulate inflammation and angiogenesis, it would be a natural extension of this work to explore how LA alters IgE-mediated

responses of mast cells. Therefore, variously sourced mast cells underwent activation via IgE crosslinking in the presence or absence of LA to determine how this alters IgE-mediated activation.

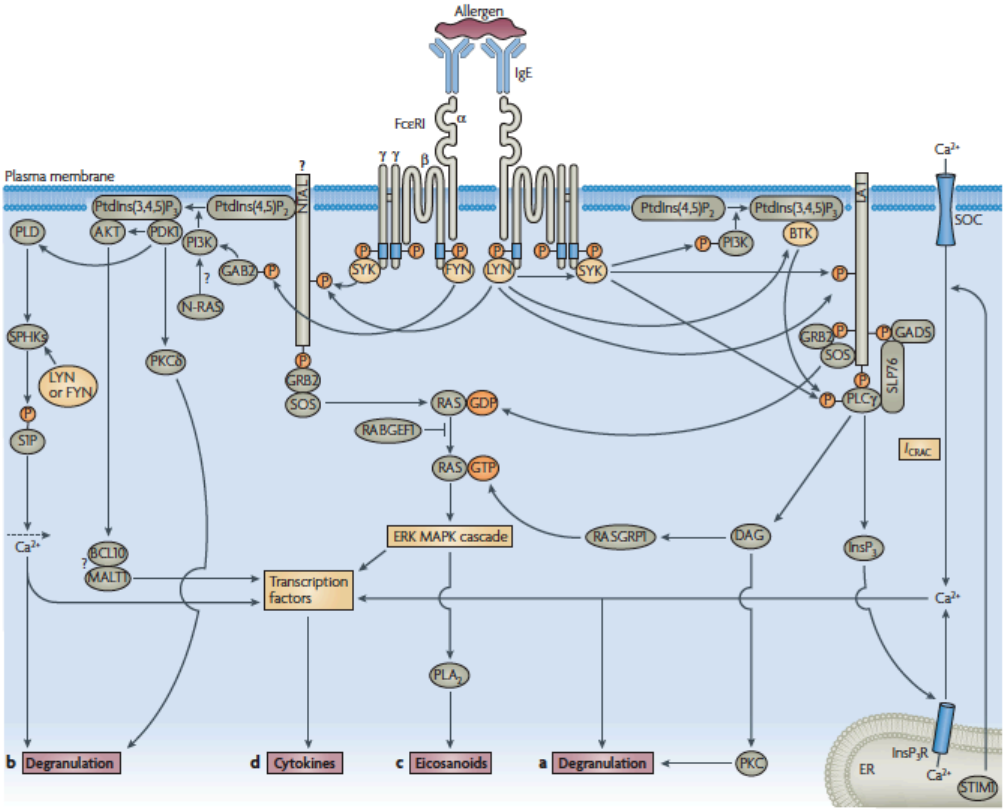

FIGURE 4.1 Mast cell IgE signaling pathway (153) IgE-Ag crosslinking promotes the aggregation of FcεRI and activation of various downstream signaling mediators. These signaling events are mediated by tyrosine phosphorylation of ITAMs by Lyn on the β-chain, which recruits more Lyn as well as Fyn on the β-chain ITAMs and Syk docking to ITAMs on the γ-chains. From there, various mediators are activated that lead to the immediate release of pre-formed mediators, in addition to promoting the *de novo* synthesis of cytokines and chemokines.

IV.3 MATERIALS AND METOHDS

IV.3.1 Animals

C57BL/6J male and female mice were purchased from The Jackson Laboratory (Bar Harbor, ME), bred in the VCU animal care facility, and used at a minimum of 6 weeks old, with approval from the Virginia Commonwealth University institutional animal care and use committee (IACUC).

IV.3.2 Mouse Mast Cell Cultures

BMMC were derived by harvesting bone marrow from C57BL/6 mouse femurs, followed by culture in complete RPMI (cRPMI) 1640 medium (Invitrogen Life Technologies, Carlsbad, CA) containing 10% FBS, 2mM L-glutamine, 100 U/ml penicillin, 100 μg/ml streptomycin, 1mM sodium pyruvate, and 1mM HEPES (all from Corning, Corning, NY), supplemented with IL-3-containing supernatant from WEHI-3B cells and SCF-containing supernatant from BHK-MKL cells. The final concentrations of IL-3 and SCF were adjusted to 1.5ng/ml and 15ng/ml, respectively, as measured by ELISA. BMMC were used after 3 weeks of culture, at which point these primary populations were >90% mast cells, based on staining for c-Kit and FcεRI expression. Mouse peritoneal mast cells were obtained by collecting peritoneal lavage from C57BL/6 mice, which cultured in cRPMI supplemented with recombinant mouse IL-3 and SCF at 10ng/mL each. Peritoneal mast cells were used after 14 days, at which these *ex vivo* expanded cells were approximately 85% mast cells, based on staining for c-Kit and FcεRI expression.

IV.3.3 Cytokines and Reagents

Recombinant mouse IL-3 and SCF, as well as mouse IL-6, TNF, and MCP-1 (CCL-2) ELISA kits were purchased from BioLegend (San Diego, CA). Mouse MIP-1α (CCL-3) and VEGF ELISA kits were purchased from PeproTech (Rocky Hill, NJ). Mouse IL-13 ELISA kits were purchased from eBioscience (San Diego, CA). L-(+)-lactic acid and Sodium L-lactate were purchased from Sigma-Aldrich (St. Louis, MO). Human TNF and MCP-1 ELISA kits were purchased from BD OptEIA (BD Biosciences; Franklin Lakes, NJ).

IV.3.4 Cell Culture Conditions

For IgE crosslinking, BMMC and PMC were incubated with 500 ng/mL of anti-DNP IgE overnight. BMMC and PMC were then washed and were cultured (at $2x10^6$ cells/mL) in 20ng/mL of IL-3 and SCF in cRPMI. An equal volume of 25mM LA in cRPMI was added to the cell suspension, resulting in a final cell concentration of $1x10^6$ cells/ml, 10ng/mL of IL-3 and SCF, and 12.5mM LA. Control conditions received cRPMI in place of LA. After 24 hours of pretreatment in LA media, cells then received 50ng/mL of DNP-HSA for 16 hours, after which supernatants were collected. pH was measured for media alone, lactic acid, and lactate-conditioned media using the Beckman Phi 45 pH meter.

IV.3.5 Degranulation Assay

Mast cells were first given IgE (500 ng/mL) overnight and then treated with 12.5 mM LA for 24 hours. During that 24 hour treatment with LA, the last 4 hours were done in the absence of IL-3 and SCF to starve the mast cells prior to activation. Then mast cells were activated by crosslinking IgE with DNP. 10 minutes after DNP is given, cells were

washed twice with PBS and stained for degranulation using two antibodies, PE anti-CD63 and APC anti-CD107a (BioLegend, San Diego, CA). Cells were washed twice with PBS, resuspended in FACS buffer, and analyzed via FACS.

IV.3.6 In Vitro Angiogenesis Assay

Angiogenesis was measured using the Angiogenesis Starter Kit from ThermoFisher Scientific (catalog no. A1460901, Waltham, MA). The assay entailed first culturing human umbilical vein endothelial cells (HUVECs) in T175 flasks in M200 media supplemented with Gibco Large Vessel Endothelial Supplement. When HUVECs reached approximately 80% confluency, media was removed and trypsin was added to remove cells from the flasks. Concurrently, 48-well plates were coated with Geltrex Basement Membrane Matrix, which was allowed to polymerize at 37°C for 1 hour. After matrix polymerization, HUVECs were seeded on top and allowed to migrate into the matrix. Next, conditioned media was added on top of the matrix to promote endothelial tube formation. 16 hours after conditioned media was added, images were captured of endothelial tube networks. Quantification was done by doing a blinded count of the number of tubes present in each field of view. A tube was characterized as a connection between two different nodes of cells.

IV.3.7 Human Skin Mast Cell Culture

As approved by the Internal Review Board at the University of South Carolina, surgical skin samples were collected from the Cooperative Human Tissue Network of the National Cancer Institute. Skin mast cells (SkMC) were harvested and cultured from 5

human donors as previously described (107). After 6-10 weeks, mast cells were used at which time purity was nearly 100%, as confirmed with toluidine blue staining.

IV.3.8 Surface Staining with Flow Cytometry

BMMC were given IgE (500 ng/mL) overnight and then treated with 12.5 mM LA for 24 hours. Following LA treatment, BMMC were stained with a PE-anti IgE antibody to determine if LA exposure stripped IgE off the surface of mast cells. Additionally, some BMMC were not given IgE but incubated with LA and stained with a APC-anti-FcεRIα antibody to determine if treatment altered expression of the IgE receptor FcεRI. Cells were run and analyzed on the FACSCelesta.

IV.3.9 PhosFlow

BMMC were given IgE (500 ng/mL) overnight and then treated with 12.5 mM LA for 24 hours. During the last 4 hours of LA treatment, cells were starved from IL-3 and SCF to remove any phosphorylation signals in response to those growth factors. Antigen was given to induce activation and 10 minutes later, cells were fixed by incubating in 1.6% paraformaldehyde. For permeabilization, cells were washed and then slowly added to ice-cold methanol solution while vortexing. Cells were then washed and stained with APC labeled antibodies against pERK1/2, pSyk, and pBtk. Cells were then run and analyzed on the FACSCelesta

IV.3.10 Passive Systemic Anaphylaxis

Age-matched C57BL/6 mice (12 week old mice) first received subcutaneous injections of 1mg/kg ketoprofen from Spectrum Chemical (New Brunswick, NJ) and then 30 minutes later intraperitoneal injections of 4mg/kg of 4% (w/v) LA. 24 hours later, all mice were injected intraperitoneally with anti-DNP IgE (50 μg) and 16 hours later given intraperitoneal injections of DNP (100 μg) to induce anaphylaxis. For histamine-induced anaphylaxis, mice were given the same ketoprofen and LA injections and were given an intraperitoneal injection of 8 mg of histamine 24 hours after the LA injection. The core body temperature of each mouse was measured using a rectal thermometer probe (Physitemp Instruments). Mice were then euthanized via CO_2 asphyxiation and blood was collected by cardiac puncture and centrifuged to isolate plasma.

III.3.12 Statistical Analysis

Data are presented as mean ± SE and analyzed using GraphPad Prism 6 software (GraphPad, La Jolla, CA). Comparisons between two groups were done using unpaired Student's *t* test and comparisons between multiple groups were done using one-way analysis of variance with Tukey's post-hoc test. All p values <0.05 were deemed significant.

IV.4 RESULTS

IV.4.1 Kinetics of LA enhancement of IgE-mediated cytokine secretion

In order to determine LA on IgE-mediated cytokine secretion, time-course and concentration-response experiments were performed. First, BMMC were sensitized with IgE overnight, then treated with various concentraton of LA for 24 hours. DNP-HSA was

then given to cross-link IgE, and 16 hours later supernatants were collected and analyzed via ELISA. Figure 4.2A shows that in response to increasing doses of LA, IL-6 and MCP-1 secretion was enhanced. At 25mM, cytokine production was no longer enhanced, which corresponded to a decrease in cell viability (data not shown). Therefore, for the remainder of this work LA was used at 12.5mM. To determine the optimal duration of pre-exposure with LA, BMMC were incubated with IgE overnight and then given 12.5mM LA for periods of time ranging from 48 hours to 0 hours (i.e. simultaneously with DNP-HSA). DNP-HSA was then added, and 16 hours later supernatants were collected and analyzed via ELISA. Figure 4.2B shows that after 12 hours of LA treatment, IgE-mediated secretion of IL-6 was enhanced, as well as after 24 and 48 hours. At the 48-hour mark, cell viability began to decrease, which led us to select 24 hours as the optimal duration for LA pre-exposure.

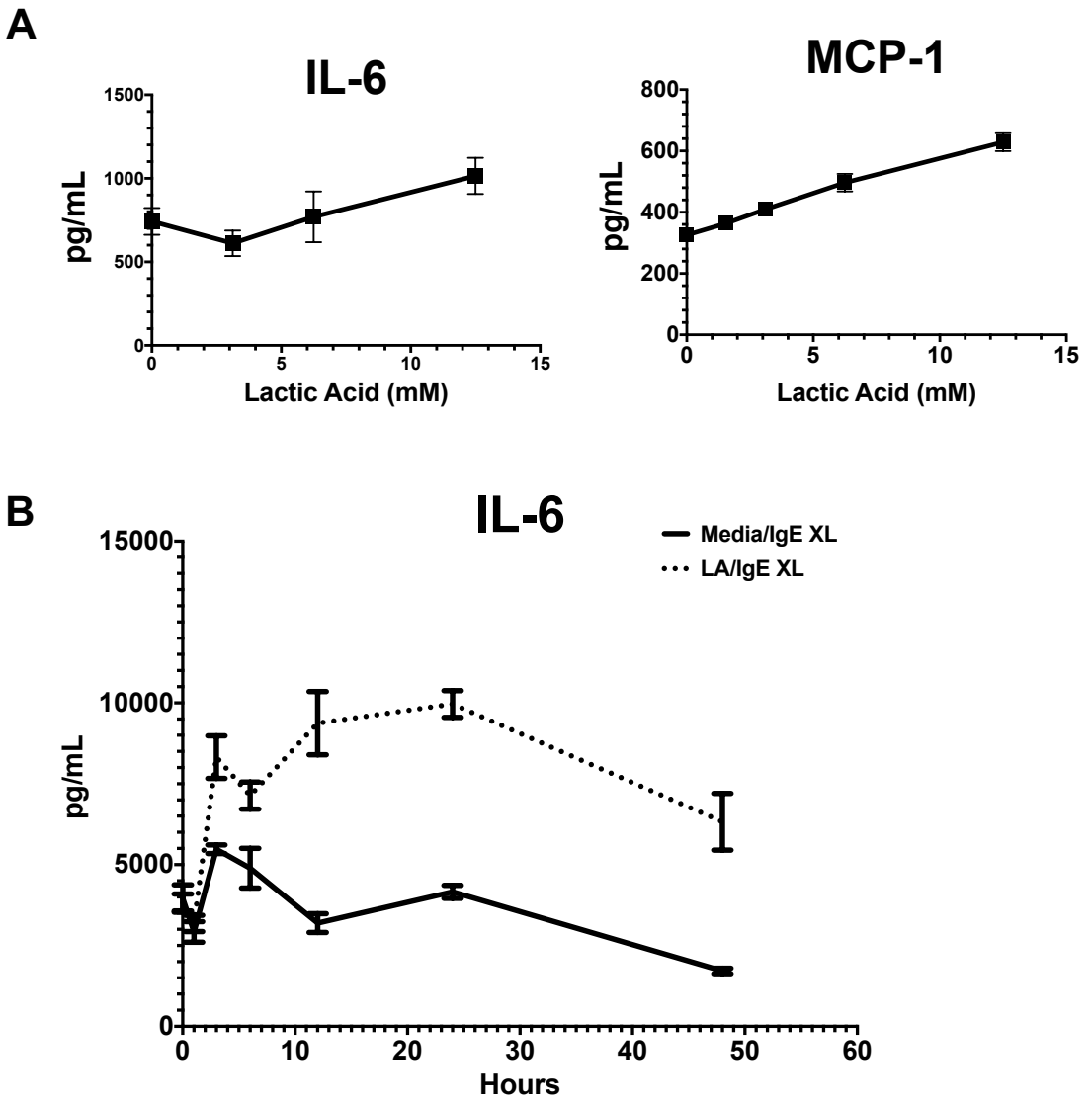

FIGURE 4.2 Kinetics of LA enhancement of IgE-mediated cytokine secretion A) BMMC were pretreated with lactic acid prior to IgE-Ag crosslinking. Supernatants were collected 16 hrs after activation. A) Dose-response and B) time-course experiments were done to determine kinetics of lactic acid effects on BMMC cytokine production. 24 hours and 12.5mM were the optimal conditions for lactic acid pretreatment. Supernatants were analyzed by ELISA. Results are representative of three independent experiments using 3 BMMC populations each, and expressed as mean ±SEM. *, $p<0.05$; **, $p<0.01$; ***, $p<0.001$; ****, $p<0.0001$; NS, not significant.

IV.4.2 Lactic acid enhances IgE-mediated cytokine production from BMMC

While Figure 4.2 displayed changes in IL-6 and MCP-1 secretion in response to LA, it is important to determine if other cytokines and chemokines change accordingly with LA treatment. BMMC were given IgE overnight and then treated with LA for 24 hours, followed with IgE crosslinking with DNP-HSA. 16 hours later supernatants were collected and analyzed via ELISA. Figure 4.3 shows that the inflammatory cytokines IL-6 and TNF, as well as the chemokines MCP-1 and MIP-1α were elevated in response to LA. IL-13 secretion, a classic marker of IgE-mediated inflammation, was also increased in response to LA. Interestingly, the anti-inflammatory and pro-angiogenic growth factor VEGF was induced in response to LA. In conclusion, a panel of IgE-mediated inflammatory cytokines and chemokines were elevated in response to LA, as well as the angiogenic cytokine VEGF.

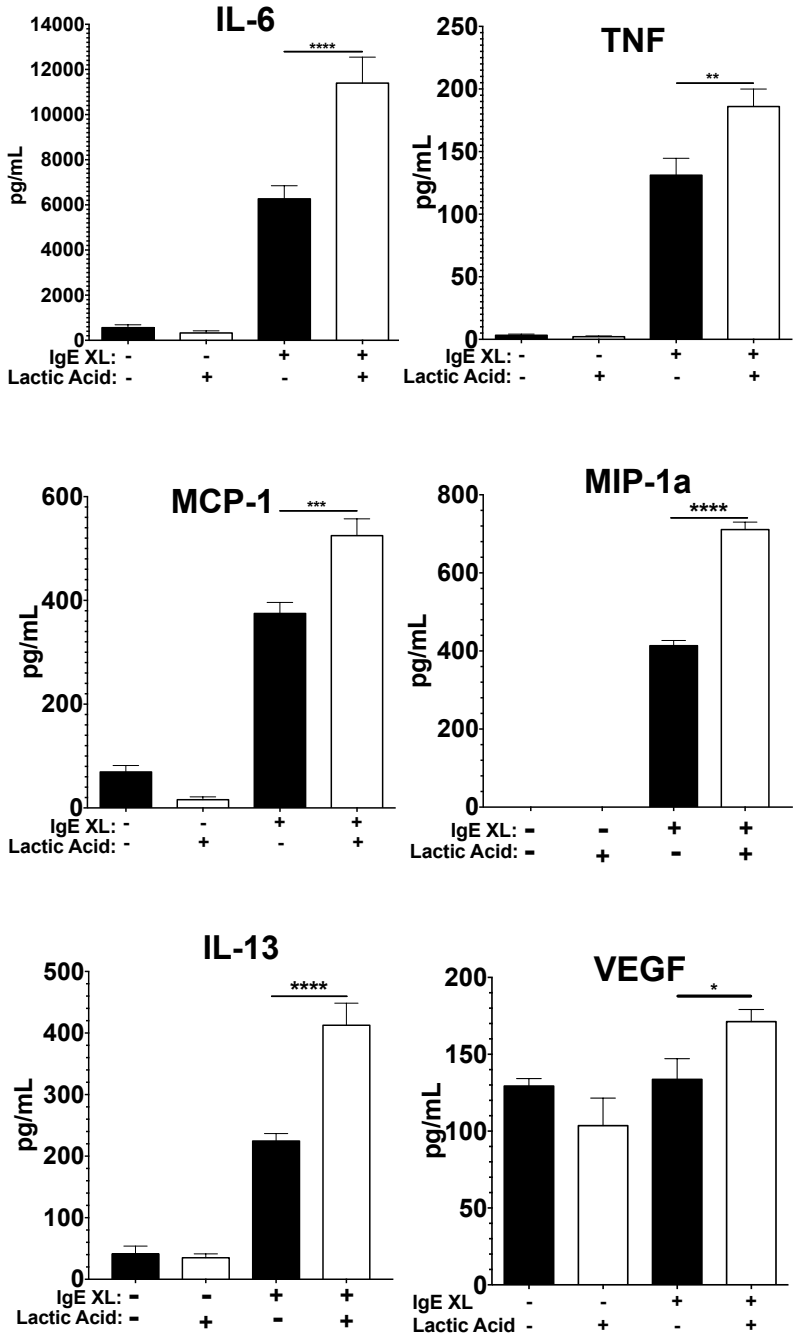

FIGURE 4.3 LA enhances IgE-mediated cytokine production BMMC were pretreated with 12.5 mM lactic acid prior to IgE-Ag crosslinking. Supernatants were collected 16 hrs after activation. Supernatants were analyzed by ELISA. Various cytokines and chemokines were measured. Results are representative of three independent experiments using 3 BMMC populations each, and expressed as mean ±SEM. *, $p<0.05$; **, $p<0.01$; ***, $p<0.001$; ****, $p<0.0001$; NS, not significant.

IV.4.3 *Lactic acid does not affect IgE-mediated BMMC degranulation*

A critical response to IgE crosslinking in mast cell biology is degranulation, which involves the rapid release of pre-formed mediators, such as histamine, proteases, arachidonic acid metabolites, and some cytokines (154). As the preformed granules move to the cell membrane to release their contents during degranulation, unique cell surface markers arise that can be used to measure degranulation via flow cytometry. Two such surface markers are CD63 and CD107a (155, 156). Therefore to determine if LA alters IgE-mediated degranulation, surface expression of CD63 and CD107a were measured. After overnight incubation with IgE, BMMC were treated with LA for 24 hours, then activated with DNP-HSA. Because degranulation is a rapid response, 15 minutes after crosslinking cells were washed and stained for CD63 and CD107a. Figure 4.4 shows that CD63 and CD107a surface expression increases with IgE crosslinking, and that LA does not change the expression of those markers. Therefore LA does not alter appear to alter IgE-mediated degranulation.

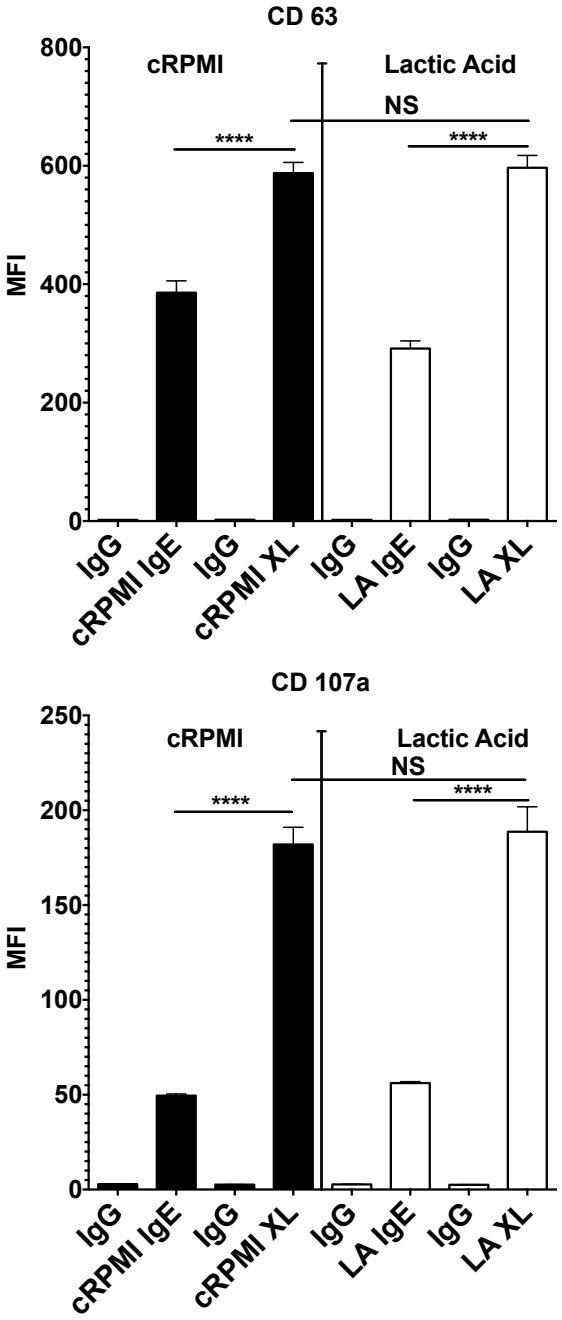

FIGURE 4.4 LA does not alter IgE-mediated degranulation BMMC were pretreated with 12.5 mM lactic acid prior to IgE-Ag crosslinking. 10 minutes after crosslinking, cells were washed, stained for CD63 and CD107a, washed, and analyzed via FACS. Results are representative of three independent experiments using 3 BMMC populations each, and expressed as mean ±SEM. *, $p<0.05$; **, $p<0.01$; ***, $p<0.001$; ****, $p<0.0001$; NS, not significant.

IV.4.4 LA enhances IgE-mediated angiogenesis

To determine if the increase in VEGF production is indicative of mast cell angiogenic activity, supernatants from BMMC exposed to LA and IgE crosslinking were used in an *in vitro* angiogenesis assay. Conditioned supernatants from BMMC were added to the HUVEC cultures. 16 hours after conditioned supernatants were added, images were taken of any tube networks that formed. Analysis entailed counting the number of tubes formed between different nodes of HUVECs. As shown in Figure 4.5, the media alone and LA alone groups were not different, as well as the IgE crosslinked group. However, the supernatants from BMMC treated with LA and IgE crosslinked promoted robust tube formation among HUVECs in Matrigel. Therefore, LA was able to enhance IgE-mediated angiogenesis.

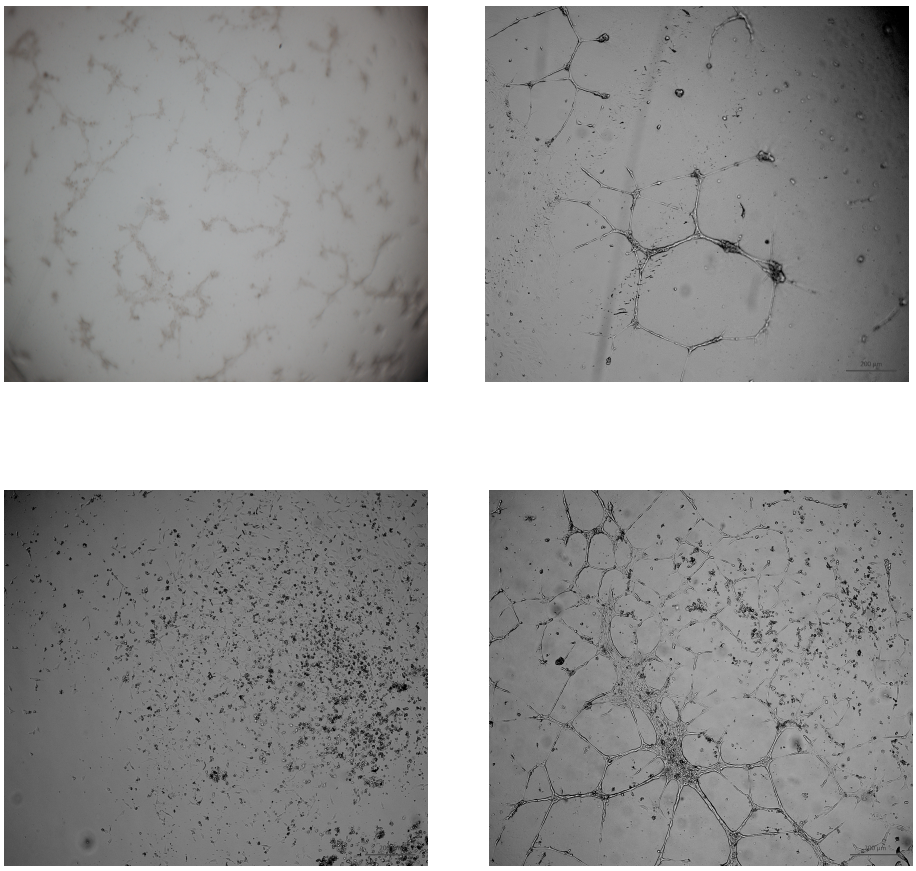

FIGURE 4.5 LA enhances IgE-mediated angiogenesis HUVEC were seeded into a Geltrex matrix and then exposed to conditioned supernatants from IgE-Ag crosslinked BMMC pre-treated with LA. 16 hours following supernatant treatment, images were captured of capillary tube network formation. Using ImageJ, images were analyzed by quantifying tube formation by counting tubes between nodes of cells. Results are one experiment conducted in triplicate and expressed as mean ±SEM. *, $p<0.05$; **, $p<0.01$; ***, $p<0.001$; ****, $p<0.0001$; NS, not significant.

IV.4.5 *LA suppresses IgE-mediated cytokine production from peritoneal mast cells*

To determine if LA can also alter IgE responses from *ex vivo* derived mast cells, murine peritoneal mast cells (PMC) were treated with LA. PMC were given IgE overnight, then treated with LA at 12.5 mM for 24 hours, and activated with DNP-HSA. 16 hours later, supernatants were collected and analyzed via ELISA. Surprisingly, Figure 4.6 shows that in response to LA, IgE-mediated inflammatory cytokine secretion from PMC is suppressed. This contradicts the previous findings with BMMC, where LA enhanced inflammatory cytokines secretion. However, one consistent aspect of the responses from BMMC and PMC is that LA enhanced IgE-mediated VEGF secretion. There appears to be a consistent angiogenic phenotype developed in response to LA treatment. PMC are *ex vivo*-derived cells and not differentiated *in vitro*, which makes them more physiologically relevant. To further this work, we next studied human mast cells.

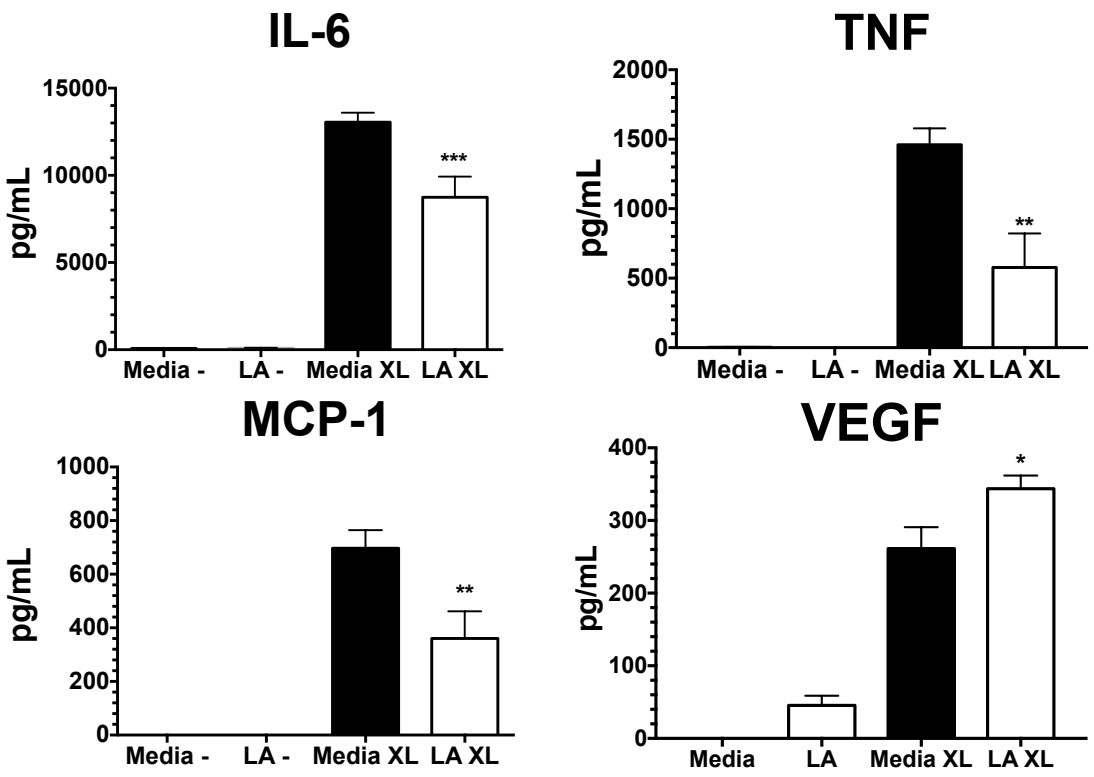

FIGURE 4.6. LA suppresses IgE-mediated cytokine production from peritoneal mast cells Peritoneal mast cells (PMC) were harvested from C57BL/6 mice and expanded *in vitro* for 2 weeks. PMC were then given IgE overnight, treated with 12.5 mM for 24 hours, and then activated via IgE-Ag crosslinking. 16 hours later, supernatnats were collected and analyzed via ELISA. Results are three experiments conducted in triplicate and expressed as mean ±SEM. *, $p<0.05$; **, $p<0.01$; ***, $p<0.001$; ****, $p<0.0001$; NS, not significant.

IV.4.6 LA suppresses IgE-mediated cytokine production from human skin mast cells

SkMC from human donors, which mature in vivo and are expanded ex vivo, are conceivably one of the most physiologically relevant sources for mast cells. This work was done in collaboration with Carole Oskeritzian at the University of South Carolina. As before, SkMC were sensitized with IgE overnight, treated with 12.5 mM LA for 24 hours, then activated with antigen. 16 hours later, supernatants were collected and analyzed via ELISA. As shown in Figure 4.7, LA treatment dramatically reduced IgE-mediated cytokine production, confirming the PMC findings in Figure 4.7. This consistency prompted us to continue our studies using PMC.

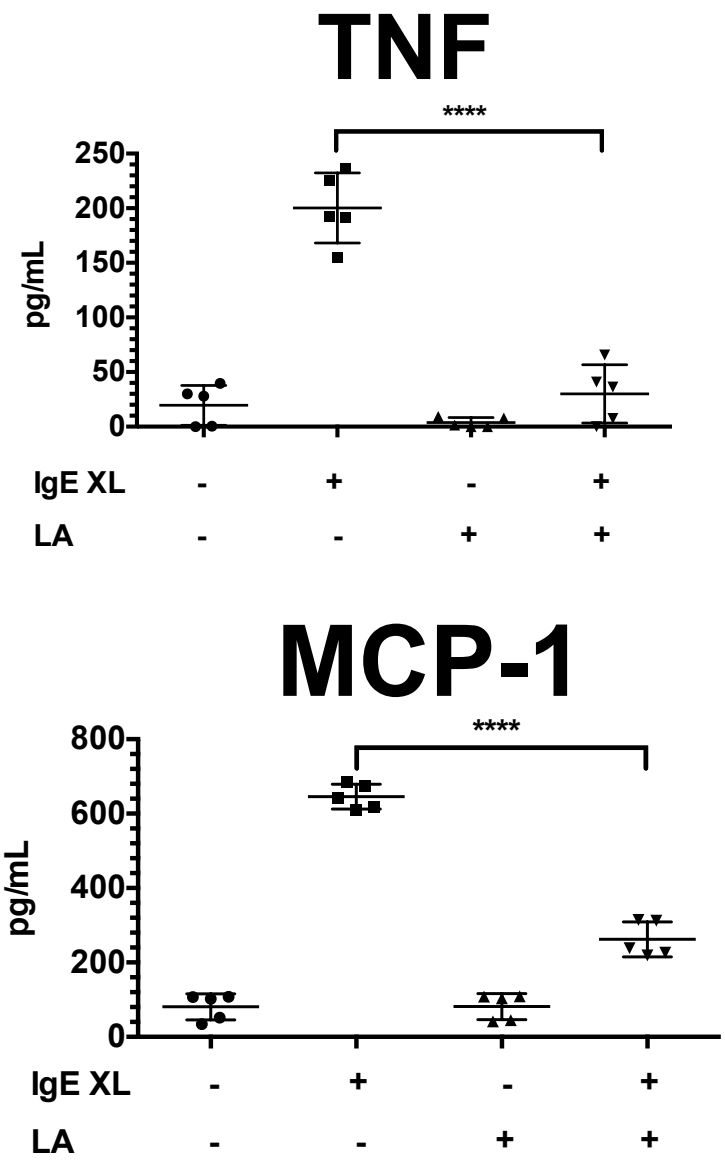

FIGURE 4.7 LA suppresses IgE-mediated cytokine production from human skin mast cells Primary human skin mast cells cultured from 5 donors were treated with either media alone or 12.5 mM lactic acid for 24 hours, then activated with IgE-Ag cross linking (IgE XL). Supernatants were collected 16 hours later and analyzed by ELISA. *, p<0.05; **, p<0.01; ***, p<0.001; ****, p<0.0001; N.S., not significant.

IV.4.7 LA does not strip IgE from the cell surface or alter FcεRIα levels

To better understand how LA suppresses IgE-mediated cytokine production in PMCs, surface expression and occupancy of the high-affinity IgE receptor, FcεRI, was measured via flow cytometry. Since acid pH has been used to strip IgE from FcεRI (157), we also determined if LA treatment affected IgE receptor occupancy. After incubating cells overnight with IgE, then 12.5 mM LA for 24 hours, cells were stained for surface-bound IgE and analyzed via flow cytometry. Figure 4.8A shows that LA treatment does not change FcεRI surface expression. Additionally, Figure 4.8B demonstrates that LA treatment does not change the levels of IgE present on the cell surface. In conclusion, the ability of LA to alter IgE-mediated responses is not due to changes in FcεRI surface receptor expression or occupancy.

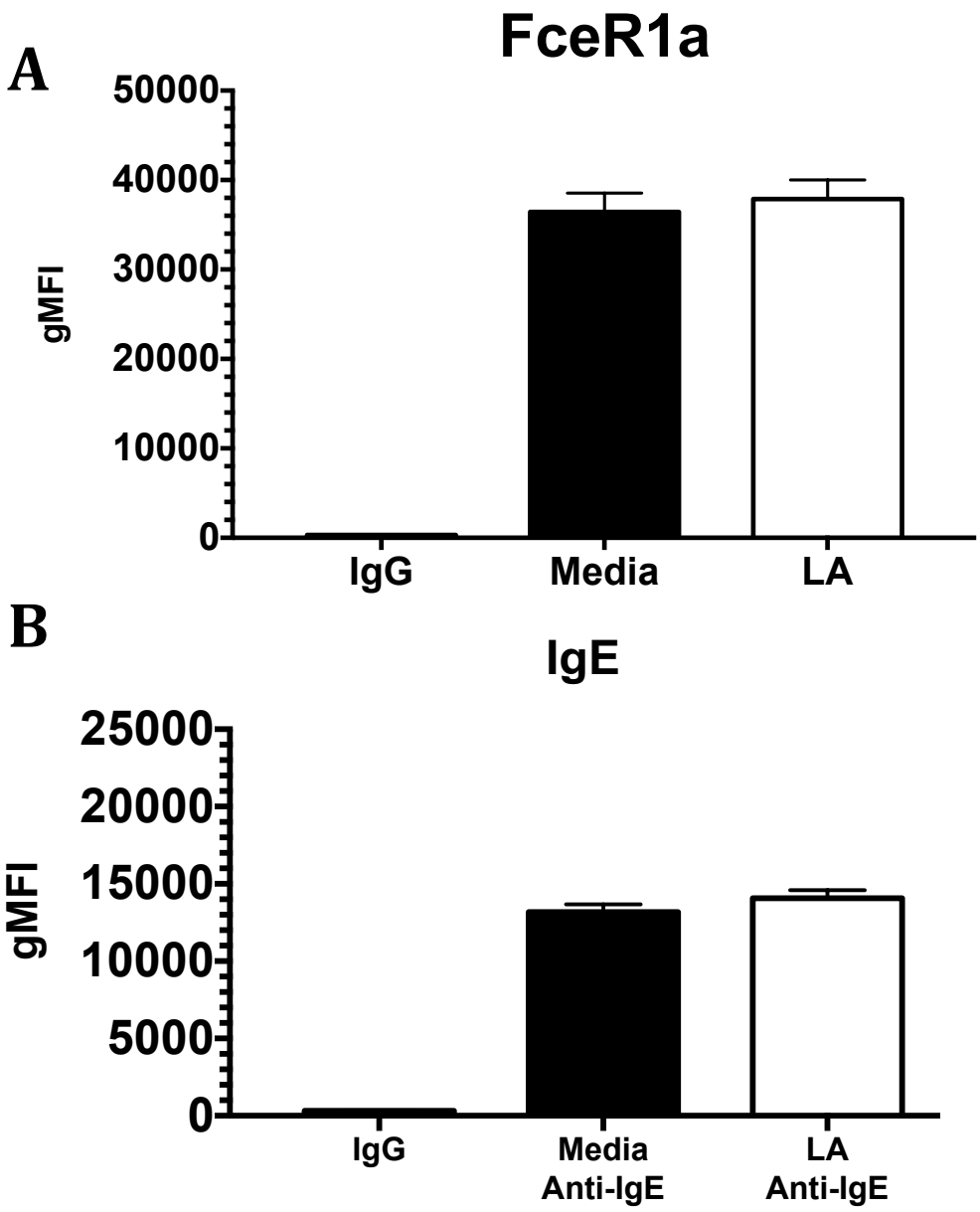

FIGURE 4.8 LA does not strip IgE from the surface or alter FcεRIα levels A) PMC were treated with 12.5 mM LA for 24 hours and then stained for FcεRIα to examine any changes in surface expression. B) PMC were given IgE overnight, and then treated with 12.5 mM for 24 hours. Cells were then stained for surface-bound IgE to determine if LA strips off IgE from the surface of mast cells. Results are three experiments conducted in triplicate and expressed as mean ±SEM.*, $p<0.05$; **, $p<0.01$; ***, $p<0.001$; ****, $p<0.0001$; N.S., not significant.

IV.4.8 *LA suppress IgE-mediated cytokine production in a pH- and MCT-1-dependent manner*

In the previous chapter, we showed that LA suppresses IL-33-induced cytokine production in a pH- and MCT-1-dependent manner (158). We therefore determined if similar mechanism explains LA effects on IgE signaling. First, PMCs were incubated overnight with IgE and then treated with either media alone, 12.5 mM LA, or 12.5 mM sodium lactate (NaLA). After treatment for 24 hours, PMC were activated with antigen for 16 hours, and supernatants were analyzed via ELISA. Figure 4.9A shows that while LA suppressed IgE-mediated TNF secretion, NaLA did not affect TNF secretion relative to media alone. This shows that LA suppresses in a pH-dependent manner. To determine if the effect of LA is MCT-1-dependent, PMCs were first incubated overnight with IgE and then treated with an inhibitor of MCT-1 and MCT-2, AR-C155858. Since we previously found that mast cell do not to express MCT2, any changes with AR-C155858 would be due to MCT-1 (158). After 1-hour incubation with vehicle (DMSO) or AR-C155858, PMC were treated with media alone or 12.5 mM LA for 24 hours, then activated for 16 hours with antigen and analyzed via ELISA. Figure 4.9B shows that in the vehicle alone group, LA suppressed IgE-mediated secretion of TNF as expected. Howvere, in the presence of AR-C155858 LA no longer decreased TNF secretion. We concluded that, as with IL-33, LA suppresses IgE-mediated mast cell activation in a pH- and MCT-1-dependent manner.

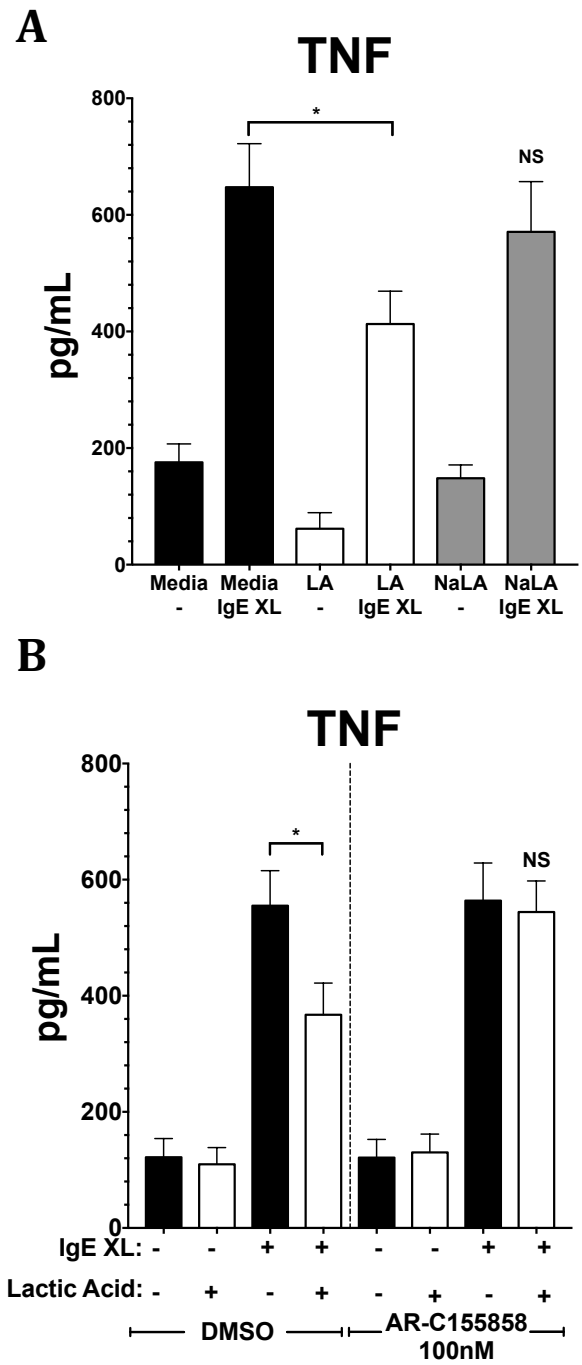

FIGURE 4.9. LA suppress IgE-mediated cytokine production in a pH- and MCT-1-dependent manner A) PMC were treated with either 12.5 mM LA or 12.5 mM sodium lactate for 24 hours and then activated via IgE-Ag crosslinking. B) PMC were pre-treatd with either an MCT-1/2 inhibitor AR-C155858 (100 nM) or DMSO (vehicle) for 1 hour, treated with 12.5 mM for 24 hours, and then activated via IgE-Ag crosslinking. 16 hours later supernatants were collected and analyzed via ELISA. Results are two experiments conducted in triplicate and expressed as mean ±SEM.*, $p<0.05$; **, $p<0.01$; ***, $p<0.001$; ****, $p<0.0001$; N.S., not significant.

IV.4.9 *LA alters IgE-mediated signaling*

To better understand how LA alters IgE-mediated responses in mast cells, IgE signaling was analyzed in the presence of LA. PMC were incubated overnight with IgE then treated with either media alone or 12.5 mM LA for 24 hours. DNP-HSA was used to activate PMC. 5 minutes after activation, cells were fixed using methanol, permeabilized with 1.6% paraformaldehyde, and stained using antibodies against phospho-Syk, phospho-Btk, and phospho-ERK1/2 before flow cytometry analysis. Figure 4.10 demonstrates that LA treatment reduces phosphorylation of Syk, Btk, and ERK 1/2, showing that LA does in fact alter IgE signaling events. The suppression of Syk phosphorylation is noteworthy because in Syk-deficient mast cells, IgE-mediated degranulation, calcium flux, and cytokine production are abolished (153, 159). In conclusion, LA suppresses the activation of key signaling proteins in the IgE signaling cascade.

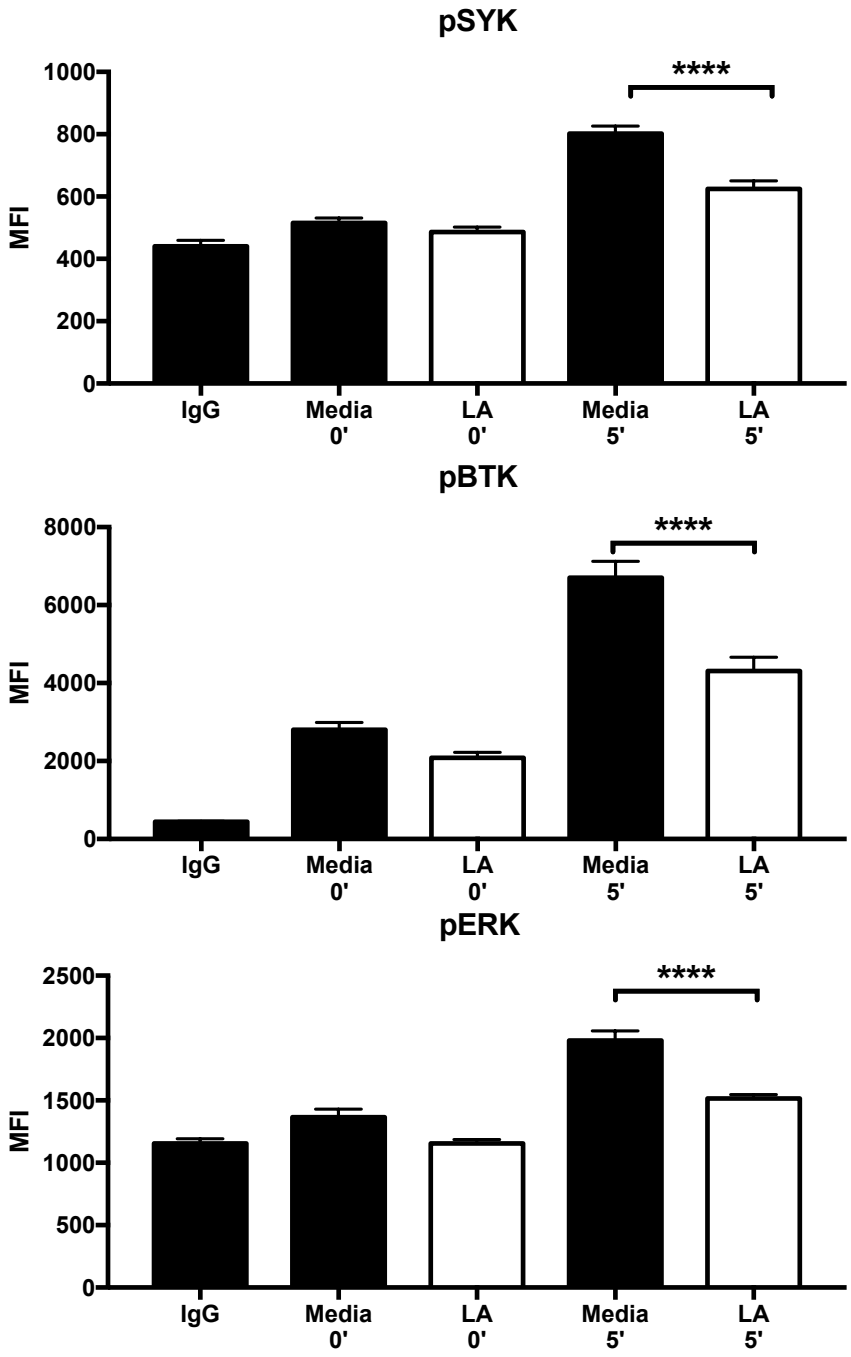

FIGURE 4.10. LA alters IgE-mediated signaling PMC were given IgE overnight and then treated with 12.5 mM LA for 24 hours. During those last 4 hours, PMC were starved from IL-3 and SCF. Cells were then given Ag (50 ng/mL) to induce activation via IgE-Ag crosslinking. 10 minutes after activation, cells were fixed and permeabilized, stained for phosphorylation of key signaling mediators of the IgE signaling pathway, and run on the FACSCelesta and analyzed for changes in phosphorylation levels. Results are three experiments conducted in triplicate and expressed as mean ±SEM.*, $p<0.05$; **, $p<0.01$; ***, $p<0.001$; ****, $p<0.0001$; N.S., not significant.

IV.4.10 LA alters passive systemic anaphylaxis

Lastly, we wanted determined if LA alters IgE-mediated mast cell responses *in vivo*. Therefore, we used the mast cell-mediated PSA model. C57BL/6 mice were injected with IgE, and the next day injected first with ketoprofen to alleviate pain associated with LA, and then either PBS or LA at 4mg/kg. 24 hours after PBS or LA injections, mice were injected with antigen to induce anaphylaxis. Core body temperature was measured over the course of 2 hours using a rectal probe. Figure 4.11 shows that mice receiving LA underwent less severe anaphylaxis based on core body temperature change. Because this is both a mast cell- and histamine-dependent model, it is possible that LA changed vasculature responsiveness to histamine, and not mast cell behavior (154). Therefore, we conducted another PSA study in which we induced anaphylaxis with histamine injections, rather than IgE and antigen, after injecting mice with either PBS or LA. In histamine-induced PSA, there was no difference in temperature drop between mice that received PBS or LA, indicating no changes in the responsiveness of the endothelium to histamine. This demonstrates that LA can functionally alter mast cell IgE-mediated behavior *in vivo*.

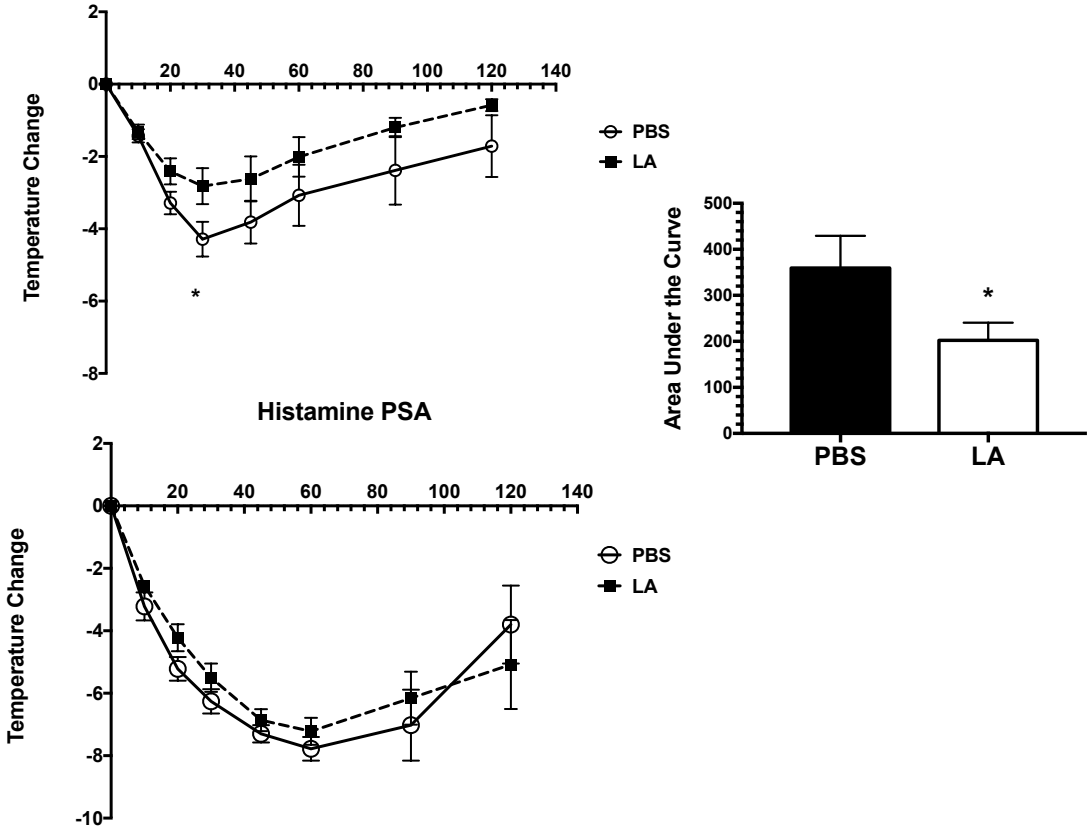

FIGURE 4.11. LA alters passive systemic anaphylaxis Age-matched C57BL/6 mice were first subcutaneously injected with ketoprofen, 30 minutes later intraperitoneally injected with LA, 24 hours later intraperitoneally injected with IgE (50 μg), and then 16 hours later injected with Ag (100 μg) to induce passive systemic anaphylaxis. Histamine-induced passive systemic anaphylaxis was done by intraperitoneally injecting 8 mg of histamine, rather than IgE and Ag. Results shown are from 5 mice in each group and expressed as mean ±SEM.*, p<0.05; **, p<0.01; ***, p<0.001; ****, p<0.0001; N.S., not significant.

IV.5 DISCUSSION

In this study, LA was shown to alter IgE-mediated activation, with variable effects based on the source of mast cells used. We initially showed that LA enhanced cytokine production from BMMC. This enhancement included several inflammatory cytokines: TNF, IL-6, MCP-1, MIP-1α, and IL-13, as well as VEGF. An *in vitro* angiogenesis assay demonstrated showed that LA-treated, IgE-activated BMMC secreted pro-angiogenic factors, as tube formation was dramatically increased. While we have detected VEGF, our current experiments does not prove that VEGF is required for the angiogenic activity, and we suspect other pro-angiogenic mediators are enhanced by LA treatment. This is in keeping with prior papers showing angiogenic factors produced by mast cells (40, 46, 160). Further investigation will be necessary to determine how LA alters the expression of these other angiogenic factors in the context of IgE crosslinking. The mechanism by which VEGF is induced in mast cells is still being elucidated, but a Fyn-dependent mechanism has been reported (44). Additionally, more recent work has shown that IgE-mediated mast cell production of leukotriene B_4 and 12(S)-hydroxyeicosatetraenoic acid, ligands of leukotriene B_4 receptor 2 (BLT2), play a critical role in VEGF production. BLT2 ligands are produced in response to IgE crosslinking, nd appear to provide positive feedback via BLT2, promoting VEGF synthesis (161). These provide new targets in studying how LA enhances IgE-mediated VEGF production.

We demonstrated the ability of LA to reduce activation of key signaling molecules in the IgE signaling cascade: Syk, Btk, and ERK. Syk activation is a critical, apical transducer of FcεRI signaling, driving degranulation, calcium flux, and cytokine production (153, 159). By nature of working with a populations where relatively few

cells are obtained from tissue harvesting, measuring changes in cell signaling proteins is challenging with PMC. For this reason we employed flow cytometry versus western blotting (162). This limited our analyses, due to reagent availability. Thus it will be important to expand this study to further explore how LA alters IgE-mediated signaling in PMCs.

When expanding our studies beyond BMMC to PMC and SkMC, an unexpected response occurred. While LA enhanced IgE-mediated cytokines with BMMC, it suppressed this response in PMC and SkMC. These discrepancies in response to LA might be attributed to mast cell heterogeneity. In the mouse system, mast cells are divided into mucosal mast cells (MMC) and connective tissue mast cells (CTMC), whereas in the human system mast cells are divided based on the their granular contents. Human mast cells with granules containing proteases that are mostly tryptases are referred to as mast cell tryptase (MC_T), and mast cells expressing both chymases and tryptases are referred to as mast cell tryptase-chymase (MC_{TC}). Based on granular content, the mouse mucosal mast cell is analogous to the human MC_T, and the mouse connective tissue mast cell to the human MC_{TC}. The PMC used in this work are CTMC, and the human SkMCs are the analogous MC_{TC} (60, 163, 164). In contrast, the BMMC used more closely resemble MMC (165). Thus lineage-specific effects may explain the differences in our results. This is supported by recent work demonstrating that the heterogenic differences in mast cell populations can lead to divergent expression profiles (57). However, it is important to note that BMMC are differentiated in vitro, while PMC and SkMC differentiate in vivo and expand ex vivo. For these reasons, we place a greater

emphasis on results from PMC and SkMC studies. Future work will include assessing the response of in vivo-derived MMC, to further assess lineage-specific effects.

The ability of LA to suppress IgE-mediated responses was further validated by the results of the *in vivo* PSA experiment, where mice injected with LA had a reduced temperature drop, indicating that those mice underwent less severe anaphylaxis. Mice injected with LA showed no difference compared to mice injected with PBS when undergoing histamine-induced PSA, demonstrating that LA is not acitng on the endothelium but rather suppressing IgE- and mast cell-mediated responses *in vivo*.

IV.6 CONCLUSION

In this study we demonstrate that LA enhances IgE-mediated cytokine production by BMMC. This enhancement includes VEGF, which correlated with angiogenic effects in an *in vitro* assay. Interestingly, when mast cells were sourced from either the peritoneum of mice or from skin biopsies from human donors, LA suppressed IgE-mediated cytokine production. Given that these two mast cell populations matured *in vivo*, they are of greater physiological relevance and PMCs were used throughout the rest of the study. While LA suppressed IgE-mediated inflammatory cytokine production in PMCs, VEGF secretion was still enhanced. LA-mediated suppression of IgE crosslinked PMCs was shown to be pH- and MCT-1-dependent. Additionally, LA suppressed the phosphorylation of Syk, Btk, and ERK, key mediators in IgE signaling. Lastly, LA was able to suppress IgE and mast cell-mediated responses *in vivo*, reducing the temperature drop in passive systemic anaphylaxis. Collectively, these data demonstrate that LA to promotes an anti-inflammatory and pro-angiogenic phenotype in mast cells.

CHAPTER V: CONCLUSIONS AND FUTURE WORK

V.I SUMMARY

Mast cells are a tissue resident cell population of the innate immune system that have been shown to play a critical role in inflammatory responses to biomaterials. Improving biomaterial design is critical to overcoming fibrotic responses for many implants. Previous work demonstrated how increasing scaffold pore size is needed for promoting improved tissue integration, as well as reducing macrophage M1 polarization. However little work has explored how biomaterials can be manipulated to alter mast cell responses, particularly with regard to scaffold architecture and degradative byproducts.

In Chapter 2, IL-33- and LPS-mediated cytokine and chemokine production was measured from BMMC cultured on electrospun polydioxanone of varying geometries. First, the two electrospun scaffolds used were a 60 mg/mL scaffold and a 140 mg/mL scaffold, where the 140 mg/mL scaffold had larger pore and fiber diameters. In response to IL-33 and LPS, BMMC cultured on the 140 mg/mL scaffold had reduced IL-6, TNF, MCP-1, and MIP-1α secretion but enhanced VEGF secretion, when compared to the 60mg/mL scaffold. This pro-angiogenic phenotype was also true at the mRNA level, where in response to IL-33, BMMC cultured on the 140 mg/mL scaffold showed greater VEGF and MMP-9 expression. When trying to isolate the role of scaffold pore size, 60 mg/mL polydioxanone scaffolds were electrospun on an air-flow mandrel. In response to this increased pore size, LPS- and IL-33-mediated IL-6 and TNF production were dramatically reduced. Interestingly, reducing pore size of 140 mg/mL scaffolds using a hydraulic press only partially reduced IL-33- and LPS-mediated inflammatory cytokine production. Together these data emphasize the importance of pore dimension, but also suggest that larger fibers are less inflammatory and less dependent on pore size. These

data can help guide design of implanted materials to promote wound healing and reduce inflammation and chronic fibrosis.

In Chapter 3, we explored how degradative byproducts of synethetic polymers could alter also alter IL-33-mediated mast cell activation. We did this by pre-treating BMMC with LA that were then activated with IL-33. LA pre-treatment suppressed inflammatory cytokine and chemokine production while enhancing VEGF, a phenotype that mimics what we saw in Chapter 2 with scaffolds of increased pore size. Changes in IL-33-meidated cytokine production were also true of *ex vivo*-derived peritoneal mast cells. These effects were pH- and MCT-1-dependent, and selectively suppressed key proteins involved in IL-33 signaling. The enhancement of VEGF was shown to be Akt1-dependent based on siRNA experiments.

LA treatment enhanced HIF-1α expression which we found to negatively regulate miR-155-5p levels. Further, LA-mediated suppression of IL-33-induced cytokine production required miR-155-5p suppression, since miR-155-5p overexpression reversed LA effects. Because miR-155-5p promotes inflammation, LA-mediated miR-155-5p suppression corroborates the proposed anti-inflammatory role for LA. Furthermore, these data were consistent in vivo. LA injection reduced the stimulatory effects of IL-33 on plasma cytokine levels. Lastly, skin mast cells from human donors showed that LA abolished the ability of IL-33 to enhance IgE-mediated cytokine production, an effect shown to be MCT-dependent. These data suggest that LA, an important degradative by-product of PLLA polymers, suppresses IL-33-mediated pro-inflammatory cytokines while promoting angiogenic factor secretion.

Given how potent IgE crosslinking is in activating mast cells, as well as the ability of IgE crosslinking to potentiate inflammation and angiogenesis, the work in Chapter 4 explored how LA alters IgE signaling in mast cells. We were surprised to find that, when added to BMMC cultures, LA enhanced IgE-mediated inflammatory cytokine production, as well as VEGF secretion. Supernatants from these cultures promoted robust endothelial cell tube formation, confirming LA promotes an angiogenic phenotype in mast cells. Investigating the effects of LA on IgE crosslinked mast cells was extended to include peritoneal mast cells and human skin mast cells. These experiments demonstrated inhibitory effects of LA, consistent with our IL-33 studies. LA similarly reduced the severity of IgE- and mast cell-mediated passive systemic anaphylaxis *in vivo*. We concluded that there may be lineage- or culture-dependent effects, and that on balance, LA effects are largely anti-inflammatory. Using peritoneal mast cells, we determined that the ability of LA to suppress IgE-mediated cytokine production was pH- and MCT-1-dependent and not due to changes in surface expression of the IgE receptor FcεRI. Lastly, LA reduced activation of key IgE signaling molecules, including Syk, Btk, and ERK. Collectively LA appears to be a potent suppressor of mast cell inflammatory responses, while promoting angiogenesis. These properties, along with knowledge of spatial/structural considerations, provide insight for designing biologically useful polymers.

V.II FUTURE WORK

The work done in Chapter 2 would be better served by conducting several more experiments. In order to better understand the mechanism by which scaffold structure

alters IL-33- and LPS-mediated responses, measuring changes in signaling via flow cytometry would be helpful. Trying to measure changes in signaling events proved to be difficult using western blotting, and flow cytometry provides the advantage of being more high-throughput and requiring fewer cells. Another productive experiment would be to determine if scaffold structural changes lead alter mast cell responses at the transcriptional level, particularly for AP-1 and NF-κB, which are critical for IL-33 and LPS effects. Lastly, another future experiment would include subcutaneously implanting 60 and 140 mg/mL polydioxanone scaffolds into C57BL/6 mice. After 4 weeks, mice would be perfused with a contrast agent (e.g. Microfil) and changes in the local vasculature would be measured using microCT. Additionally, scaffolds would be excised and analyzed histologically for fibrous capsule formation and macrophage polarization. The role of mast cells would be determined by including mast cell-deficient $Kit^{W\text{-}sh/W\text{-}sh}$ mouse.

While the LA and IL-33 story is more complete, there are still questions left to be answered. We need to determine what miR-155 is targeting in this system. One way to find out would be to mine through different software algorithms, such as the DIANA micro-T tool, that assist in identifying targets based on the miR recognition elements that are validated experimentally. Once a target is identified, we can measure its expression in the presence of LA, and then knockdown expression of that target using siRNAs to determine if it is a necessary component for LA effects. Additionally, an important experiment to conduct would also be to electrospin poly-lactic acid scaffolds, incubate them in media to allow for scaffold degradation over time, and treat mast cells with that

conditioned media to determine if this alters IL-33- or IgE-mediated activation of mast cells.

Future work with LA and IgE-activated mast cells would include repeating the *in vitro* angiogenesis experiment with conditioned supernatants from IgE-crosslinked PMC, since LA suppressed inflammatory cytokine production in these cells. While VEGF was enhanced, it would be helpful to confirm if LA promoted a functional angiogenic phenotype with the PMC as well. Lastly, given that PMC and SkMC, considered to be connective tissue mast cells, responded to LA differently than BMMC, a mucosal mast cell, it would be important to use a mucosal mast cell that matured *in vivo* and determine if their response to LA mimics the BMMC.

V. CONCLUDING REMARKS

In summary, this work demonstrates that altering scaffold structure alters mast cell inflammatory and angiogenic responses. Additionally, the degradative byproducts of synthetic polymers from biomaterials can also dictate inflammatory and angiogenic responses. Mast cell responses to biomaterials warrants further investigation, particularly in the presence of signals like IL-33. Hopefully this work will help shed light on how to improve biomaterial design to mitigate inflammation and promote wound healing.

LITERATURE CITED

Literature Cited

1. Molan, P. C. 2001. Potential of Honey in the Treatment of Wounds and Burns. *American Journal of Clinical Dermatology* 2: 13–19.

2. Kaul, H., and Y. Ventikos. 2015. On the Genealogy of Tissue Engineering and Regenerative Medicine. *Tissue Engineering Part B: Reviews* 21: 203–217.

3. Vacanti, C. 2006. The history of tissue engineering. *J Cell Mol Med* 1: 569–576.

4. Schultheiss, D., D. A. Bloom, J. Wefer, and U. Jonas. 2000. Tissue engineering from Adam to the zygote: historical re ¯ections. *World Journal of Urology* 18: 84–90.

5. Mazzarello, P. 1999. A unifying concept: the history of cell theory. *Nature Cell Biology* 1: E13–E15.

6. Vasil, I. K. 2008. A history of plant biotechnology: from the Cell Theory of Schleiden and Schwann to biotech crops. *Plant Cell Rep* 27: 1423–1440.

7. Kumar, D. R., E. Hanlin, I. Glurich, J. J. Mazza, and S. H. Yale. 2010. Virchow's Contribution to the Understanding of Thrombosis and Cellular Biology. *Clinical Medicine & Research* 8: 168–172.

8. Bagot, C. N., and R. Arya. 2008. Virchow and his triad: a question of attribution. *British Journal of Haematology* 143: 180–190.

9. Riedel, S. 2004. Edward Jenner and the history of smallpox and vaccination. *BUMC Proceedings* 18: 21–25.

10. Berche, P. 2012. Louis Pasteur, from crystals of life to vaccination. *Clinical Microbiology and Infection* 18: 1–6.

11. Silverstein, A. M. 1996. History of Immunology. *Cellular Immunology* 174: 1–6.

12. Gensini, G. F., A. A. Conti, and D. Lippi. 2007. The contributions of Paul Ehrlich to infectious disease. *Journal of Infection* 54: 221–224.

13. Winau, F., O. Westphal, and R. Winau. 2004. Paul Ehrlich — in search of the magic bullet. *Microbes and Infection* 6: 786–789.

14. Chernyak, L., and A. Tauber. 1988. History of Immunology. *Cellular Immunology* 117: 218–233.

15. Dranoff, G. 2004. Cytokines in cancer pathogenesis and cancer therapy. *Nat Rev Cancer* 4: 11–22.

16. Becker, A. J., E. A. McCullock, and J. E. Till. 1963. Cytological Demonstration of the Clonal Nature of Spleen Colonies derived from Transplanted Mouse Marrow Cells. *Nature* 197: 452–454.

17. Langer, R., and J. P. Vacanti. 1993. Tissue Engineering. *Science* 260: 920–926.

18. Wolter, J. R., and R. F. Meyer. 1984. Sessile Macrophages Forming Clear Endothelium-like Membrane on Inside of Successful Keratoprosthesi. *Graefes Archive for Clinical and Experimental Opthamology* 222: 109–117.

19. Cao, Y., J. P. Vacanti, K. T. Paige, J. Upton, and C. A. Vacanti. 1997. Transplantation of Chondrocytes Utilizing a Polymer-Cell Construct to Produce Tissue-Engineered Cartilage in the Shape of a Human Ear. *Plastic and Reconstructive Surgery* 100: 297–302.

20. Klopfleisch, R., and F. Jung. 2016. The pathology of the foreign body reaction against biomaterials. *J. Biomed. Mater. Res.* 105: 927–940.

21. Harrison, P., and E. Martin Cramer. 1993. Platelet α-granules. *Blood Reviews* 7: 52–

62.

22. Blair, P., and R. Flaumenhaft. 2009. Platelet α-granules: Basic biology and clinical correlates. *Blood Reviews* 23: 177–189.

23. Enoksson, M., K. Lyberg, C. Moller-Westerberg, P. G. Fallon, G. Nilsson, and C. Lunderius-Andersson. 2011. Mast Cells as Sensors of Cell Injury through IL-33 Recognition. *The Journal of Immunology* 186: 2523–2528.

24. Rutz, S., Want, X., and Ouyang, W. 2014. The IL-20 Subfamily of Cytokines - from Host Defence to Tissue Homeostasis. *Nature Reviews Immunology* 14(12): 783 - 795.

25. Molofsky, A. B., A. K. Savage, and R. M. Locksley. 2015. Interleukin-33 in Tissue Homeostasis, Injury, and Inflammation. *Immunity* 42: 1005–1019.

26. Chinetti-Gbaguidi, G., Colin, S., and Staels, B. 2015. Macrophage Subsets in Atherosclerosis. *Nature Reviews* Cardiology 12: 10-17.

27. Murray, P. J., J. E. Allen, S. K. Biswas, E. A. Fisher, D. W. Gilroy, S. Goerdt, S. Gordon, J. A. Hamilton, L. B. Ivashkiv, T. Lawrence, M. Locati, A. Mantovani, F. O. Martinez, J.-L. Mege, D. M. Mosser, G. Natoli, J. P. Saeij, J. L. Schultze, K. A. Shirey, A. Sica, J. Suttles, I. Udalova, J. A. van Ginderachter, S. N. Vogel, and T. A. Wynn. 2014. Macrophage Activation and Polarization: Nomenclature and Experimental Guidelines. *Immunity* 41: 14–20.

28. Galli, S. J., N. Borregaard, and T. A. Wynn. 2011. Phenotypic and functional plasticity of cells of innate immunity: macrophages, mast cells and neutrophils. *Nat. Immunol*. 12: 1035–1044.

29. Schmitz, J., A. Owyang, E. Oldham, Y. Song, E. Murphy, T. K. McClanahan, G. Zurawski, M. Moshrefi, J. Qin, X. Li, D. M. Gorman, J. F. Bazan, and R. A. Kastelein.

2005. IL-33, an Interleukin-1-like Cytokine that Signals via the IL-1 Receptor-Related Protein ST2 and Induces T Helper Type 2-Associated Cytokines. *Immunity* 23: 479–490.

30. Andrade, M. V., S. Iwaki, C. Ropert, R. T. Gazzinelli, J. R. Cunha-Melo, and M. A. Beaven. 2011. Amplification of cytokine production through synergistic activation of NFAT and AP-1 following stimulation of mast cells with antigen and IL-33. *Eur. J. Immunol.* 41: 760–772.

31. Wang, J. X., S. Kaieda, S. Ameri, N. Fishgal, D. Dwyer, A. Dellinger, C. L. Kepley, M. F. Gurish, and P. A. Nigrovic. 2014. IL-33/ST2 axis promotes mast cell survival via BCLXL. *Proceedings of the National Academy of Sciences* 111: 10281–10286.

32. Moulin, D., O. Donzé, D. Talabot-Ayer, F. Mézin, G. Palmer, and C. Gabay. 2007. Interleukin (IL)-33 induces the release of pro-inflammatory mediators by mast cells. *Cytokine* 40: 216–225.

33. Iikura, M., H. Suto, N. Kajiwara, K. Oboki, T. Ohno, Y. Okayama, H. Saito, S. J. Galli, and S. Nakae. 2007. IL-33 can promote survival, adhesion and cytokine production in human mast cells. *Lab. Invest.* 87: 971–978.

34. Nilsson, G. 2012. Mast cells respond to cell injury through the recognition of IL-33. 1–9.

35. Ali, S., A. Mohs, M. Thomas, J. Klare, R. Ross, M. L. Schmitz, and M. U. Martin. 2011. The Dual Function Cytokine IL-33 Interacts with the Transcription Factor NF- B To Dampen NF- B-Stimulated Gene Transcription. *The Journal of Immunology* 187: 1609–1616.

36. Enoksson, M., C. Möller-Westerberg, G. Wicher, P. G. Fallon, K. Forsberg-Nilsson, C. Lunderius-Andersson, and G. Nilsson. 2013. Intraperitoneal influx of neutrophils in

response to IL-33 is mast cell-dependent. *Blood* 121: 530–536.

37. Desmouliere, A., I. A. Darby, B. Laverdet, and F. Bonté. 2014. Fibroblasts and myofibroblasts in wound healing. *CCID* Volume 7: 301–11.

38. Garg, K., N. A. Pullen, C. A. Oskeritzian, J. J. Ryan, and G. L. Bowlin. 2013. Macrophage functional polarization (M1/M2) in response to varying fiber and pore dimensions of electrospun scaffolds. *Biomaterials* 34: 4439–4451.

39. Avula, M. N., A. N. Rao, L. D. McGill, D. W. Grainger, and F. Solzbacher. 2014. Foreign body response to subcutaneous biomaterial implants in a mast cell-deficient Kitw-Sh murine model. *Acta Biomaterialia* 10: 1856–1863.

40. Norrby, K. 2002. Mast cells and angiogenesis. Review article. *APMIS* 110: 355–371.

41. Abdel-Majid, R. M., and J. S. Marshall. 2003. Prostaglandin E2 Induces Degranulation-Independent Production of Vascular Endothelial Growth Factor by Human Mast Cells. *The Journal of Immunology* 172: 1227–1236.

42. Shalik-Dasthagirisaheb, Y. B., G. Varvara, G. Murmura, A. Saggini, G. Potalivo, A. Caraffa, P. Antinolfi, S. Tete, D. Tripodi, F. Conti, E. Cianchetti, E. Toniato, M. Rosati, P. Conti, L. Speranza, A. Pantalone, R. Saggini, T. C. Theoharides, and F. Pandolfi. 2013. Vascular Endothelial Growth Factor (VEGF), Mast Cells and Inflammation. *International Journal of Immunopathology and Pharmacology* 26: 327–335.

43. Ribatti, D., G. Ranieri, B. Nico, V. Benagiano, and E. Crivellato. 2011. Tryptase and chymase are angiogenic in vivo in the chorioallantoic membrane assay. *Int. J. Dev. Biol.* 55: 99–102.

44. nez-Andrade, G. Y. J., A. I.-S. nchez, D. G. lez, M. N. Lamas, and C. G. lez-Espinosa. 2013. Immunoglobulin E induces VEGF production in mast cells and

potentiates their pro-tumorigenic actions through a Fyn kinase-dependent mechanism. *Journal of Hematology & Oncology* 6: 1–1.

45. Lee, A.-J., M. Ro, and J.-H. Kim. 2016. Leukotriene B 4Receptor 2 Is Critical for the Synthesis of Vascular Endothelial Growth Factor in Allergen-Stimulated Mast Cells. *The Journal of Immunology* 197: 2069–2078.

46. Hiromatsu, Y., and S. Toda. 2003. Mast cells and angiogenesis. *Microsc. Res. Tech.* 60: 64–69.

47. Chillo, O., E. C. Kleinert, T. Lautz, M. Lasch, J.-I. Pagel, Y. Heun, K. Troidl, S. Fischer, A. Caballero-Martinez, A. Mauer, A. R. M. Kurz, G. Assmann, M. Rehberg, S. M. Kanse, B. Nieswandt, B. Walzog, C. A. Reichel, H. Mannell, K. T. Preissner, and E. Deindl. 2016. Perivascular Mast Cells Govern Shear Stress- Induced Arteriogenesis by Orchestrating Leukocyte Function. *CellReports* 16: 2197–2207.

48. Bryers, J. D., C. M. Giachelli, and B. D. Ratner. 2012. Engineering Biomaterials to Integrate and Heal: The Biocompatibility Paradigm Shifts. *Biotechnology and Bioengineering* 109: 1898–1911.

49. Brown, B. N., B. D. Ratner, S. B. Goodman, S. Amar, and S. F. Badylak. 2012. Macrophage polarization: An opportunity for improved outcomes in biomaterials and regenerative medicine. *Biomaterials* 33: 3792–3802.

50. Klopfleisch, R., and F. Jung. 2016. The pathology of the foreign body reaction against biomaterials. *J. Biomed. Mater. Res.* 105: 927–940.

51. Veiseh, O., J. C. Doloff, M. Ma, A. J. Vegas, H. H. Tam, A. R. Bader, J. Li, E. Langan, J. Wyckoff, W. S. Loo, S. Jhunjhunwala, A. Chiu, S. Siebert, K. Tang, J. Hollister-Lock, S. Aresta-Dasilva, M. Bochenek, J. Mendoza-Elias, Y. Wang, M. Qi, D.

M. Lavin, M. Chen, N. Dholakia, R. Thakrar, I. Lacík, G. C. Weir, J. Oberholzer, D. L. Greiner, R. Langer, and D. G. Anderson. 2015. Size- and shape-dependent foreign body immune response to materials implanted in rodents and non-human primates. *Nat Mater* 14: 643–651.

52. Badylak, S. F., and T. W. Gilbert. 2008. Immune response to biologic scaffold materials. *Seminars in Immunology* 20: 109–116.

53. Stout, R. D., C. Jiang, B. Matta, I. Tietzel, S. K. Watkins, and J. Suttles. 2005. Macrophages Sequentially Change Their Functional Phenotype in Response to Changes in Microenvironmental Influences. *The Journal of Immunology* 175: 342–349.

54. Gordon, S. 2003. Alternative activation of macrophages. *Nat. Rev. Immunol.* 3: 23–35.

55. Martinez, F. O., A. Sica, A. Mantovani, and M. Locati. 2008. Macrophage activation and polarization. *Front Biosci (Landmark Ed)* 13: 453–461.

56. Ribatti, D., and E. Crivellato. 2012. Mast cells, angiogenesis, and tumour growth. *BBA - Molecular Basis of Disease* 1822: 2–8.

57. Dwyer, D. F., D. F. Dwyer, N. A. Barrett, K. F. Austen, E. Y. Kim, M. B. Brenner, L. Shaw, B. Yu, A. Goldrath, S. Mostafavi, A. Regev, A. Rhoades, D. Moodley, H. Yoshida, D. Mathis, C. Benoist, T. Nabekura, V. Lam, L. L. Lanier, B. Brown, M. Merad, V. Cremasco, S. Turley, P. Monach, M. L. Dustin, Y. Li, S. A. Shinton, R. R. Hardy, T. Shay, Y. Qi, K. Sylvia, J. Kang, K. Fairfax, G. J. Randolph, M. L. Robinette, A. Fuchs, M. Colonna, N. A. Barrett, and K. F. Austen. 2016. Expression profiling of constitutive mast cells reveals a unique identity within the immune system. *Nat. Immunol.* 1–12.

58. Amin, K. 2012. The role of mast cells in allergic inflammation. *Respir Med* 106: 9–14.

59. Thevenot, P. T., D. W. Baker, H. Weng, M.-W. Sun, and L. Tang. 2011. The pivotal role of fibrocytes and mast cells in mediating fibrotic reactions to biomaterials. *Biomaterials* 32: 8394–8403.

60. Galli, S. J., N. Borregaard, and T. A. Wynn. 2011. Phenotypic and functional plasticity of cells of innate immunity: macrophages, mast cells and neutrophils. *Nat. Immunol*. 12: 1035–1044.

61. Madden, L. R., D. J. Mortisen, E. M. Sussman, S. K. Dupras, J. A. Fugate, J. L. Cuy, K. D. Hauch, M. A. Laflamme, C. E. Murry, and B. D. Ratner. 2010. Proangiogenic scaffolds as functional templates for cardiac tissue engineering. *Proceedings of the National Academy of Sciences* 107: 15211–15216.

62. Saino, E., M. L. Focarete, C. Gualandi, E. Emanuele, A. I. Cornaglia, M. Imbriani, and L. Visai. 2011. Effect of Electrospun Fiber Diameter and Alignment on Macrophage Activation and Secretion of Proinflammatory Cytokines and Chemokines. *Biomacromolecules* 12: 1900–1911.

63. Wulff, B. C., and T. A. Wilgus. 2013. Mast cell activity in the healing wound: more than meets the eye? *Exp Dermatol* 22: 507–510.

64. Douaiher, J., J. Succar, L. Lancerotto, M. F. Gurish, D. P. Orgill, M. J. Hamilton, S. A. Krilis, and R. L. Stevens. 2014. *Development of Mast Cells and Importance of Their Tryptase and Chymase Serine Proteases in Inflammation and Wound Healing*, 1st ed. Elsevier Inc.; :211–252.

65. Spiller, K. L., S. Nassiri, C. E. Witherel, R. R. Anfang, J. Ng, K. R. Nakazawa, T. Yu,

and G. Vunjak-Novakovic. 2015. Sequential delivery of immunomodulatory cytokines to facilitate the M1-to-M2 transition of macrophages and enhance vascularization of bone scaffolds. *Biomaterials* 37: 194–207.

66. Spiller, K. L., R. R. Anfang, K. J. Spiller, J. Ng, K. R. Nakazawa, J. W. Daulton, and G. Vunjak-Novakovic. 2014. The role of macrophage phenotype in vascularization of tissue engineering scaffolds. *Biomaterials* 35: 4477–4488.

67. Brown, B. N., J. E. Valentin, A. M. Stewart-Akers, G. P. McCabe, and S. F. Badylak. 2009. Macrophage phenotype and remodeling outcomes in response to biologic scaffolds with and without a cellular component. *Biomaterials* 30: 1482–1491.

68. Brown, B. N., B. M. Sicari, and S. F. Badylak. 2014. Rethinking Regenerative Medicine: A Macrophage-Centered Approach. *Front Immunol* 5: 349–11.

69. Garg, K., J. J. Ryan, and G. L. Bowlin. 2011. Modulation of mast cell adhesion, proliferation, and cytokine secretion on electrospun bioresorbable vascular grafts. *J. Biomed. Mater. Res.* 97A: 405–413.

70. Lin, F., X.-D. Ren, Z. Pan, L. Macri, W.-X. Zong, M. G. Tonnesen, M. Rafailovich, D. Bar-Sagi, and R. A. F. Clark. 2011. Fibronectin Growth Factor-Binding Domains Are Required for Fibroblast Survival. *Journal of Investigative Dermatology* 131: 84–98.

71. Liu, T., W. Zhou, B. Cai, J. Chu, G. Shi, H. Teng, J. Xu, J. Xiao, and Y. Wang. 2015. IRX2-mediated upregulation of MMP-9 and VEGF in a PI3K/AKT-dependent manner. *Mol Med Report* 1–6.

72. McClure, M. J., P. S. Wolfe, D. G. Simpson, S. A. Sell, and G. L. Bowlin. 2012. The use of air-flow impedance to control fiber deposition patterns during electrospinning. *Biomaterials* 33: 771–779.

73. Helander, H. F., and G. D. Bloom. 1974. Quantitative Analysis of Mast Cell Structure. *Journal of Microscopy* 100: 315–321.

74. Madurantakam, P. A., C. P. Cost, D. G. Simpson, and G. L. Bowlin. 2009. Science of nanofibrous scaffold fabrication: strategies for next generation tissue-engineering scaffolds. *Nanomedicine* 4: 193–206.

75. Zilla, P., D. Bezuidenhout, and P. Human. 2007. Prosthetic vascular grafts: Wrong models, wrong questions and no healing. *Biomaterials* 28: 5009–5027.

76. MBChB, T. P., P. Z. M. PhD, and D. B. PhD. 2013. Differentiating transmural from transanastomotic prosthetic graft endothelialization through an isolation loop-graft model. *Journal of Vascular Surgery* 58: 1053–1061.

77. Boland, E. D., J. A. Matthews, K. J. Pawlowski, D. G. Simpson, G. E. Wnek, and G. L. Bowlin. 2004. Electrospinning collagen and elastin: preliminary vascular tissue engineering. *Front Biosci* 9: 1422–1432.

78. Keselowsky, B. G., A. W. Bridges, K. L. Burns, C. C. Tate, J. E. Babensee, M. C. LaPlaca, and A. J. García. 2007. Role of plasma fibronectin in the foreign body response to biomaterials. *Biomaterials* 28: 3626–3631.

79. Caballero-George, C., Marin, and Briceño. 2013. Critical evaluation of biodegradable polymers used in nanodrugs. *IJN* 3071–21.

80. Ulery, B. D., L. S. Nair, and C. T. Laurencin. 2011. Biomedical applications of biodegradable polymers. *J. Polym. Sci. B Polym. Phys.* 49: 832–864.

81. Nair, L. S., and C. T. Laurencin. 2007. Biodegradable polymers as biomaterials. *Progress in Polymer Science* 32: 762–798.

82. Nair, L. S., and C. T. Laurencin. 2007. Biodegradable polymers as biomaterials.

Progress in Polymer Science 32: 762–798.

83. Sarasua, J. R., N. López-Rodríguez, E. Zuza, S. Petisco, B. Castro, M. del Olmo, T. Palomares, and A. Alonso-Varona. 2011. Crystallinity assessment and in vitro cytotoxicity of polylactide scaffolds for biomedical applications. *J Mater Sci: Mater Med* 22: 2513–2523.

84. Ercolani, E., C. Del Gaudio, and A. Bianco. 2013. Vascular tissue engineering of small-diameter blood vessels: reviewing the electrospinning approach. *J Tissue Eng Regen Med* 9: 861–888.

85. Kalesnikoff, J., and S. J. Galli. 2008. New developments in mast cell biology. *Nat. Immunol.* 9: 1215–1223.

86. Finkelman, F. D. 2007. Anaphylaxis: lessons from mouse models. *J. Allergy Clin. Immunol.* 120: 506–515.

87. Burton, O. T., and H. C. Oettgen. 2011. Beyond immediate hypersensitivity: evolving roles for IgE antibodies in immune homeostasis and allergic diseases. *Immunol. Rev.* 242: 128–143.

88. Metcalfe, D. D., R. D. Peavy, and A. M. Gilfillan. 2009. Mechanisms of mast cell signaling in anaphylaxis. *J. Allergy Clin. Immunol.* 124: 639–648.

89. Ho, L. H., T. Ohno, K. Oboki, N. Kajiwara, H. Suto, M. Iikura, Y. Okayama, S. Akira, H. Saito, S. J. Galli, and S. Nakae. 2007. IL-33 induces IL-13 production by mouse mast cells independently of IgE-FcepsilonRI signals. *J. Leukoc. Biol.* 82: 1481–1490.

90. Silver, M. R., A. Margulis, N. Wood, S. J. Goldman, M. Kasaian, and D. Chaudhary. 2010. IL-33 synergizes with IgE-dependent and IgE-independent agents to promote mast

cell and basophil activation. *Inflamm. Res*. 59: 207–218.

91. Liew, F. Y., N. I. Pitman, and I. B. McInnes. 2010. Disease-associated functions of IL-33: the new kid in the IL-1 family. *Nat. Rev. Immunol*. 10: 103–110.

92. Hsu, C.-L., C. V. Neilsen, and P. J. Bryce. 2010. IL-33 Is Produced by Mast Cells and Regulates IgE- Dependent Inflammation. *PLoS ONE* 5: e11944.

93. Hsu, P. P., and D. M. Sabatini. 2008. Cancer cell metabolism: Warburg and beyond. *Cell* 134: 703–707.

94. Quail, D. F., and J. A. Joyce. 2013. Microenvironmental regulation of tumor progression and metastasis. *Nat. Med*. 19: 1423–1437.

95. Maturu, P., W. W. Overwijk, J. Hicks, S. Ekmekcioglu, E. A. Grimm, and V. Huff. 2014. Characterization of the inflammatory microenvironment and identification of potential therapeutic targets in wilms tumors. *Transl Oncol* 7: 484–492.

96. Gottfried, E., L. A. Kunz-Schughart, S. Ebner, W. Mueller-Klieser, S. Hoves, R. Andreesen, A. Mackensen, and M. Kreutz. 2006. Tumor-derived lactic acid modulates dendritic cell activation and antigen expression. *Blood* 107: 2013–2021.

97. Chanmee, T., P. Ontong, K. Konno, and N. Itano. 2014. Tumor-associated macrophages as major players in the tumor microenvironment. *Cancers (Basel)* 6: 1670–1690.

98. Fischer, K., P. Hoffmann, S. Voelkl, N. Meidenbauer, J. Ammer, M. Edinger, E. Gottfried, S. Schwarz, G. Rothe, S. Hoves, K. Renner, B. Timischl, A. Mackensen, L. Kunz-Schughart, R. Andreesen, S. W. Krause, and M. Kreutz. 2007. Inhibitory effect of tumor cell-derived lactic acid on human T cells. *Blood* 109: 3812–3819.

99. Semenza, G. L. 2009. Regulation of cancer cell metabolism by hypoxia-inducible

factor 1. *Semin. Cancer Biol*. 19: 12–16.

100. Zhang, Y., P. Yang, and X.-F. Wang. 2014. Microenvironmental regulation of cancer metastasis by miRNAs. *Trends Cell Biol*. 24: 153–160.

101. Colegio, O. R., N.-Q. Chu, A. L. Szabo, T. Chu, A. M. Rhebergen, V. Jairam, N. Cyrus, C. E. Brokowski, S. C. Eisenbarth, G. M. Phillips, G. W. Cline, A. J. Phillips, and R. Medzhitov. 2014. Functional polarization of tumour-associated macrophages by tumour-derived lactic acid. *Nature* 513: 559–563.

102. Jensen, J. C., C. Buresh, and J. A. Norton. 1990. Lactic acidosis increases tumor necrosis factor secretion and transcription in vitro. *J. Surg. Res*. 49: 350–353.

103. Samuvel, D. J., K. P. Sundararaj, A. Nareika, M. F. Lopes-Virella, and Y. Huang. 2009. Lactate boosts TLR4 signaling and NF-kappaB pathway-mediated gene transcription in macrophages via monocarboxylate transporters and MD-2 up-regulation. *J. Immunol*. 182: 2476–2484.

104. Beghdadi, W., L. C. Madjene, M. Benhamou, N. Charles, G. Gautier, P. Launay, and U. Blank. 2011. Mast cells as cellular sensors in inflammation and immunity. *Front Immunol* 2: 37.

105. DiGirolamo, M., F. D. Newby, and J. Lovejoy. 1992. Lactate production in adipose tissue: a regulated function with extra-adipose implications. *FASEB J*. 6: 2405–2412.

106. Livak, K. J., and T. D. Schmittgen. 2001. Analysis of Relative Gene Expression Data Using Real-Time Quantitative PCR and the 2−ΔΔCT Method. *Methods* 25: 402–408.

107. Kambe, N., M. Kambe, J. P. Kochan, and L. B. Schwartz. 2001. Human skin-derived mast cells can proliferate while retaining their characteristic functional and

protease phenotypes. *Blood* 97: 2045–2052.

108. Withers, R. T., W. M. Sherman, D. G. Clark, P. C. Esselbach, S. R. Nolan, M. H. Mackay, and M. Brinkman. 1991. Muscle metabolism during 30, 60 and 90 s of maximal cycling on an air-braked ergometer. *European Journal of Applied Physiology* 63: 354–362.

109. Ruan, G. X., and A. Kazlauskas. 2013. Lactate Engages Receptor Tyrosine Kinases Axl, Tie2, and Vascular Endothelial Growth Factor Receptor 2 to Activate Phosphoinositide 3-Kinase/Akt and Promote Angiogenesis. *J. Biol. Chem.* 288: 21161–21172.

110. Ostroukhova, M., N. Goplen, M. Z. Karim, L. Michalec, L. Guo, Q. Liang, and R. Alam. 2012. The role of low-level lactate production in airway inflammation in asthma. *AJP: Lung Cellular and Molecular Physiology* 302: L300–L307.

111. Peter, K., M. Rehli, K. Singer, K. Renner-Sattler, and M. Kreutz. 2015. Lactic acid delays the inflammatory response of human monocytes. *Biochemical and Biophysical Research Communications* 1–7.

112. Dietl, K., K. Renner, K. Dettmer, B. Timischl, K. Eberhart, C. Dorn, C. Hellerbrand, M. Kastenberger, L. A. Kunz-Schughart, P. J. Oefner, R. Andreesen, E. Gottfried, and M. P. Kreutz. 2010. Lactic Acid and Acidification Inhibit TNF Secretion and Glycolysis of Human Monocytes. *The Journal of Immunology* 184: 1200–1209.

113. Vegran, F., R. Boidot, C. Michiels, P. Sonveaux, and O. Feron. 2011. Lactate Influx through the Endothelial Cell Monocarboxylate Transporter MCT1 Supports an NF- B/IL-8 Pathway that Drives Tumor Angiogenesis. *Cancer Research* 71: 2550–2560.

114. Le Floch, R., J. Chiche, I. Marchiq, T. Naiken, K. Ilc, C. M. Murray, S. E.

Critchlow, D. Roux, M.-P. Simon, and J. Pouyssegur. 2011. CD147 subunit of lactate/H+ symporters MCT1 and hypoxia-inducible MCT4 is critical for energetics and growth of glycolytic tumors. *Proceedings of the National Academy of Sciences* 108: 16663–16668.

115. Cortes-Campos, C., R. Elizondo, C. Carril, F. Martínez, K. Boric, F. Nualart, and M. A. Garcia-Robles. 2013. MCT2 Expression and Lactate Influx in Anorexigenic and Orexigenic Neurons of the Arcuate Nucleus. *PLoS ONE* 8: e62532–15.

116. Lin, R. Y., J. C. Vera, R. S. K. Chaganti, and D. W. Golde. 1998. Human Monocarboxylate Transporter 2 (MCT2) Is a High Affinity Pyruvate Transporter. *J. Biol. Chem*. 273: 28959–28965.

117. Hosoya, K.-I., T. Kondo, M. Tomi, H. Takanaga, S. Ohtsuki, and T. Terasaki. 2001. MCT1-Mediated Transport of L-Lactic Acid at the Inner Blood–Retinal Barrier: A Possible Route for Delivery of Monocarboxylic Acid Drugs to the Retina. *Pharmaceutical Research* 18: 1669–1676.

118. Andrade, M. V., S. Iwaki, C. Ropert, R. T. Gazzinelli, J. R. Cunha-Melo, and M. A. Beaven. 2011. Amplification of cytokine production through synergistic activation of NFAT and AP-1 following stimulation of mast cells with antigen and IL-33. *Eur. J. Immunol*. 41: 760–772.

119. ZHANG, Q., C. OH, D. MESSADI, H. DUONG, A. KELLY, C. SOO, L. WANG, and A. LE. 2006. Hypoxia-induced HIF-1 α accumulation is augmented in a co-culture of keloid fibroblasts and human mast cells: Involvement of ERK1/2 and PI-3K/Akt. *Experimental Cell Research* 312: 145–155.

120. Liu, T., W. Zhou, B. Cai, J. Chu, G. Shi, H. Teng, J. Xu, J. Xiao, and Y. Wang. 2015. IRX2-mediated upregulation of MMP-9 and VEGF in a PI3K/AKT-dependent

manner. *Mol Med Report* 1–6.

121. Ji, Y., C. Wrzesinski, Z. Yu, J. Hu, S. Gautam, N. V. Hawk, W. G. Telford, D. C. Palmer, Z. Franco, M. Sukumar, R. Roychoudhuri, D. Clever, C. A. Klebanoff, C. D. Surh, T. A. Waldmann, N. P. Restifo, and L. Gattinoni. 2015. miR-155 augments CD8+ T-cell antitumor activity in lymphoreplete hosts by enhancing responsiveness to homeostatic γc cytokines. *Proc. Natl. Acad. Sci. U.S.A.* 112: 476–481.

122. De Saedeleer, C. J., T. Copetti, P. E. Porporato, J. Verrax, O. Feron, and P. Sonveaux. 2012. Lactate activates HIF-1 in oxidative but not in Warburg-phenotype human tumor cells. *PLoS ONE* 7: e46571–12.

123. Zuo, R.-J., X.-W. Gu, Q.-R. Qi, T.-S. Wang, X.-Y. Zhao, J.-L. Liu, and Z.-M. Yang. 2015. Warburg-like Glycolysis and Lactate Shuttle in Mouse Decidua during Early Pregnancy. *J. Biol. Chem.* 290: 21280–21291.

124. Babar, I. A., J. Czochor, A. Steinmetz, J. B. Weidhaas, P. M. Glazer, and F. J. Slack. 2014. Inhibition of hypoxia-induced miR-155 radiosensitizes hypoxic lung cancer cells. *Cancer Biology & Therapy* 12: 908–914.

125. Hu, R., Y. Zhang, X. Yang, J. Yan, Y. Sun, Z. Chen, and H. Jiang. 2015. Isoflurane attenuates LPS-induced acute lung injury by targeting miR-155-HIF1-alpha. *Front Biosci (Landmark Ed)* 20: 139–156.

126. Bruning, U., L. Cerone, Z. Neufeld, S. F. Fitzpatrick, A. Cheong, C. C. Scholz, D. A. Simpson, M. O. Leonard, M. M. Tambuwala, E. P. Cummins, and C. T. Taylor. 2011. MicroRNA-155 Promotes Resolution of Hypoxia-Inducible Factor 1 Activity during Prolonged Hypoxia. *Molecular and Cellular Biology* 31: 4087–4096.

127. Lu, L.-F., T.-H. Thai, D. P. Calado, A. Chaudhry, M. Kubo, K. Tanaka, G. B. Loeb,

H. Lee, A. Yoshimura, K. Rajewsky, and A. Y. Rudensky. 2009. Foxp3-Dependent MicroRNA155 Confers Competitive Fitness to Regulatory T Cells by Targeting SOCS1 Protein. *Immunity* 30: 80–91.

128. Sung, H.-J., C. Meredith, C. Johnson, and Z. S. Galis. 2004. The effect of scaffold degradation rate on three-dimensional cell growth and angiogenesis. *Biomaterials* 25: 5735–5742.

129. Marichal, T., M. Tsai, and S. J. Galli. 2013. Mast Cells: Potential Positive and Negative Roles in Tumor Biology. *Cancer Immunol Res* 1: 269–279.

130. Coussens, L. M., W. W. Raymond, G. Bergers, M. Laig-Webster, O. Behrendtsen, Z. Werb, G. H. Caughey, and D. Hanahan. 1999. Inflammatory mast cells up-regulate angiogenesis during squamous epithelial carcinogenesis. *Genes Dev*. 13: 1382–1397.

131. Benítez-Bribiesca, L., A. Wong, D. Utrera, and E. Castellanos. 2001. The role of mast cell tryptase in neoangiogenesis of premalignant and malignant lesions of the uterine cervix. *J. Histochem. Cytochem*. 49: 1061–1062.

132. Gilfillan, A. M., and M. A. Beaven. 2011. Regulation of mast cell responses in health and disease. *Crit. Rev. Immunol*. 31: 475–529.

133. Nareika, A., L. He, B. A. Game, E. H. Slate, J. J. Sanders, S. D. London, M. F. Lopes-Virella, and Y. Huang. 2005. Sodium lactate increases LPS-stimulated MMP and cytokine expression in U937 histiocytes by enhancing AP-1 and NF-kappaB transcriptional activities. *Am. J. Physiol. Endocrinol. Metab*. 289: E534–42.

134. Marchiq, I., and J. Pouyssegur. 2015. Hypoxia, cancer metabolism and the therapeutic benefit of targeting lactate/H+ symporters. *J Mol Med* 1–17.

135. Bruning, U., L. Cerone, Z. Neufeld, S. F. Fitzpatrick, A. Cheong, C. C. Scholz, D.

A. Simpson, M. O. Leonard, M. M. Tambuwala, E. P. Cummins, and C. T. Taylor. 2011. MicroRNA-155 promotes resolution of hypoxia-inducible factor 1alpha activity during prolonged hypoxia. *Molecular and Cellular Biology* 31: 4087–4096.

136. Huang, C.-J., P. N. N. Nguyen, K. B. Choo, S. Sugii, K. Wee, S. K. Cheong, and T. Kamarul. 2014. Frequent Co-Expression of miRNA-5p and -3p Species and Cross-Targeting in Induced Pluripotent Stem Cells. *Int. J. Med. Sci.* 11: 824–833.

137. Choo, K. B., Y. L. Soon, P. N. N. Nguyen, M. S. Y. Hiew, and C.-J. Huang. 2014. MicroRNA-5p and -3p co-expression and cross-targeting in colon cancer cells. *J Biomed Sci* 21: 892–14.

138. Kuchenbauer, F., S. M. Mah, M. Heuser, A. McPherson, J. Ruschmann, A. Rouhi, T. Berg, L. Bullinger, B. Argiropoulos, R. D. Morin, D. Lai, D. T. Starczynowski, A. Karsan, C. J. Eaves, A. Watahiki, Y. Wang, S. A. Aparicio, A. Ganser, J. Krauter, H. Dohner, K. Dohner, M. A. Marra, F. D. Camargo, L. Palmqvist, C. Buske, and R. K. Humphries. 2011. Comprehensive analysis of mammalian miRNA* species and their role in myeloid cells. *Blood* 118: 3350–3358.

139. Kamide, Y., T. Ishizuka, M. Tobo, H. Tsurumaki, H. Aoki, C. Mogi, T. Nakakura, M. Yatomi, A. Ono, Y. Koga, K. Sato, T. Hisada, K. Dobashi, M. Yamada, and F. Okajima. 2015. Acidic environment augments FcεRI-mediated production of IL-6 and IL-13 in mast cells. *Biochemical and Biophysical Research Communications* 464: 949–955.

140. Lu, J., J. Kang, C. Zhang, and X. Zhang. 2015. The role of IL-33/ST2L signals in the immune cells. *Immunology Letters* 164: 11–17.

141. Rak, G. D., L. C. Osborne, M. C. Siracusa, B. S. Kim, K. Wang, A. Bayat, D. Artis,

and S. W. Volk. 2016. IL-33-Dependent Group 2 Innate Lymphoid Cells Promote Cutaneous Wound Healing. *Journal of Investigative Dermatology* 136: 487–496.

142. Schmitz, J., A. Owyang, E. Oldham, Y. Song, E. Murphy, T. K. McClanahan, G. Zurawski, M. Moshrefi, J. Qin, X. Li, D. M. Gorman, J. F. Bazan, and R. A. Kastelein. 2005. IL-33, an Interleukin-1-like Cytokine that Signals via the IL-1 Receptor-Related Protein ST2 and Induces T Helper Type 2-Associated Cytokines. *Immunity* 23: 479–490.

143. Cherry, W. B., J. Yoon, K. R. Bartemes, K. Iijima, and H. Kita. 2008. A novel IL-1 family cytokine, IL-33, potently activates human eosinophils. *Journal of Allergy and Clinical Immunology* 121: 1484–1490.

144. Holdom, M. D., A. M. Davies, J. E. Nettleship, S. C. Bagby, B. Dhaliwal, E. Girardi, J. Hunt, H. J. Gould, A. J. Beavil, J. M. McDonnell, R. J. Owens, and B. J. Sutton. 2011. Conformational changes in IgE contribute to its uniquely slow dissociation rate from receptor FcεRI. *Nat Struct Mol Biol* 18: 571–576.

145. Kraft, S., and J.-P. Kinet. 2007. New developments in FcεRI regulation, function and inhibition. *Nat. Rev. Immunol.* 7: 365–378.

146. Oskeritzian, C. A., S. E. Alvarez, N. C. Hait, M. M. Price, S. Milstien, and S. Spiegel. 2008. Distinct roles of sphingosine kinases 1 and 2 in human mast-cell functions. *Blood* 111: 4193–4200.

147. Dehlink, E., B. Platzer, A. H. Baker, J. LaRosa, M. Pardo, P. Dwyer, E. H. Yen, Z. Szépfalusi, S. Nurko, and E. Fiebiger. 2011. A Soluble Form of the High Affinity IgE Receptor, Fc-Epsilon-RI, Circulates in Human Serum. *PLoS ONE* 6: e19098–8.

148. Siraganian, R. P., R. O. de Castro, E. A. Barbu, and J. Zhang. 2010. Mast cell signaling: The role of protein tyrosine kinase Syk, its activation and screening methods

for new pathway participants. *FEBS Letters* 584: 4933–4940.

149. Ryan, J. J. 2014. Too much of a good thing: beta-chain overexpression blocks FcεRI signalling by capturing Lyn in the cytosol. *Clin Exp Allergy* 44: 154–156.

150. Nunomura, S. 2005. Role of the Fc RI -chain ITAM as a signal regulator for mast cell activation with monomeric IgE. *International Immunology* 17: 685–694.

151. Kelly D Stone MD, P., C. P. MD, and D. D. M. MD. 2010. IgE, mast cells, basophils, and eosinophils. *Journal of Allergy and Clinical Immunology* 125: S73–S80.

152. da Silva, E. Z. M., M. C. Jamur, and C. Oliver. 2014. Mast Cell Function. *J. Histochem. Cytochem.* 62: 698–738.

153. Kraft, S., and J.-P. Kinet. 2007. New developments in FcεRI regulation, function and inhibition. *Nat. Rev. Immunol.* 7: 365–378.

154. Qayum, A. A., A. Paranjape, D. Abebayehu, E. M. Kolawole, T. T. Haque, J. J. A. McLeod, A. J. Spence, H. L. Caslin, M. T. Taruselli, A. P. Chumanevich, B. Baker, C. A. Oskeritzian, and J. J. Ryan. 2016. IL-10–Induced miR-155 Targets SOCS1 To Enhance IgE-Mediated Mast Cell Function. *The Journal of Immunology* 196: 4457–4467.

155. Kolawole, E. M., J. J. A. McLeod, V. Ndaw, D. Abebayehu, B. O. Barnstein, T. Faber, A. J. Spence, M. Taruselli, A. Paranjape, T. T. Haque, A. A. Qayum, Q. A. Kazmi, D. S. Wijesinghe, J. L. Sturgill, C. E. Chalfant, D. B. Straus, C. A. Oskeritzian, and J. J. Ryan. 2016. Fluvastatin Suppresses Mast Cell and Basophil IgE Responses: Genotype-Dependent Effects. *J. Immunol.* 196: 1461–1470.

156. Raposo, G., D. Tenza, S. Mecheri, R. Peronet, C. Bonnerot, and C. Desaymard. 1997. Accumulation of Major Histocompatibility Complex Class II Molecules in Mast Cell Secretory Granules and Their Release upon Degranulation. *Molecular Biology of the*

Cell 8: 2631–2645.

157. Greer, A. M., N. Wu, A. L. Putnam, P. G. Woodruff, P. Wolters, J.-P. Kinet, and J.-S. Shin. 2014. Serum IgE clearance is facilitated by human FcεRI internalization. *J. Clin. Invest*. 124: 1187–1198.

158. Abebayehu, D., A. J. Spence, A. A. Qayum, M. T. Taruselli, J. J. A. McLeod, H. L. Caslin, A. P. Chumanevich, E. M. Kolawole, A. Paranjape, B. Baker, V. S. Ndaw, B. O. Barnstein, C. A. Oskeritzian, S. A. Sell, and J. J. Ryan. 2016. Lactic Acid Suppresses IL-33-Mediated Mast Cell Inflammatory Responses via Hypoxia-Inducible Factor-1α-Dependent miR-155 Suppression. *J. Immunol*. 197: 2909–2917.

159. Gilfillan, A. M., and J. Rivera. 2009. The tyrosine kinase network regulating mast cell activation. *Immunol. Rev*. 228: 149–169.

160. Ucuzian, A. A., A. A. Gassman, A. T. East, and H. P. Greisler. 2010. Molecular Mediators of Angiogenesis. *Journal of Burn Care & Research* 31: 158–175.

161. Lee, A.-J., M. Ro, and J.-H. Kim. 2016. Leukotriene B 4Receptor 2 Is Critical for the Synthesis of Vascular Endothelial Growth Factor in Allergen-Stimulated Mast Cells. *The Journal of Immunology* 197: 2069–2078.

162. Faber, T. W., N. A. Pullen, J. F. A. Fernando, E. M. Kolawole, J. J. A. McLeod, M. Taruselli, K. L. Williams, K. O. Rivera, B. O. Barnstein, D. H. Conrad, and J. J. Ryan. 2014. ADAM10 is required for SCF-induced mast cell migration. *Cellular Immunology* 290: 80–88.

163. Feger, F., S. Varadaradjalou, Z. Gao, S. N. Abraham, and M. Arock. 2002. The role of mast cells in host defense and their subversion by bacterial pathogens. *Trends in Immunology* 23: 151–158.

164. Tsai, M., S. Li-Sun, G. F. J. Newlands, T. Takeishi, K. E. Langley, K. M. Zsebo, H. R. P. Miller, E. N. Geissler, and S. J. Galli. 2003. The Rat c-Kit Ligand, Stem Cell Factor, Induces the Develepment of Connective Tissue-Type and Mucosal Mast Cells In Vivo. Analysis by Anatomical Distribution, Histochemistry, and Protease Phenotype. *Journal of Experimental Medicine* 174: 125–131.

165. Macdonald, A. J., J. Pick, E. Y. Bissonnette, and A. D. Befus. 2006. Rat mucosal mast cells: the cultured bone marrow-derived mast cell is biochemically and functionally analgous to its counterpart in vivo. *Immunology* 93: 533–539.

VITA

VITA

Daniel Abebayehu was born on August 30th 1989 in St. Mary's Hospital in Milwaukee, Wisconsin and is a citizen of the United States of America. The only child of Dr. Abebayehu Tegene and Ms. Konjit Eskender, he moved to the Washington D.C. Metropolitan area with his family at only 6 months old. He graduted from Hayfield Secondary School in Alexandria, Virginia in 2007. He later received a Bachelor of Science degree in Biomedical Engineering from the University of Virginia in Charlottesville, Virginia in 2011. Following two and a half years spent working in the lab of Dr. Edward Botchwey in the Department of Biomedical Engineering, he applied and enrolled in a graduate program to pursue a PhD in Biomedical Engineering at Virginia Commonwealth University. Daniel currently resides in Richmond, Virginia with his wife, Mary Catherine, and his two sons, James and Eli.